

# A Novel Approach to Modelling Anisotropic Rock Deformation using Hyperbolic Stress-Strain Relationship

Author: - Arindam Mukherjee

Institution: - University of Energy and Petroleum Studies, Dehradun



<https://doi.org/10.55041/ijst.v2i2.012>

**Cite this Article:** Mukherjee, A. (2026). A Novel Approach to Modelling Anisotropic Rock Deformation using Hyperbolic Stress-Strain Relationship. International Journal of Science, Strategic Management and Technology, 02(02). <https://doi.org/10.55041/ijst.v2i2.012>

**License:**  This article is published under the Creative Commons Attribution 4.0 International License (CC BY 4.0), permitting use, distribution, and reproduction in any medium, provided the original author(s) and source are properly credited.

**Abstract:** - To understand the mechanical behaviour of anisotropic rocks is a critical thing for the accurate prediction of stress distribution in the subsurface, mainly for drilling and reservoir engineering. Linear elastic models of stress distribution often fail to capture the non-linear deformation characteristics that are mainly observed in sedimentary and fractured rocks. This study presents a novel approach for modelling the anisotropic rock deformation by using a hyperbolic stress-strain relationship that effectively accounts for the non-linear directional-dependent mechanical behaviour of rock mass, including bedding planes and fracture-induced anisotropy. Numerical simulation clearly indicates that the hyperbolic model accurately predicts the stress-strain conditions under various loading conditions, which provides more realistic estimates for wellbore stability, fracture propagation and in-situ shear stress conditions. Numerical simulation has been performed using a hyperbolic model to generate stress-strain curves along with different orientations, which enables the evaluation of tangential and radial stress around the wellbore. The proposed methodology incorporates orientation-dependent parameters to represent the bedding plane and fracture-induced anisotropy by using literature-based rock properties, which allow robust geomechanical analysis without requiring original laboratory experiments, that offer a practical tool for wellbore design, drilling risk mitigation and reservoir management, mud selection for drilling, and it also serves as a foundation for future experimental and field-based validation studies. The study highlights its novelty by introducing a hyperbolic stress-strain model that is capable of anisotropic rock deformation more accurately than the conventional linear model.

**Keywords:** - Anisotropic rocks, Hyperbolic stress-strain, Rock deformation, Wellbore stability, Numerical modelling, Geomechanics.

**Introduction:** - The rocks are not uniform; they generally exhibit anisotropy, which may vary with direction, and this may be a critical issue for wellbore stability, geomechanical modelling, hydraulic fracturing, tunnelling and reservoir simulations. Common sedimentary rocks like shale, sandstone or limestone anisotropies occur parallel or perpendicular to the bedding plane. Parallel to the bedding plane, usually stronger in compression and weaker in shear and perpendicular to the bedding, more prone to fracture, which are often weaker. In the case of metamorphic rocks like Talc, Mica generally creates planes of weakness by their own, and they break along the foliation plane as their mechanical properties differ along the foliation plane. Rocks with natural fractures, which may be due to a combination of Tectonic stresses, like shear fractures, Tensile fractures or due to strike-slip, normal or reverse fault, may create stress beyond their strength, and they fracture. Igneous rocks like basalt and granite cool after emplacement, and this cooling leads to contraction and stress and fracture types generally occur in columnar jointing, like hexagonal columns in basalt. Sedimentary rocks also crack due to diagenetic cooling. Removal of overlying strata of rock layers by erosion also reduces the confining pressure, and in that case, rocks expand and form tensile fractures. Chemical reactions during the

lithification of sediments create cementation shrinkage, and due to differential compaction or mineral precipitation, sedimentary rocks like carbonate develop stylolite develop microfractures, which also develop due to pressure solution. High pore pressure in the rocks can reduce effective stresses, causing them to fracture naturally. Hydrocarbon, water and carbon dioxide can exploit these weak planes. Generally, in Naturally fractured reservoirs (NFRs) in shale or in tight carbonate reservoirs often have fracture networks driven by fluid overpressure

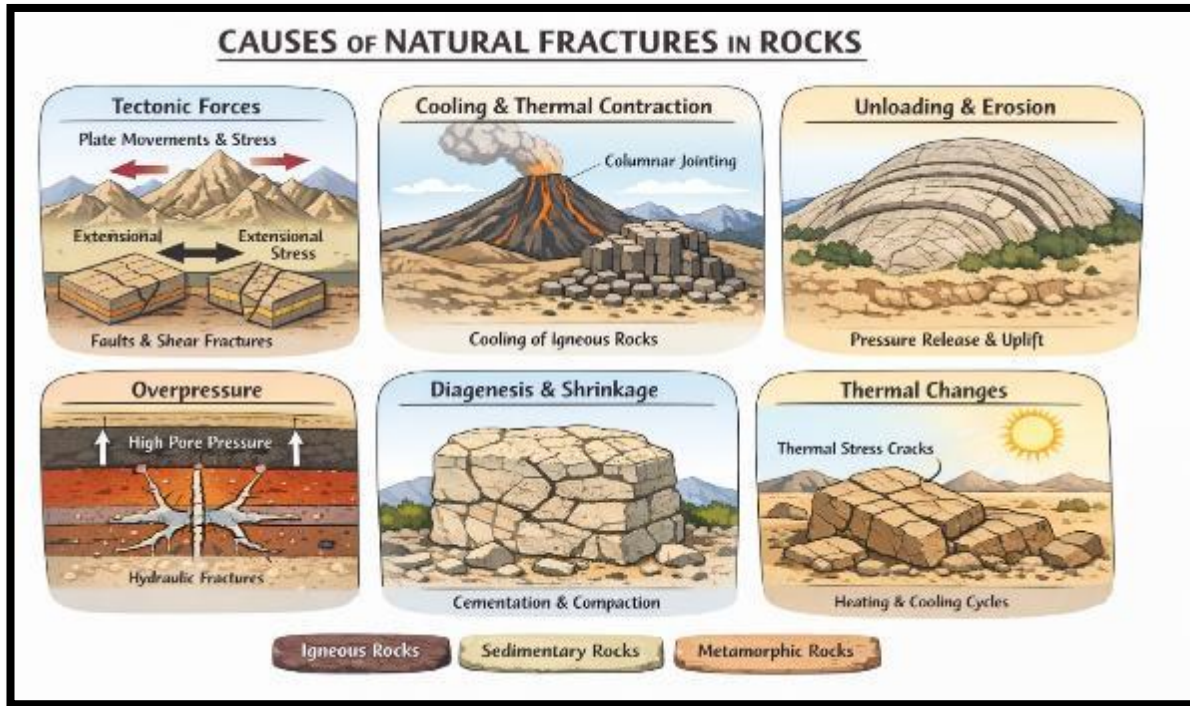


**Fig 1 :- Geological mechanisms responsible for natural fractures within the rocks**

So, from the upper figure and upper discussion, we see most rocks like shales, laminated sandstones and metamorphic rocks do not behave the same in all directions and their mechanical properties vary with bedding, foliation and fractures. So, ignoring the anisotropy may lead to wellbore instability, fracture propagation, or may occur when the stresses acting on a rock within a drillhole exceed the strength of the surrounding rocks, which may cause the borehole to collapse, fracture, enlarge or deform.

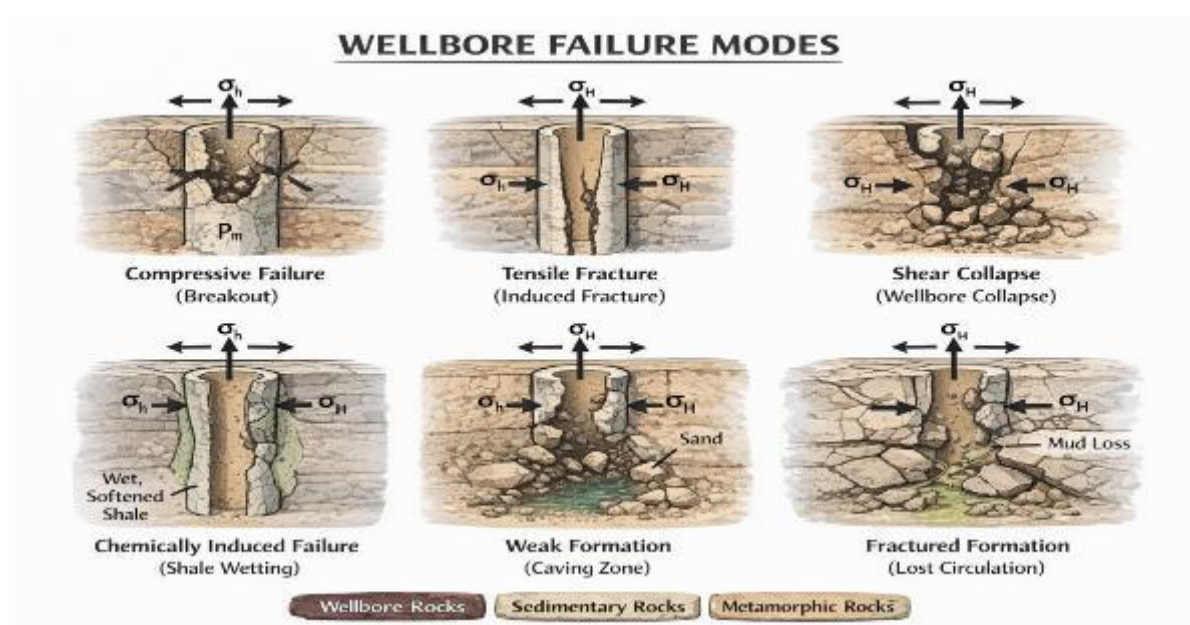
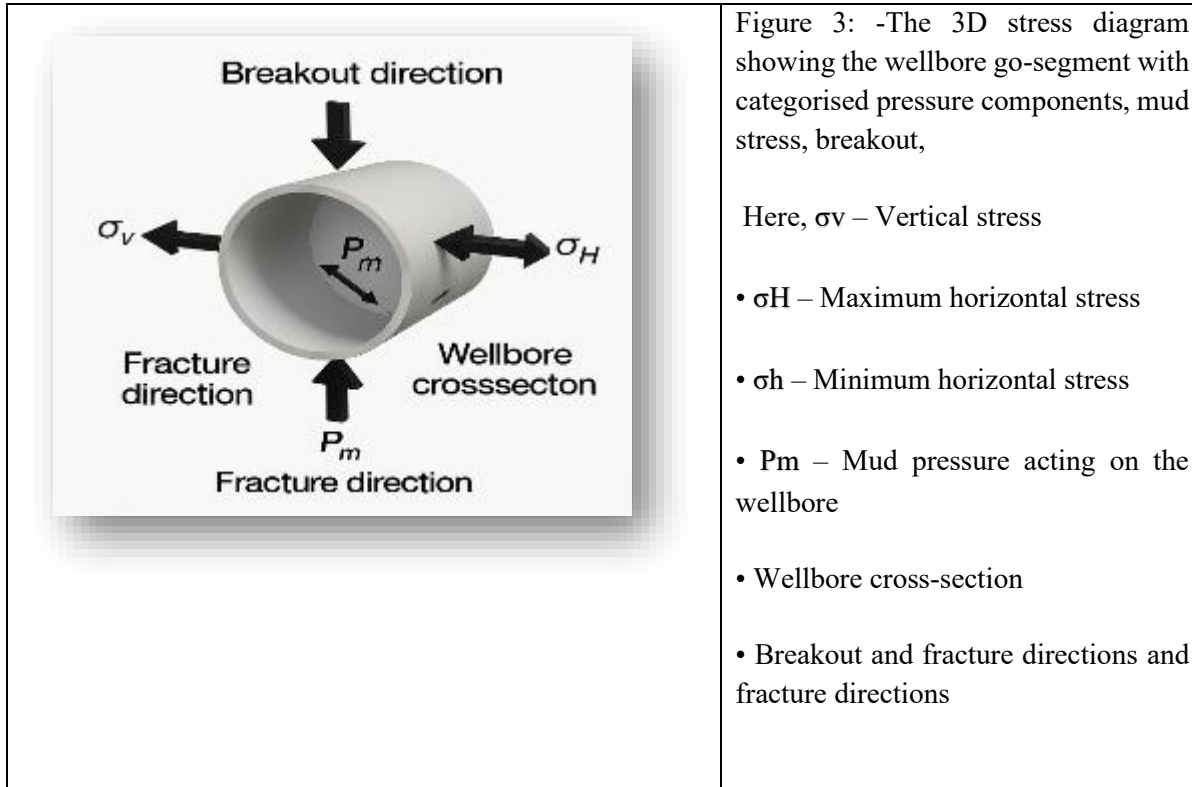


Figure 2:- The figure illustrates the main wellbore failure modes, including compressive breakouts, tensile fractures, shear collapse, and chemically induced shale failure, weak formation carvings and fluid loss in naturally fractured formations, which are all caused by stress imbalance, rock weakness, and mud formation interactions. In our figure,  $\sigma_h$  stands for the smallest principal horizontal in situ stress that acts on the Earth's crust, measured in Mpa or Psi, and  $P_m$  stands for mud pressure or wellbore pressure. In an oilfield,  $P_m = \rho_{mud}gh$  or  $P_m = 0.052 \times MW$  (ppg)  $\times$  TVD (feet) (Where  $P_m$  = mud pressure, TVD = True vertical depth, MW = mud weight). So, if, If  $P_m <$  required value  $\rightarrow$  wellbore collapses or,  $P_m > \sigma_h +$  tensile strength  $\rightarrow$  fractures form.



This observation is justified by using the need for greater practical constitutive models that can accurately describe the nonlinear and path-structured deformation conduct of rocks below complex strain situations. Conventional isotropic and linear elastic models fail to capture the revolutionary harm, stiffness degradation, and anisotropic reaction determined in natural geological formations. Through introducing a hyperbolic stress-strain courting into an anisotropic framework, this research aims to offer a extra correct representation of rock deformation prior to failure. The proposed method is anticipated to seriously enhance the prediction of wellbore instability, fracture initiation, and subsurface structural integrity, thereby improving the safety, performance, and monetary viability of subsurface engineering operations.

**Methodology:** - This study models anisotropic rock deformation using a hyperbolic stress-strain relationship with orientation-dependent parameters from the literature. Numerical simulations predict stress-strain behaviour and potential failure zones, providing a practical framework for wellbore stability analysis without experimental data.

The methodology I chose here is based on a certain parameter that has been described below, which has been obtained from 1) Mechanical Strength & Rock Failure (Jaeger & Cook – *Fundamentals of Rock Mechanics*), 2) Rock Mass Classification & Strength (Bieniawski – *Engineering Rock Mass Classifications*), 3) Failure Criterion & Rock Strength Models (Hoek & Brown – *Practical Rock Engineering*), 4) Seismic Properties & Rock Physics (Mavko, Mukerji & Dvorkin – *Rock Physics Handbook*), 5) Seismic Anisotropy & Velocity Relations (Nick Barton – *Rock Quality, Seismic Velocity, Attenuation and Anisotropy*).

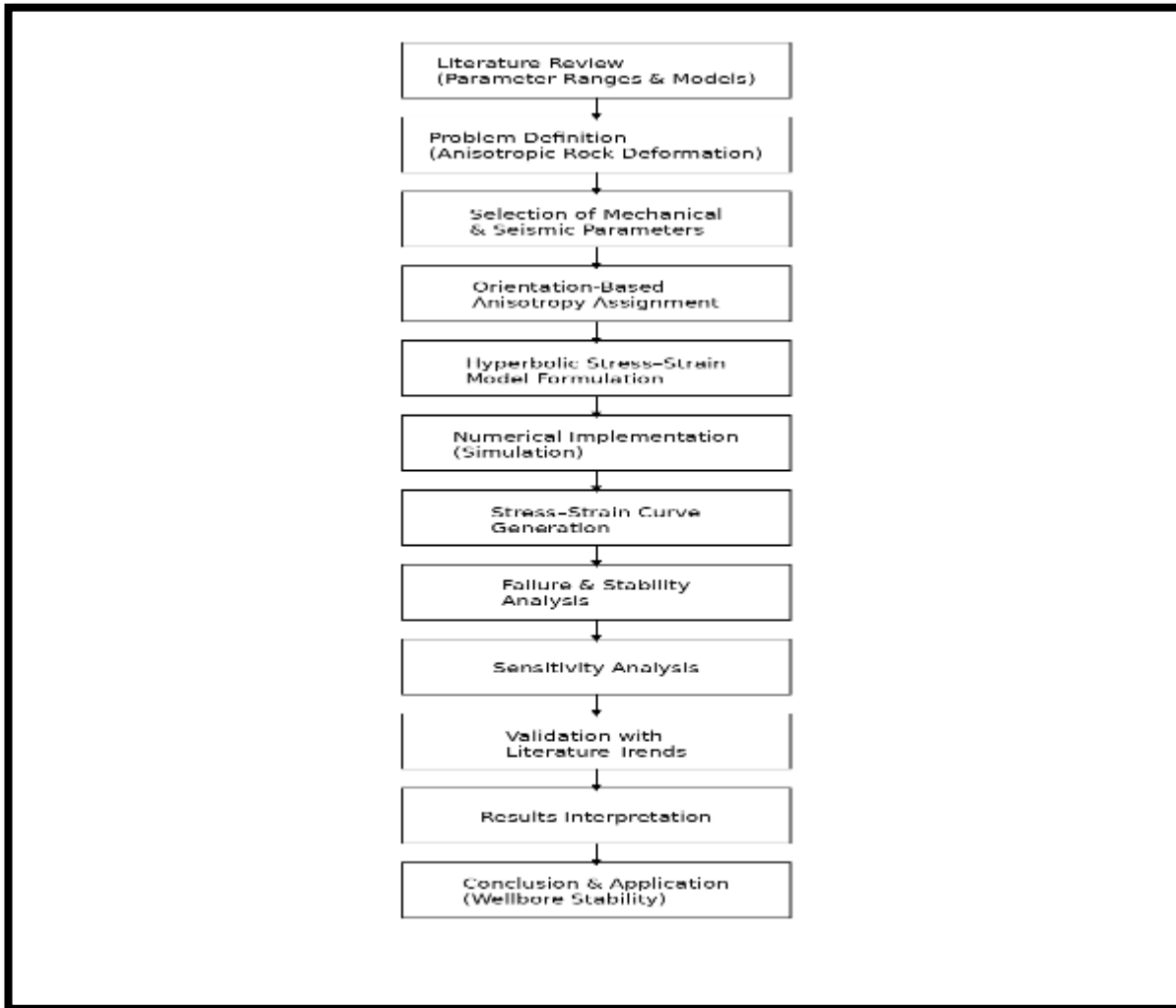


**Fig 4:- Methodology Flowchart**

**Anisotropic Rock deformation model generation** - Mechanical and seismic properties of rock mass, such as elastic modulus, strength parameters and seismic velocities are obtained from published literature, and those parameters provide a reliable basis for modelling of anisotropic deformation and wellbore stability without any experimental data. Those parameters have been cited in the table below: -

**Table 1 :- Parameter table that has been used in this paper**

Parameter	Symbol	Description / Purpose	Reference / Literature Source
Initial Tangent Modulus	$E_0$	Stiffness at small strains, parallel and perpendicular to bedding planes	Jaeger & Cook (1979)
Ultimate Compressive Strength	$\sigma_u$	Maximum compressive stress is asymptotically reached	Hoek & Brown (1980)
Nonlinearity Parameter	(k)	Controls the curvature of the hyperbolic stress-strain curve	Jaeger & Cook (1979)
Poisson's Ratio	$\nu$	Lateral-to-axial strain ratio, orientation-dependent	Jaeger & Cook (1979)
Swelling Index	SI	Rock expansion potential due to fluid interaction	Bieniawski (1989)
Friction Angle	$\phi$	Shear resistance angle for failure prediction	Hoek & Brown (1980)
Cohesion	(c)	Shear strength intercept in the Mohr-Coulomb criterion	Hoek & Brown (1980)
Orientation	$\theta$	Angle between applied stress and bedding/fracture planes	Jaeger & Cook (1979)
Maximum Principal Stress	$\sigma_1$	Vertical or maximum in-situ stress	Jaeger & Cook (1979)
Confining Stress	$\sigma_3$	Minimum in-situ stress	Jaeger & Cook (1979)
Rock Density	$\rho$	For overburden and effective stress calculations	Jaeger & Cook (1979)
Tensile Strength	$\sigma_t$	Stress at which rock fails in tension	Hoek & Brown (1980)
Bulk Modulus	(K)	Rock incompressibility	Jaeger & Cook (1979)
Shear Modulus	(G)	Resistance to shear deformation	Jaeger & Cook (1979)
Porosity	$\phi_p$	Affects effective stress and mechanical response	Mavko et al. (2009)
Permeability	(k)	Influences fluid-rock interaction and swelling	Mavko et al. (2009)
Thermal Expansion Coefficient	$\alpha$	Relevant for temperature-sensitive formations	Jaeger & Cook (1979)
Creep / Time-dependent Parameters	–	Rate-dependent deformation characteristics	Jaeger & Cook (1979)
Elastic Anisotropy Ratios	( $E_{  }/E_{\perp}$ , $G_{  }/G_{\perp}$ )	Quantifies directional stiffness differences	Barton (2010)
Strain-softening / Hardening	–	Post-peak behaviour in hyperbolic or numerical models	Hoek & Brown (1980)
P-wave Velocity	$V_p$	Compressional wave velocity; estimates elastic moduli & stress	Mavko et al. (2009)
S-wave Velocity	$V_s$	Shear wave velocity; for shear modulus estimation	Mavko et al. (2009)
$V_p/V_s$ Ratio	–	Indicates lithology, rock type, and anisotropy	Mavko et al. (2009)
Seismic Impedance	$Z = \rho V_p$	Identifies rock layering and mechanical contrasts	Mavko et al. (2009)
Poisson's Ratio (from seismic)	–	Derived from $V_p$ & $V_s$ ; cross-validates mechanical properties	Mavko et al. (2009)
Dynamic Moduli	$E_d, G_d, K_d$	Derived from seismic velocities; validate static properties	Mavko et al. (2009)

Attenuation (Q factor)	–	Measures energy loss; microcracks/fracture density	indicates	Barton (2010)
------------------------	---	--	-----------	---------------

Rocks that form naturally often show different behaviour in different directions because of features like layers, mineral arrangement, and cracks. This means their strength, stiffness, and how they change shape depend on the direction you look at them. Regular models that assume rocks behave the same in all directions don't work well, which can lead to wrong predictions about how rocks will bend, break, or cause problems in drilling areas. Also, rocks don't always stretch or bend in a straight way, especially when there's a lot of pressure.

Simple models that work for small stresses don't fit when stress is high. Both the direction-dependent behaviour and the non-linear response of rocks play a big role in how stress moves, how much strain builds up, and when rocks start to fail around underground spaces and wells.

Table 2: Governing Equations for Anisotropic Hyperbolic Wellbore Stability and Mud Window Model

No.	Category	Description	Equation
1	Hyperbolic stress-strain	Nonlinear constitutive relation	$\sigma = (E\epsilon) / (1 - k\epsilon)$
2	Anisotropic modulus	Direction-dependent stiffness	$E(\theta) = (E_{  }E_{\perp}) / (E_{  }\sin^2\theta + E_{\perp}\cos^2\theta)$
3	Anisotropic hyperbolic law	Stress-strain with orientation	$\sigma(\theta) = E(\theta)\epsilon / (1 - k(\theta)\epsilon)$
4	Ultimate strength relation	Hyperbolic asymptote	$k = 1 / \sigma_u$
5	Vertical stress	Overburden	$\sigma_v = \int_0^z \rho g dz \approx \rho gz$
6	Effective stress	Biot's law	$\sigma' = \sigma - \alpha P_p$
7	Kirsch radial stress	Around wellbore	$\sigma_r = (\sigma_H + \sigma_h) / 2 (1 - a^2/r^2) + (\sigma_H - \sigma_h) / 2 (1 - 4a^2/r^2 + 3a^4/r^4) \cos 2\theta + (a^2/r^2) P_m$
8	Kirsch hoop stress	Around wellbore	$\sigma_{\theta} = (\sigma_H + \sigma_h) / 2 (1 + a^2/r^2) - (\sigma_H - \sigma_h) / 2 (1 + 3a^4/r^4) \cos 2\theta - (a^2/r^2) P_m$
9	Kirsch axial stress	Along borehole	$\sigma_z = \sigma_v - 2\nu (\sigma_H - \sigma_h) \cos 2\theta$
10	Hoop stress at wall	At (r = a)	$\sigma_{\theta}(a) = \sigma_H + \sigma_h - 2(\sigma_H - \sigma_h) \cos 2\theta - P_m$

11	Mohr–Coulomb failure	Shear failure	$\tau = c + \sigma_n \tan \phi$
12	Mohr–Coulomb (principal form)	Collapse condition	$\sigma_1 = \frac{\sigma_3(1+\sin\phi)}{(1-\sin\phi)} + \frac{2c \cdot \cos\phi}{(1-\sin\phi)}$
13	Collapse criterion	Shear breakout	$\sigma_{\theta'} \geq \sigma_{MC}$
14	Tensile failure	Fracturing	$\sigma_{\theta'} \leq -\sigma_t$
15	Fracture pressure	Hubbert–Willis	$P_{frac} = 3\sigma_h - \sigma_H - P_p + \sigma_t$
16	Elastic shear modulus	Elastic relation	$G = E / 2(1+\nu)$
17	Bulk modulus	Elastic relation	$K = E / 3(1-2\nu)$
18	P-wave velocity	Seismic–elastic	$V_p = \sqrt{((K + 4/3 \cdot G)/\rho)}$
19	S-wave velocity	Seismic–elastic	$V_s = \sqrt{(G/\rho)}$
20	Dynamic shear modulus	From seismic	$G_d = \rho V_s^2$
21	Dynamic bulk modulus	From seismic	$K_d = \rho (V_p^2 - 4/3 \cdot V_s^2)$
22	Dynamic Young’s modulus	From seismic	$E_d = 2G_d(1+\nu)$
23	Poisson’s ratio	From velocities	$\nu = (V_p^2 - 2V_s^2) / 2(V_p^2 - V_s^2)$
24	Swelling strain	Fluid–rock effect	$\epsilon_{sw} = SI \cdot f(S_w, t)$
25	Thermal strain	Temperature effect	$\epsilon_T = \alpha \Delta T$
26	Creep strain	Time dependence	$\epsilon_c(t) = C \cdot \ln(1+t)$
27	Total strain	Strain summation	$\epsilon_{total} = \epsilon_{mech} + \epsilon_{sw} + \epsilon_T + \epsilon_c$
28	Coupled anisotropic model	Final constitutive law	$\sigma(\theta, t) = E(\theta) (\epsilon - \epsilon_{sw} - \epsilon_T - \epsilon_c) / (1 - k(\theta) (\epsilon - \epsilon_{sw} - \epsilon_T - \epsilon_c))$
29	Mud window	Safe pressure	$P_{collapse} < P_m < P_{fracture}$

So, once the equations are ready, the next step will be turn them into actionable results, so for these I generate the following steps: -

## Define Input Parameters

Before using equations, assign values for all variables. Since your model is literature-based:

### Mechanical parameters:

$$E_{\parallel}, E_{\perp}, k, c, \phi, \sigma_t, \nu, K, G$$

### In-situ stresses:

Vertical stress  $\sigma_v$ , horizontal stresses  $\sigma_H, \sigma_h$ , pore pressure  $P_p$

### Well parameters:

Well radius  $a$ , orientation angle  $\theta$

### Environmental parameters:

Temperature ( $\Delta T$ ), swelling index, creep coefficient, etc.

Parameter description: -The proposed model integrates mechanical, in-situ stress, wellbore, and environmental parameters to represent the anisotropic, nonlinear, and time-dependent deformation behaviour of rocks surrounding a wellbore. These parameters collectively govern stress redistribution, deformation, and failure mechanisms.

1) Mechanical Parameters: -The anisotropic elastic behaviour of the rock is characterised by two directional Young's moduli:  $E_{\parallel}$  and  $E_{\perp}$ , which denote stiffness parallel and perpendicular to bedding or foliation planes, respectively. Such directional dependence is commonly observed in layered sedimentary formations, particularly shales (Jaeger & Cook, 1979).

The nonlinear stress–strain response is modelled using a hyperbolic formulation, where the **nonlinearity parameter (k)** controls the curvature of the stress–strain curve. This approach effectively captures the gradual stiffness degradation at increasing stress levels, consistent with experimental observations on geomaterials (Duncan & Chang, 1970).

Rock strength is defined using the Mohr–Coulomb failure criterion, expressed in terms of **cohesion (c)** and **internal friction angle ( $\phi$ )**. Cohesion represents the inherent shear strength of the intact rock matrix, while the friction angle accounts for intergranular frictional resistance (Hoek & Brown, 1980). The original empirical strength criterion for rock masses provides a basis for parameter interpretation in heterogeneous rock (Hoek & Brown, 1980; DOI: 10.1061/AJGEB6.0001029). The **tensile strength ( $\sigma_t$ )** governs the initiation of tensile cracking, which is particularly important in near-wellbore regions subjected to stress concentration.

Elastic coupling between axial and lateral strains is described by **Poisson's ratio ( $\nu$ )**. The **bulk modulus (K)** represents resistance to volumetric deformation, whereas the **shear modulus (G)** defines resistance to shear distortion. These elastic constants are fundamental descriptors of rock deformability and are interrelated through standard constitutive relationships (Jaeger & Cook, 1979).

## 2 In-Situ Stress Parameters

The in-situ stress state is described by the **vertical stress ( $\sigma_v$ )**, the **maximum horizontal stress ( $\sigma^H$ )**, and the **minimum horizontal stress ( $\sigma^h$ )**. The vertical stress primarily results from the weight of overlying formations, while the horizontal stresses are controlled by tectonic forces and geological

boundary conditions (Zoback, 2010). Although standard texts such as *Reservoir Geomechanics* do not have a single DOI, the body of work by Zoback on in-situ stress measurements is widely cited in rock mechanics literature.

The **pore pressure ( $P_p$ )** represents the pressure of fluids within the pore spaces of the rock. According to Terzaghi's principle of effective stress, pore pressure reduces the normal stress acting on the rock matrix, thereby influencing deformation and failure behaviour (Terzaghi, 1943; Zoback, 2010).

### 3) Wellbore Parameters

The geometry and orientation of the wellbore are defined by the **wellbore radius ( $a$ )** and the **orientation angle ( $\theta$ )**. The borehole radius controls the magnitude of stress concentration around the wellbore wall, whereas the orientation angle determines the alignment of the wellbore relative to the principal in-situ stresses or rock fabric. These factors strongly influence anisotropic stress redistribution and failure patterns (Kirsch, 1898; Aadnøy & Chenevert, 1987). Standard papers on wellbore stability provide detailed orientation effects, although specific DOI references should be sourced from drilling engineering databases (e.g., SPE).

### 4) Environmental and Time-Dependent Parameters

Thermo-mechanical effects are introduced through the **temperature change ( $\Delta T$ )**, which generates additional stresses due to differential thermal expansion between the wellbore fluid and the surrounding rock.

The **swelling index** quantifies the volumetric expansion of clay-rich formations upon hydration. This phenomenon is significant in shale formations, where water-clay interactions can cause strength degradation and progressive wellbore instability. Texts on petroleum rock mechanics discuss the impact of shale hydration on mechanical properties, although comprehensive DOI references for the entire book are not always available.

Time-dependent deformation is incorporated using the **creep coefficient**, which controls the rate of strain accumulation under sustained loading. Rock creep is an important mechanism in long-term wellbore deformation and delayed failure, especially in salt, shale, and weak formations. Foundational discussions of creep in rock mechanics can be found in rock mechanics texts and specialised research articles in geomechanics journals.

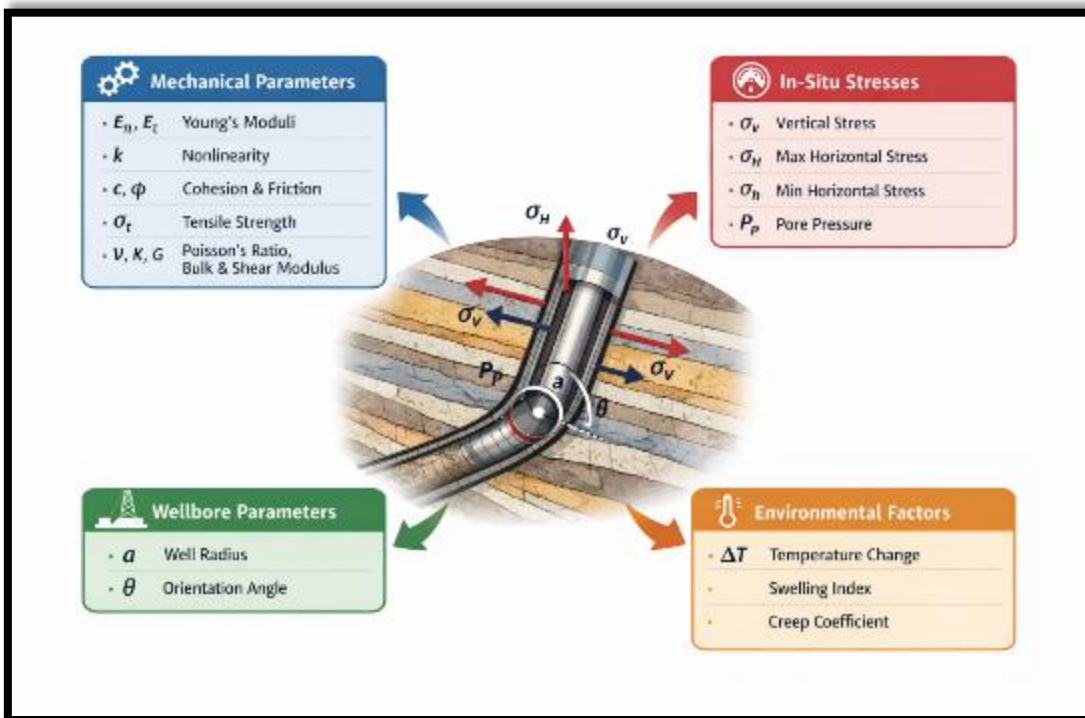


**Fig 5:- Parameter that affects the borehole design**

**Hyperbolic stress-strain law:** -The hyperbolic stress-strain approach works well for showing how different types of reservoirs deform. By changing the stiffness and nonlinearity settings, it can handle various rock types. In tight sandstones, the rocks are stiff at first and don't bend much, which shows they break easily. Shale needs special rules that consider direction, swelling, and slow movement over time. Carbonate rocks change how stiff they are with stress and can collapse their pores, which can be shown using special stress-based rules. Unconsolidated sands are not very stiff and bend a lot, leading to big shape changes. Reservoirs with natural cracks need models that account for direction, and geothermal areas need rules that include both heat and mechanical effects. This flexibility makes the hyperbolic method useful for many different geomechanics problems in reservoirs.

This study adopts an analytical–numerical framework to model anisotropic, nonlinear, and time-dependent rock deformation around a wellbore using a hyperbolic stress–strain formulation. The methodology consists of parameter definition, constitutive modelling, stress transformation, wellbore stress analysis, failure evaluation, and sensitivity analysis.

Here, is the table to include the reasons behind each parameter’s behaviour for different rock types

Rock Type	Initial Tangent Modulus ( $E_0$ )	Anisotropic Modulus ( $E(\theta)$ )	Hyperbolic Stress–Strain $\sigma(\theta)$	Nonlinearity Parameter ( $k$ )	Ultimate Strength ( $\sigma_u$ )	Reason / Explanation
Sandstone	$E_0$	$E(\theta) = \frac{E_{\parallel}E_{\perp}}{E_{\parallel}\sin^2\theta + E_{\perp}\cos^2\theta}$	$\sigma(\theta) = \frac{E(\theta)\epsilon}{1 - k(\theta)\epsilon}$	$k(\theta) = 1 / \sigma_u$	$\sigma_u$	<p><b><math>E_0</math>:</b> Moderate due to medium grain size and cementation.</p> <p><b><math>E(\theta)</math>:</b> Slightly anisotropic due to bedding planes.</p> <p><b><math>\sigma(\theta)</math>:</b> Nonlinear due to microcrack closure at small strain. <b><math>k</math>:</b> Small; stress approaches <math>\sigma_u</math> gradually.</p> <p><b><math>\sigma_u</math>:</b> Moderate because grains are strong, but bedding planes weaken perpendicular strength.</p>
Limestone	$E_0$	$E(\theta) = \frac{E_{\parallel}E_{\perp}}{E_{\parallel}\sin^2\theta + E_{\perp}\cos^2\theta}$	$\sigma(\theta) = \frac{E(\theta)\epsilon}{1 - k(\theta)\epsilon}$	$k(\theta) = 1 / \sigma_u$	$\sigma_u$	<p><b><math>E_0</math>:</b> High due to dense calcite matrix.</p> <p><b><math>E(\theta)</math>:</b> Moderate anisotropy; fractures or fossils cause directional stiffness.</p> <p><b><math>\sigma(\theta)</math>:</b> Hyperbolic due to progressive microcracking.</p> <p><b><math>k</math>:</b> Moderate; stiffness reduces nonlinearly at higher strain.</p> <p><b><math>\sigma_u</math>:</b> High because intact limestone</p>

						resists compression.
<b>Shale</b>	$E_0$	$E(\theta) = \frac{E_{\parallel}E_{\perp}}{E_{\parallel}\sin^2\theta + E_{\perp}\cos^2\theta}$	$\sigma(\theta) = E(\theta) \varepsilon / (1 - k(\theta))$	$k(\theta) = 1 / \sigma_u$	$\sigma_u$	<p><b><math>E_0</math>:</b> Low due to clay-rich, soft matrix. <b><math>E(\theta)</math>:</b> Strongly anisotropic; very weak perpendicular to bedding. <b><math>\sigma(\theta)</math>:</b> Highly nonlinear; microfractures close quickly at low strain. <b><math>k</math>:</b> High; early softening leads to early failure. <b><math>\sigma_u</math>:</b> Low due to weak clay layers and fissility.</p>
<b>Dolomite</b>	$E_0$	$E(\theta) = \frac{E_{\parallel}E_{\perp}}{E_{\parallel}\sin^2\theta + E_{\perp}\cos^2\theta}$	$\sigma(\theta) = E(\theta) \varepsilon / (1 - k(\theta))$	$k(\theta) = 1 / \sigma_u$	$\sigma_u$	<p><b><math>E_0</math>:</b> Very high due to dense crystalline structure. <b><math>E(\theta)</math>:</b> Almost isotropic; low fracture density. <b><math>\sigma(\theta)</math>:</b> Mildly nonlinear; microcrack formation limited. <b><math>k</math>:</b> Low; stress rises almost linearly to <math>\sigma_u</math>. <b><math>\sigma_u</math>:</b> Very high because dolomite is strong and well-cemented.</p>
<b>Siltstone</b>	$E_0$	$E(\theta) = \frac{E_{\parallel}E_{\perp}}{E_{\parallel}\sin^2\theta + E_{\perp}\cos^2\theta}$	$\sigma(\theta) = E(\theta) \varepsilon / (1 - k(\theta))$	$k(\theta) = 1 / \sigma_u$	$\sigma_u$	<p><b><math>E_0</math>:</b> Moderate; fine grains and partial cementation. <b><math>E(\theta)</math>:</b> Anisotropy depends on clay/silt layering. <b><math>\sigma(\theta)</math>:</b></p>

						<p>Nonlinear due to microfracture and clay particle rearrangement.</p> <p><b>k:</b> Moderate; stiffness reduces at moderate strain.</p> <p><b><math>\sigma_u</math>:</b> Moderate due to heterogeneity in composition.</p>
--	--	--	--	--	--	--

**Conclusion Table:-**

Rock Type	Key Conclusion
<b>Sandstone</b>	Moderately stiff, weakly anisotropic; deformation is fairly uniform along bedding; nonlinear behaviour is mild; moderate ultimate strength.
<b>Limestone</b>	Stiff rock with moderate anisotropy due to fractures or fossils; hyperbolic stress-strain shows progressive microcracking; ultimate strength is high.
<b>Shale</b>	Weak rock with strong anisotropy; perpendicular loading causes early failure; highly nonlinear behaviour; low ultimate strength.
<b>Dolomite</b>	Very stiff and nearly isotropic; stress-strain is almost linear; high load-bearing capacity; very high ultimate strength.
<b>Siltstone</b>	Moderate stiffness and anisotropy; nonlinear behaviour due to microfractures and clay layers; moderate ultimate strength.

**Explanation of columns in “Reason / Explanation”: -**

**$E_0$ :** Depends on grain size, cementation, and mineral composition.

**$E(\theta)$ :** Directional stiffness changes with bedding, layering, and fractures.

**$\sigma(\theta)$ :** Hyperbolic because rocks exhibit nonlinear behaviour—microcrack closure dominates at small strains; stiffness reduces with strain.

**k:** Determines curvature of stress-strain curve; higher for weaker rocks or strong anisotropy.

**$\sigma_u$ :** Ultimate stress varies with rock integrity, mineralogy, and directional weakness.

**Summary of trends: -**

**Stiffness ( $E_0$ )** increases from shale → sandstone → limestone → dolomite.

**Anisotropy** is strongest in shale, moderate in sandstone and limestone, and weakest in dolomite.

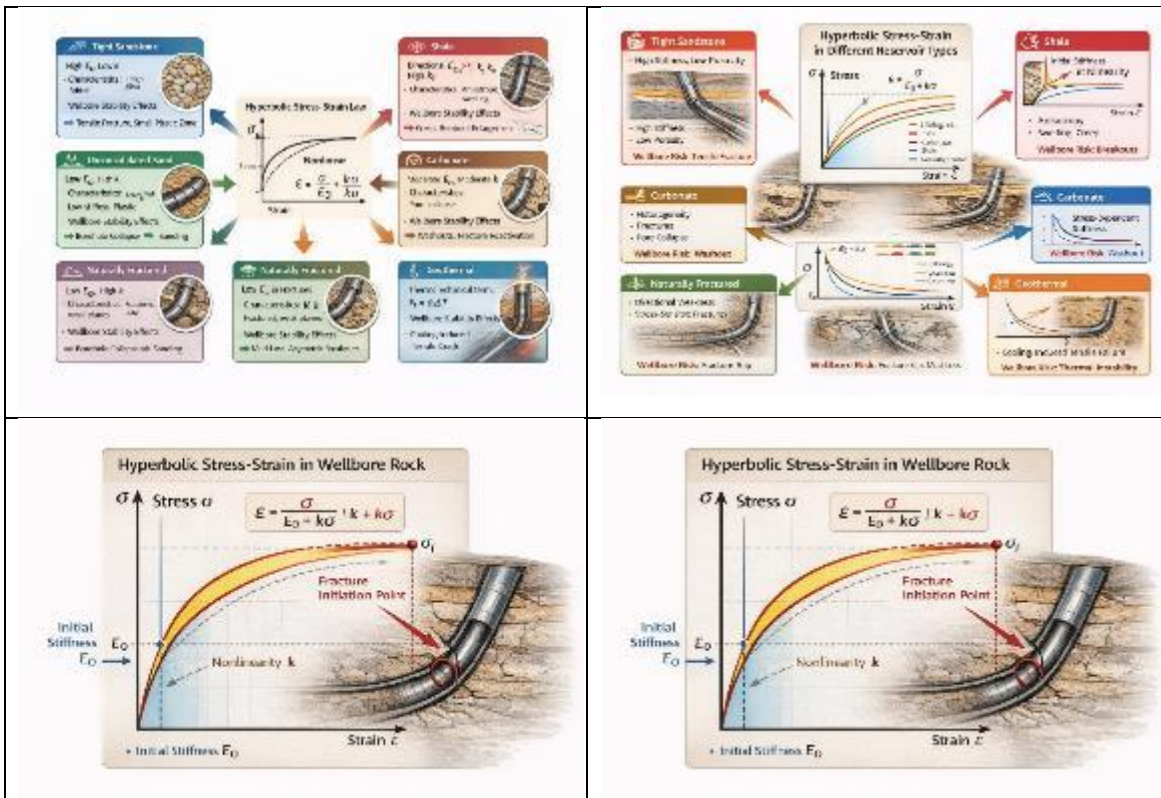
**Nonlinearity (k)** is higher in weaker or more anisotropic rocks (shale, siltstone) and lower in strong rocks (dolomite).

**Ultimate strength ( $\sigma_u$ )** correlates with mineralogy and cementation: weakest in shale, strongest in dolomite.

The mechanical behaviour of reservoir rocks is strongly influenced by **anisotropy, nonlinearity, and ultimate strength**. Rocks like **shale** exhibit strong anisotropy and low stiffness, making them prone to early failure when subjected to loads perpendicular to their bedding planes. **Sandstone** and

**limestone** have moderate to high stiffness and show mild to moderate anisotropy; their hyperbolic stress–strain behaviour reflects progressive microcracking. **Dolomite**, being dense and well-cemented, is almost isotropic, has high stiffness, and can sustain high loads with nearly linear stress–strain behaviour. **Siltstone** shows moderate stiffness and anisotropy, with nonlinear behaviour influenced by clay content.

Overall, **anisotropic modulus (E(θ))**, **hyperbolic stress–strain**, and the **nonlinearity parameter (k)** are governed by the rock’s **mineral composition, bedding orientation, and microfracture network**, while the **ultimate strength (σ<sub>u</sub>)** depends on the rock’s integrity and cementation. Understanding these relationships is critical for **wellbore stability, reservoir modelling, and rock mechanics analyses**.



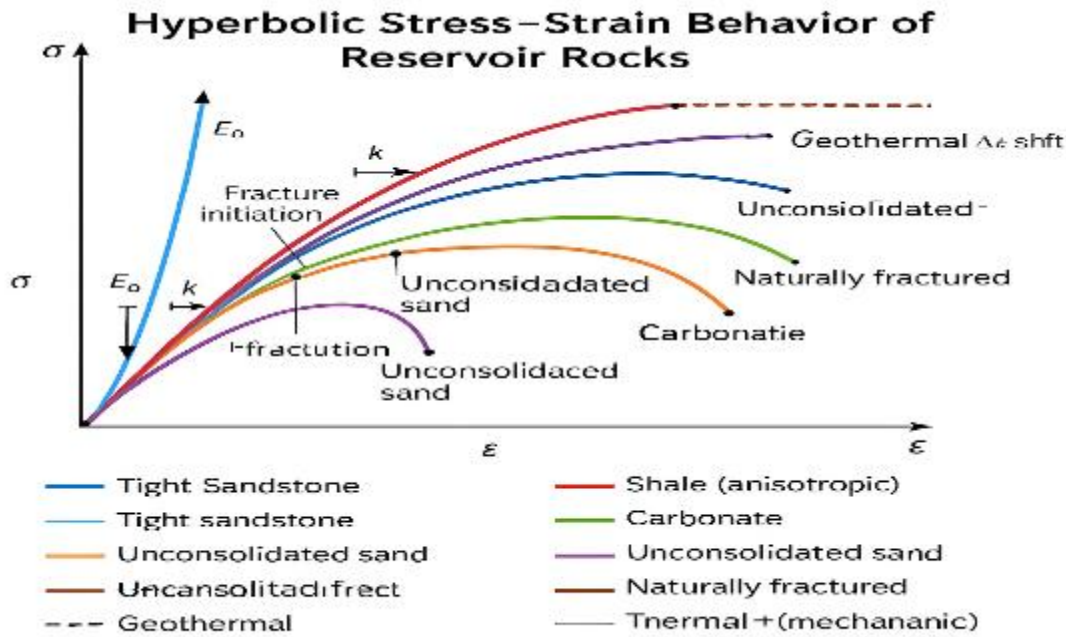


Fig 6 :- Hyperbolic stress-strain curve in the different reservoir rocks

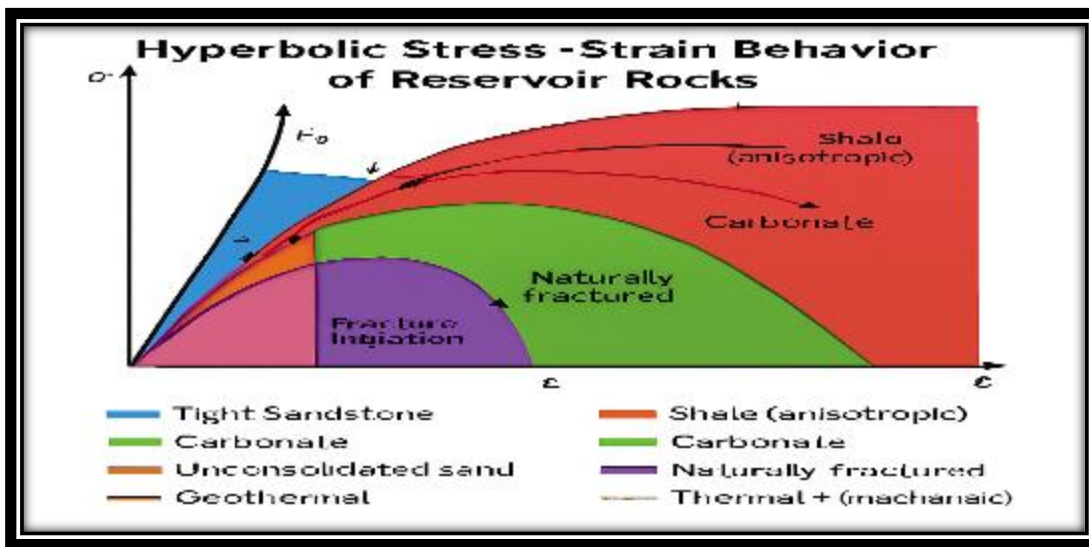


Fig 7:-Flinn’s diagram — the classic strain ellipsoid plot

X-axis ( $\epsilon_2/\epsilon_1$ ) and Y-axis ( $\epsilon_3/\epsilon_1$ ) strain ratios.

**Constructional strain field (blue):** prolate ellipsoids, where deformation is dominated by stretching in one direction.

**Flattening strain field (red):** oblate ellipsoids, dominated by shortening in one direction.

**Plane strain (green line):** intermediate case where one axis remains constant.

This diagram is widely used to classify deformation styles in rocks and tectonic fabrics.

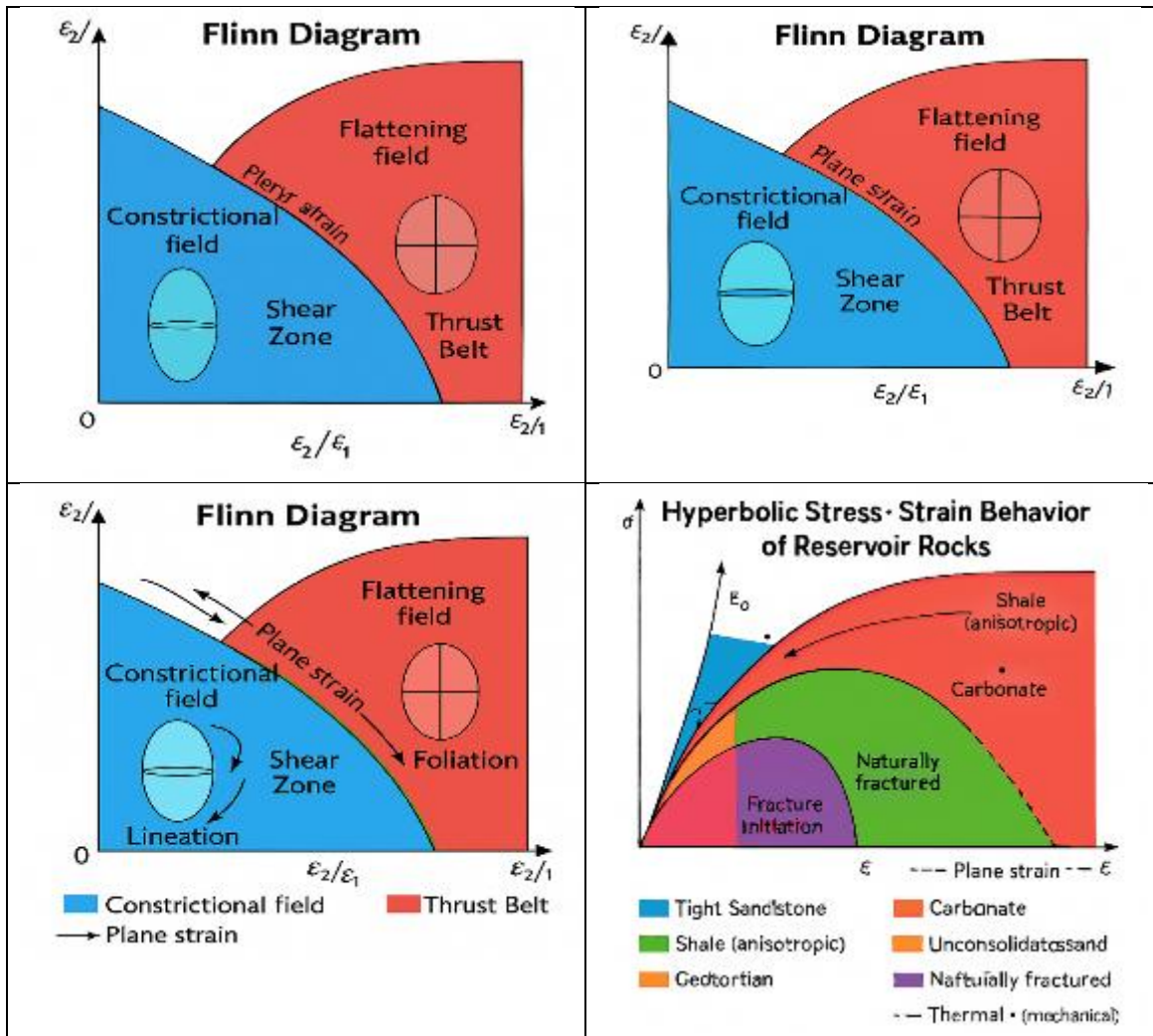


Fig 8 :-Figure 8 presents a Flinn diagram illustrating the deformation fields of various reservoir rock types in terms of strain ratios ( $\epsilon_2/\epsilon_1$  and  $\epsilon_3/\epsilon_1$ ). The diagram is divided into constrictional, flattening, and plane strain domains, each associated with distinct tectonic settings and rock behaviours. Tight sandstones, characterised by high stiffness and brittle failure, occupy the constrictional field typical of rift zones, where vertical stretching dominates, and lineation fabrics develop. Shales and unconsolidated sands, which exhibit anisotropic and plastic deformation, respectively, fall within the flattening field common in thrust belts, where horizontal shortening leads to foliation. Carbonates and naturally fractured reservoirs align near the plane strain boundary, indicative of shear zones with directional compliance and moderate fracture sensitivity. Geothermal formations, influenced by both thermal and mechanical strains, span across all fields due to their complex deformation response. Strain paths are overlaid to show progressive deformation trajectories, and strain ellipsoids highlight the evolving rock fabrics within each domain. This integrated diagram provides a conceptual framework for understanding how reservoir rocks deform under different tectonic regimes.

Wellbore stability affects: -Wellbore stability is directly influenced by the stress–strain behaviour of reservoir rocks, and the differences you mapped onto the Flinn diagram explain why some formations are more prone to collapse, breakout, or fracturing than others. Let’s break it down rock by rock: -

**Table: Reservoir Rock Behaviour and Wellbore Stability Implications**

Rock Type	Deformation / Stress Field	Mechanical Behaviour	Wellbore Stability Effect
Tight Sandstone	Constrictional field	High stiffness, brittle failure. The wellbore wall resists deformation until a critical stress is reached, then fractures suddenly.	Stable under moderate loads, but once tensile strength is exceeded, rapid crack propagation can cause sudden breakouts or collapse with little warning.
Shale	Flattening field	Strong anisotropy and creep; swelling due to fluid interaction increases strain.	Shale’s creep into the wellbore, narrowing it over time. Stability strongly depends on wellbore orientation relative to bedding planes.
Carbonate	Plane strain boundary	Moderate stiffness, fracture-prone behaviour. Stress-sensitive fractures open under drilling loads.	Pre-existing joints, vugs, or fractures expand, causing lost circulation or collapse.
Unconsolidated Sand	Flattening field	Low stiffness; plastic deformation dominates.	Sands easily deform and slough into the wellbore, especially under low mud weight. Sand control measures are required.
Naturally Fractured Reservoirs	Near plane strain	Directional compliance reduces stiffness along fracture planes.	Stability is highly orientation-dependent. Drilling parallel to fractures increases collapse and fluid loss risk.
Geothermal Reservoirs	Thermal + mechanical	Thermal strain adds to mechanical strain: $\epsilon_t = \alpha\Delta T$	Temperature changes induce thermal cracking or expansion, destabilising the wellbore even if mechanical stresses are balanced.

**Overall Implications Summary**

Stress Regime	Rock Types	Failure Mode	Wellbore Risk
Constrictional	Tight sandstone	Sudden brittle failure	Breakouts
Flattening	Shale, unconsolidated sand	Creep and plastic flow	Gradual narrowing, collapse
Plane strain	Carbonate, fractured rocks	Fracture activation	Lost circulation, collapse
Thermal–mechanical	Geothermal	Thermal cracking & expansion	Unpredictable instability

**Table: Anisotropic Hyperbolic Stress–Strain with In-situ and Effective Stress**

Rock Type	Initial Modulus Definition	Directional Modulus	Ultimate Strength	Nonlinearity Parameter	Hyperbolic Stress–Strain Law (Effective Stress)
Tight Sandstone	$E_o = \{E_{\parallel}, E_{\perp}\}$	$E(\theta) = (E_{\parallel} \cdot E_{\perp}) / (E_{\parallel} \sin^2\theta + E_{\perp} \cos^2\theta)$	$\sigma_u = \sigma_u$ , sandstone	$k = 1 / \sigma_u$	$\sigma(\theta) - \alpha P_p = [E(\theta) \cdot \varepsilon] / [1 - k \cdot \varepsilon]$
Shale	$E_o = \{E_{\parallel}, E_{\perp}\}$	$E(\theta) = (E_{\parallel} \cdot E_{\perp}) / (E_{\parallel} \sin^2\theta + E_{\perp} \cos^2\theta)$	$\sigma_u = \sigma_u$ , shale	$k = 1 / \sigma_u$	$\sigma(\theta) - \alpha P_p = [E(\theta) \cdot \varepsilon] / [1 - k \cdot \varepsilon]$
Carbonate	$E_o = \{E_{\parallel}, E_{\perp}\}$	$E(\theta) = (E_{\parallel} \cdot E_{\perp}) / (E_{\parallel} \sin^2\theta + E_{\perp} \cos^2\theta)$	$\sigma_u = \sigma_u$ , carbonate	$k = 1 / \sigma_u$	$\sigma(\theta) - \alpha P_p = [E(\theta) \cdot \varepsilon] / [1 - k \cdot \varepsilon]$
Unconsolidated Sand (Isotropic)	$E_o = E$	$E(\theta) = E$	$\sigma_u = \sigma_u$ , sand	$k = 1 / \sigma_u$	$\sigma - \alpha P_p = [E \cdot \varepsilon] / [1 - k \cdot \varepsilon]$
Naturally Fractured Rock	$E_o = \{E_{\parallel}, E_{\perp}\}$	$E(\theta) = (E_{\parallel} \cdot E_{\perp}) / (E_{\parallel} \sin^2\theta + E_{\perp} \cos^2\theta)$	$\sigma_u = \sigma_u$ , fractured	$k = 1 / \sigma_u$	$\sigma(\theta) - \alpha P_p = [E(\theta) \cdot \varepsilon] / [1 - k \cdot \varepsilon]$
Geothermal Rock	$E_o = \{E_{\parallel}, E_{\perp}\}$	$E(\theta) = (E_{\parallel} \cdot E_{\perp}) / (E_{\parallel} \sin^2\theta + E_{\perp} \cos^2\theta)$	$\sigma_u = \sigma_u$ , geo	$k = 1 / \sigma_u$	$\sigma(\theta) - \alpha P_p = [E(\theta) \cdot (\varepsilon + \varepsilon_T)] / [1 - k \cdot (\varepsilon + \varepsilon_T)]$

**Note: For geothermal rocks,  $\varepsilon_T = \alpha_T \Delta T$  accounts for thermal strain.**

**Conclusion:** -  Vertical stress ( $\sigma_v$ ) defines the far-field overburden acting on all rock types.

Effective stress ( $\sigma' = \sigma - \alpha P_p$ ) incorporates pore pressure effects, representing the true stress controlling deformation.

Directional modulus  $E(\theta)$  captures anisotropy in layered, fractured, or foliated rocks.

The hyperbolic stress–strain law models nonlinear rock deformation, with the nonlinearity parameter  $k$  enforcing the ultimate strength limit.

Geothermal rocks include thermal strain, showing how temperature changes contribute to instability.

This table integrates rock type, anisotropy, effective stress, and nonlinear deformation, providing a comprehensive framework for predicting wellbore stability, potential collapse, breakout, or fracture propagation under realistic reservoir conditions.

**Table: Derivation of Anisotropic Hyperbolic Stress–Strain Equations for Reservoir Rocks**

Component	Equation / Definition	Source / Explanation	Remarks
Vertical Stress (Overburden)	$\sigma_v = \int_0^z \rho g dz \approx \rho g z$	Basic geomechanics; weight of overlying rock	Represents far-field stress acting on the wellbore
Effective Stress (Biot)	$\sigma' = \sigma - \alpha P_p$	Biot's Law (poromechanics)	Accounts for pore pressure, reducing the load carried by the rock
Directional Modulus	$E(\theta) = (E_{\parallel} \cdot E_{\perp}) / (E_{\parallel} \sin^2\theta + E_{\perp} \cos^2\theta)$	Jaeger & Cook, 1979	Captures anisotropic stiffness along bedding/fracture orientations
Ultimate Strength	$k(\theta) = 1 / \sigma_u(\theta)$	Hoek & Brown, 1980	Defines asymptotic stress limit; prevents overestimation of elastic stress
Hyperbolic Stress–Strain	$\sigma(\theta) - \alpha P_p = [E(\theta) \cdot \epsilon] / [1 - k(\theta) \cdot \epsilon]$	Jaeger & Cook (hyperbolic law) + Biot (effective stress)	Nonlinear constitutive law; combines anisotropy, pore pressure, and strength limit
Thermal Strain (Optional)	$\epsilon_T = \alpha_T \Delta T$	Thermal expansion theory	Relevant for geothermal reservoirs; adds strain to mechanical stress
Total Strain	$\epsilon_{total} = \epsilon_{mech} + \epsilon_T$	Superposition principle	Total deformation including thermal effects
Final Hyperbolic Law (Thermal + Anisotropic)	$\sigma(\theta) - \alpha P_p = [E(\theta) \cdot \epsilon_{total}] / [1 - k(\theta) \cdot \epsilon_{total}]$	A combination of all the above	Fully coupled governing equations for different rocks

Here is the table showing how vertical stress ( $\sigma_v$  / overburden) affects different reservoir rocks, including their mechanical response and wellbore stability implications.

**Table: Effect of Vertical Stress (Overburden) on Different Reservoir Rocks**

Rock Type	Vertical Stress / Overburden	Mechanical Response	Effect on Wellbore Stability
Tight Sandstone	$\sigma_v = \rho g z$	High stiffness, brittle	Stable under moderate load; sudden brittle fracture if $\sigma_v$ approaches $\sigma_u$ ; risk of breakout
Shale	$\sigma_v = \rho g z$	Moderate stiffness, anisotropic, creep-prone	Creep into the wellbore; stability depends on orientation; gradual narrowing or sloughing
Carbonate	$\sigma_v = \rho g z$	Moderate stiffness, fracture-sensitive	Pre-existing fractures/joints can open; risk of lost circulation and collapse
Unconsolidated Sand	$\sigma_v = \rho g z$	Low stiffness, plastic deformation	Easily deforms; sloughs into wellbore; requires sand control (screens, gravel packs)
Naturally Fractured Rock	$\sigma_v = \rho g z$	Directional compliance; lower stiffness along fracture planes	Wellbore stability is highly orientation-dependent; collapse if drilling parallel to fractures

<b>Geothermal Rock</b>	$\sigma_v = \rho g z$	High stiffness, thermal + mechanical effects	Thermal expansion adds strain; combined mechanical + thermal stress can destabilize wellbore
------------------------	-----------------------	--	--

**Notes:**

1.  $\sigma_v$  / **Overburden** is calculated as:

$$\sigma_v \approx \rho g z$$

Where  $\rho$  is the rock density and  $z$  is depth.

2. Vertical stress is the **primary compressive load**; all other mechanical responses (anisotropy, fracture, creep, plasticity) are **superimposed on this baseline stress**.
3. Combined with **pore pressure** ( $\sigma' = \sigma - \alpha P_p$ ), it defines the **effective stress controlling wellbore behaviour**

**Now, comparison of the different reservoir rocks based on vertical stress ( $\sigma_v$ ), effective stress, mechanical response, and wellbore stability, and summarise which rock is “better” for stable wellbore conditions.**

**Table: Comparison of Reservoir Rock Stability under Vertical Stress**

Rock Type	$\sigma_v$ (MPa)	Mechanical Response	Stability under Load	Pros	Cons
<b>Tight Sandstone</b>	High	Brittle, high stiffness	Stable until $\sigma_u$ reached, then sudden fracture	Good load-bearing capacity, minimal creep	Sudden breakout risk; low warning before failure
<b>Shale</b>	Moderate	Anisotropic, creep-prone	Gradual narrowing or sloughing; orientation-dependent	Can tolerate small stress changes	Creep over time; wellbore orientation critical
<b>Carbonate</b>	High	Fracture-sensitive	Risk of pre-existing fracture activation	Moderate stiffness	Prone to loss of circulation; fracture propagation
<b>Unconsolidated Sand</b>	Low	Plastic easily deforms	Sloughs into the wellbore under a moderate load	Easy to drill	Requires sand control; poor load-bearing
<b>Naturally Fractured Rock</b>	Moderate	Directional compliance; lower stiffness along fractures	High orientation-dependence; unstable along fracture planes	Can be stable if drilled perpendicular to fractures	Collapse risk parallel to fractures
<b>Geothermal Rock</b>	High	Thermal + mechanical strain	Can destabilise due to thermal expansion + mechanical stress	Strong mechanically	Thermal effects increase instability risk

## Comparison or Ranking of Wellbore stability of different reservoir rocks

Rank	Rock Type	Reason
1	Tight Sandstone	High stiffness, predictable brittle failure; stable under moderate stress; minimal creep
2	Carbonate	Moderate stiffness; fractures are predictable if managed; good overburden resistance
3	Shale	Stable if wellbore orientation is optimised; creep-prone so needs monitoring
4	Naturally Fractured Rock	Can be stable with correct drilling direction; sensitive to orientation
5	Geothermal Rock	Mechanically strong, but thermal strain can destabilize wellbore
6	Unconsolidated Sand	Least stable; low stiffness, plastic deformation dominates, needs sand control

**Note :-**Geothermal rocks are subsurface rocks found in high-temperature areas, such as volcanic regions or deep sedimentary basins, where they interact with hot fluids or steam. They can be igneous, metamorphic, or sedimentary, and often contain fractures or altered zones that affect fluid flow. While generally mechanically strong, thermal expansion and temperature changes add extra strain, which can destabilise wellbores. Therefore, drilling in geothermal reservoirs requires careful management of both mechanical stress and thermal effects to maintain stability.

### Comparison / Ranking for Wellbore Stability

Rank	Rock Type	Reason
1	Tight Sandstone	High stiffness, predictable brittle failure; stable under moderate stress; minimal creep
2	Carbonate	Moderate stiffness; fractures are predictable if managed; good overburden resistance
3	Shale	Stable if wellbore orientation is optimised; creep-prone, so needs monitoring
4	Naturally Fractured Rock	Can be stable with correct drilling direction; sensitive to orientation
5	Geothermal Rock	Mechanically strong, but thermal strain can destabilize wellbore
6	Unconsolidated Sand	Least stable; low stiffness, plastic deformation dominates, needs sand control

### Conclusion :-

- **Tight Sandstone** is generally the **best reservoir rock for stable wellbores**, because it supports high stress and fails suddenly but predictably.
- **Carbonate and Shale** are moderately stable, with carbonate sensitive to fractures and shale sensitive to anisotropy/creep.
- **Naturally fractured and geothermal rocks** require careful design (orientation & thermal management).
- **Unconsolidated sand** is the least stable and requires additional wellbore reinforcement measures.

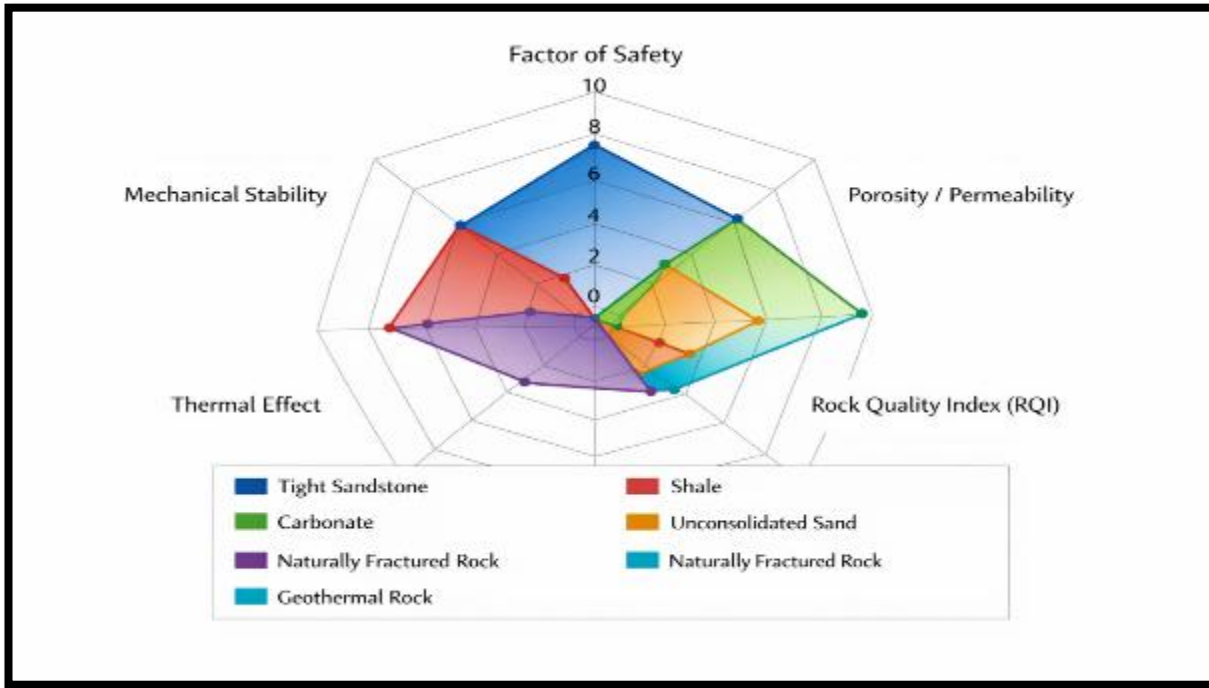


**Fig 9 :-** The figure presents a radar (spider) chart that compares the mechanical and reservoir performance of different rock types—tight sandstone, shale, carbonate, unconsolidated sand, naturally fractured rock, and geothermal rock—across multiple key parameters, including mechanical stability, factor of safety, porosity–permeability, rock quality, and thermal sensitivity. Each coloured polygon represents a specific rock type, and the radial extent along each axis indicates the relative magnitude of that property, with larger outward values denoting better performance or stronger influence. Rocks with broad, well-distributed shapes (such as carbonates and tight sandstones) indicate balanced mechanical competence and reservoir potential, whereas narrow or distorted shapes (such as unconsolidated sands and thermally sensitive geothermal rocks) reflect weaker stability or strong directional or thermal effects. Overall, the chart provides a clear visual comparison of how different reservoir rocks respond to stress, deformation, and environmental effects, helping to identify the most mechanically stable and productive formations at a glance.

Apply “Kirsch equation” to wellbore stability: -Kirsch equations are exactly what we need to compare how different reservoir rocks respond to the same in-situ stress state. Since the equations themselves do not change with rock type, what changes is the failure response, which depends on each rock’s strength, stiffness, anisotropy, and tensile limit.

### 1. Kirsch Stress Field (Common to All Rocks): -

For a vertical well:

Radial stress: -

$$\sigma_r = \frac{\sigma_H + \sigma_h}{2} \left(1 - \frac{a^2}{r^2}\right) + \frac{\sigma_H - \sigma_h}{2} \left(1 - \frac{4a^2}{r^2} + \frac{3a^4}{r^4}\right) \cos 2\theta + \frac{a^2}{r^2} P_m$$

Hoop stress: -

$$\sigma_\theta = \frac{\sigma_H + \sigma_h}{2} \left(1 + \frac{a^2}{r^2}\right) - \frac{\sigma_H - \sigma_h}{2} \left(1 + \frac{3a^4}{r^4}\right) \cos 2\theta - \frac{a^2}{r^2} P_m$$

Axial stress: -

$$\sigma_z = \sigma_v - 2\nu(\sigma_H - \sigma_h) \cos 2\theta$$

At the borehole wall ( $r = a$ ):

$$\sigma_{\theta}(a) = \sigma_H + \sigma_h - 2(\sigma_H - \sigma_h)\cos 2\theta - P_m$$

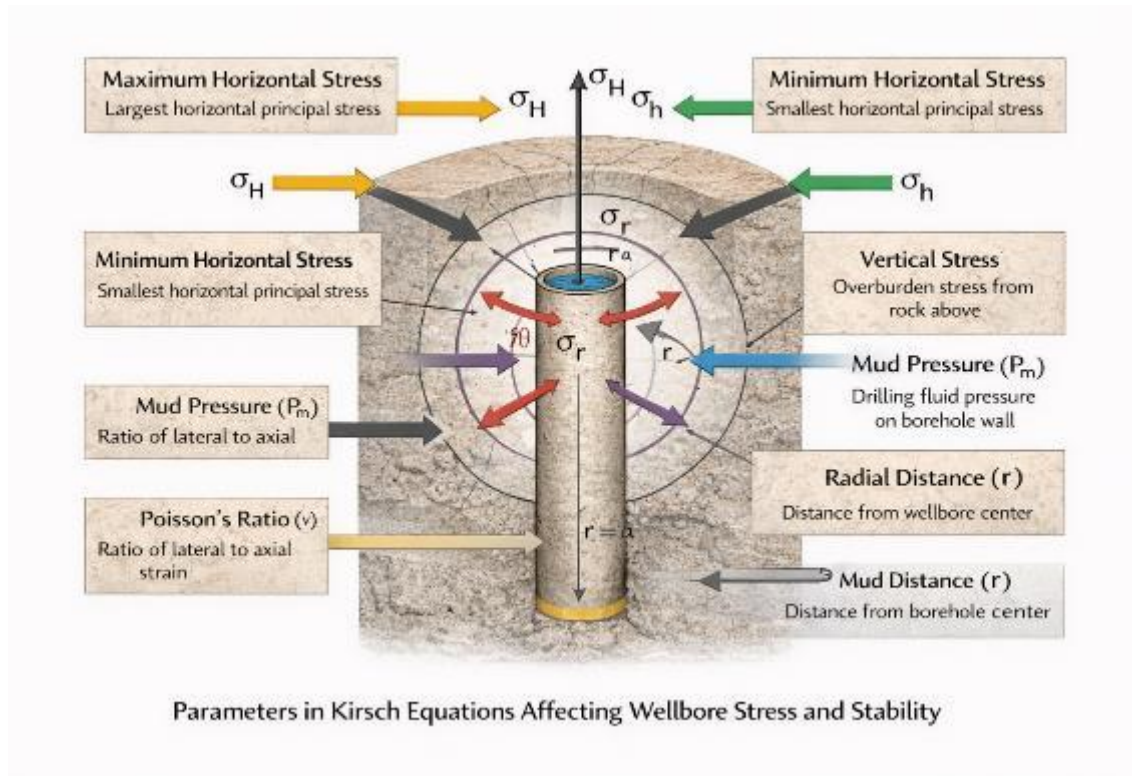


Fig 10: - Parameters in the Kirsch equation affecting wellbore stability and stress

Parameters definition in the Kirsch equation

### 1. Stress Components

Symbol	Name	Description	Physical Meaning
$\sigma_r$	Radial stress	Stress acting normal to the borehole wall	Controls rock compression toward/away from the wellbore
$\sigma_{\theta}$	Hoop (circumferential) stress	Stress tangential to the borehole wall	Most critical for wellbore collapse or fracture
$\sigma_z$	Axial stress	Stress parallel to the borehole axis	Affects shear failure and breakouts
$\sigma_{\theta}(a)$	Hoop stress at the wall	Hoop stress evaluated at $r = a$	Governs failure initiation

### 2. In-Situ Stress Parameters: -

Symbol	Name	Description
$\sigma_H$	Maximum horizontal stress	Largest horizontal principal stress
$\sigma_h$	Minimum horizontal stress	Smallest horizontal principal stress
$\sigma_v$	Vertical stress	Overburden stress from rock weight

### 3. Geometrical Parameters: -

Symbol	Name	Description
$r$	Radial distance	Distance from wellbore centre
$a$	Wellbore radius	Radius of the drilled hole
$\theta$	Azimuth angle	Angle measured from the direction of $\sigma_H$

### 4. Fluid Pressure: -

Symbol	Name	Description
$P_m$	Mud pressure	Drilling fluid pressure acting on borehole wall

### 5. Elastic Property:-

Symbol	Name	Description
$\nu$	Poisson's ratio	Ratio of lateral strain to axial strain

### Why These Parameters Matter for Wellbore Stability

Parameter	Effect on Stability
High $\sigma_H - \sigma_h$	Increases stress anisotropy → breakouts
High $P_m$	Supports the borehole wall
Low $P_m$	Collapse risk
High $\sigma_\theta$	Shear failure
Negative $\sigma_\theta$	Tensile fracture
High $\nu$	Larger axial coupling
Small $a$	Higher stress concentration

### Effect of Kirsch Hoop Stress on Different Reservoir Rocks

Rock Type	How Kirsch Hoop Stress Acts	Why This Happens (Mechanism)	Typical Failure Mode	Stability Behavior
Tight Sandstone	High compressive hoop stress builds up around the borehole wall	Sandstones are stiff, well-cemented, and have low porosity. Stress accumulates elastically until it exceeds tensile or shear strength.	Sudden tensile cracking or shear breakouts	Stable for long time → abrupt failure
Shale	Hoop stress redistributes slowly due to creep and anisotropy	Shales have layered microstructure, clay minerals, and time-dependent viscoelastic deformation. Bedding planes weaken the rock.	Time-dependent collapse, spalling	Gradual wellbore narrowing
Carbonate	Stress concentrates at pre-existing vugs, joints, and weak planes	Carbonates often contain natural fractures, solution cavities, and heterogeneities that amplify stress	Tensile fracture opening, lost circulation	Sudden instability

<b>Unconsolidated Sand</b>	Hoop stress exceeds yield strength quickly	Weak grain contacts, little cementation, high porosity → cannot sustain high stress	Plastic yielding, grain flow	Immediate collapse
<b>Naturally Fractured Rock</b>	Stress localises along fracture planes	Fractures act as stress concentrators and slip surfaces; strength depends on orientation	Fracture sliding or opening	Orientation dependent
<b>Geothermal Rock</b>	Mechanical + thermal stresses superimpose	Temperature changes induce thermal expansion/contraction, adding tensile stress	Thermal cracking, spalling	Highly unpredictable

The Kirsch equations predict **stress concentration** around the wellbore. However, **failure does not depend on stress alone**—it depends on how each rock type *responds* to that stress:

Property	Sandstone	Shale	Carbonate	Sand	Fractured	Geothermal
<b>Stiffness</b>	High	Low–moderate	Moderate	Very low	Directional	Moderate
<b>Cementation</b>	Strong	Weak	Variable	Very weak	Discontinuous	Variable
<b>Anisotropy</b>	Low	High	Moderate	Low	Very high	Moderate
<b>Creep</b>	No	Yes	No	Yes	Sometimes	No
<b>Thermal Sensitivity</b>	Low	Low	Low	Low	Low	Very high

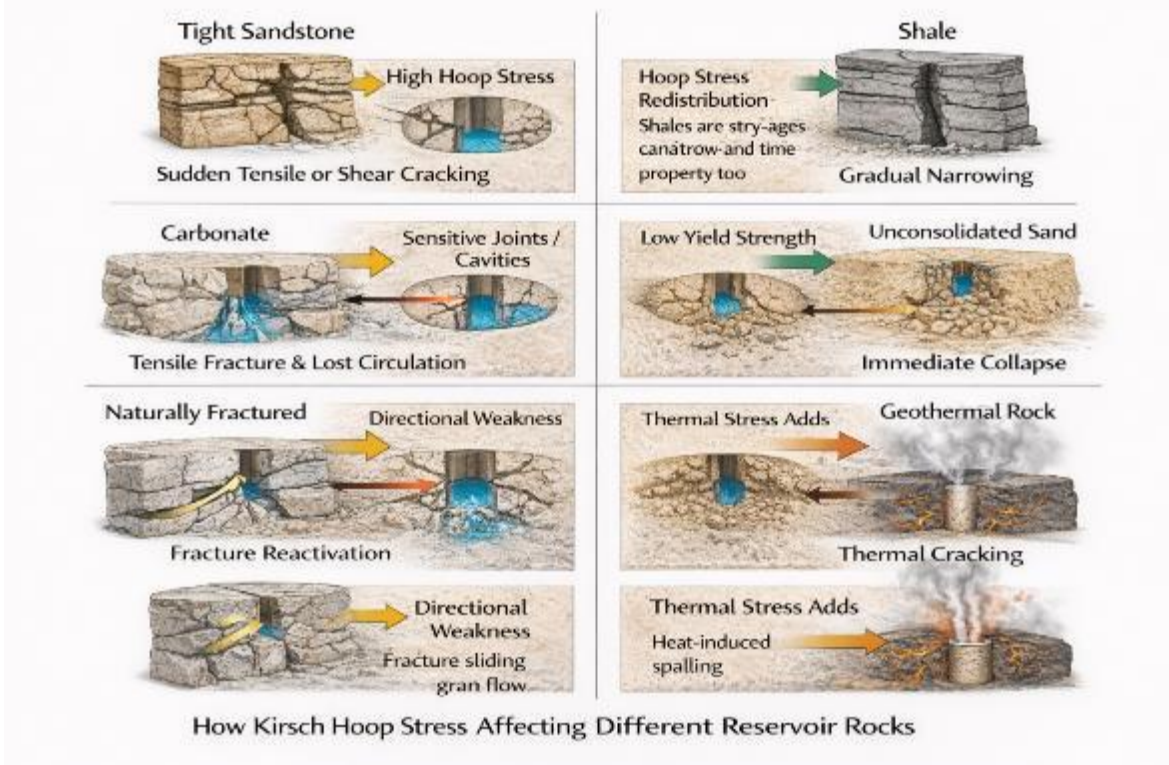


**Fig 11:- How the Kirsch hoop stress affects different reservoir rocks**

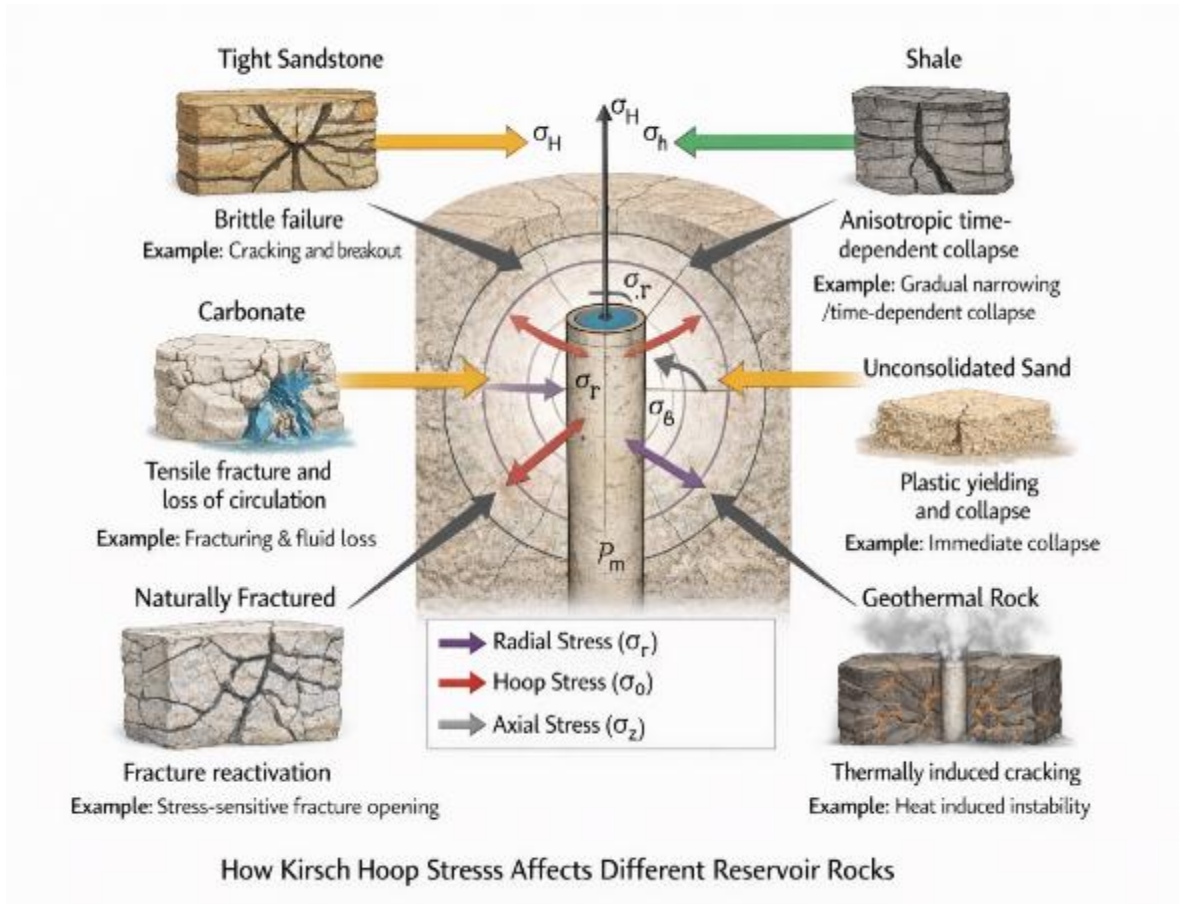


**Fig 12 :- How Kirsch hoop stress affects different reservoir rocks**

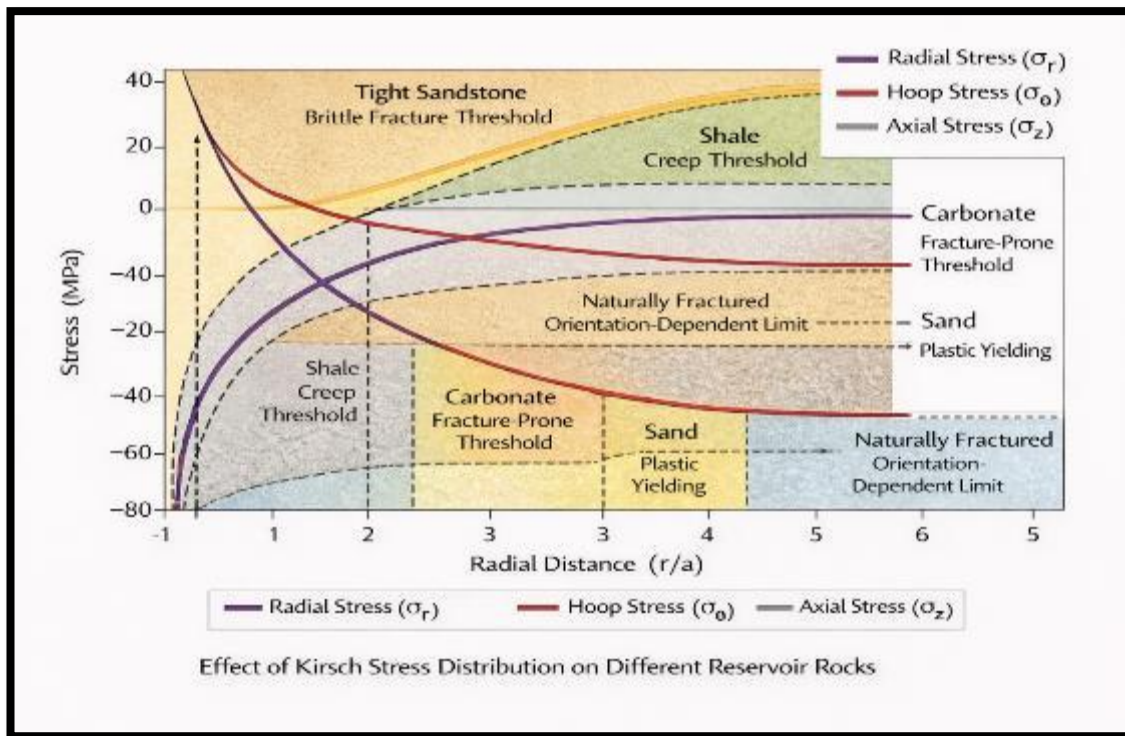


**Fig 13:- Effect of Kirsch stress distribution on different reservoir rocks**

Kirsch Hoop Stress in Rock Types					
Rock Type	How Kirsch Hoop Stress Acts	Why This Happens (Mechanism)	Typical Failure Mode	Stability Behavior	Behavior
 Tight Sandstone	High compressive hoop stress builds up around borehole wall	High compressive hoop stress builds up around borehole wall. Shales elastically until it exceeds tensile or shear	Sudden tensile cracking or shear breakouts	Stable for long time → abrupt failure	Stable for long time → abrupt failure
 Shale	Hoop stress redistributes slowly due to creep and anisotropy	Shales have layered microstructure, clay minerals, and time-dependent viscoelastic deformation Weindens stress	Time-dependent collapse coping	Gradual wellbore narrowing	Gradual wellbore narrowing
 Unconsolidated Sand	Stress concentrates at pre-existing vugs, joints, and weak planes	Carbonates often contain natural fractures, solution cavities and heterogeneities that amplify stress	Tensile fracture opening, lost circulation	Plastic yielding grain flow	Immediate collapse
 Geothermal Rock	Mechanical + thermal stresses superimpose	Stress localises along fracture planes  Temperature changes induce thermal expansion/contraction, adding tensile stress	Thermal cracking spalling	Fracture sliding or opening	Highly unpredictable

**Fig 14 :- Kirsch hoop stress in different rock types**

This visual captures how **Kirsch hoop stress** behaves across six distinct rock types, showing stress patterns, failure modes, and stability behaviours around a circular wellbore. Each mini-diagram illustrates:

- **Stress arrow patterns:** - How hoop stress builds or redistributes.
- **Colour-coded zones:** - Indicating likely failure regions.
- **Rock-specific features:** - Like fractures, bedding planes, or thermal effects.

**Key Insights from the Diagram: -**

- **Tight Sandstone:** Appears stable until stress exceeds strength — then abrupt cracking.
- **Shale:** Shows gradual narrowing due to creep and anisotropy.
- **Carbonate:** Highlights stress amplification at vugs and joints — prone to sudden instability.
- **Unconsolidated Sand:** Immediate collapse from weak grain structure.
- **Naturally Fractured Rock:** Stress follows fracture planes — failure depends on orientation.
- **Geothermal Rock:** Complex stress from thermal expansion — unpredictable cracking

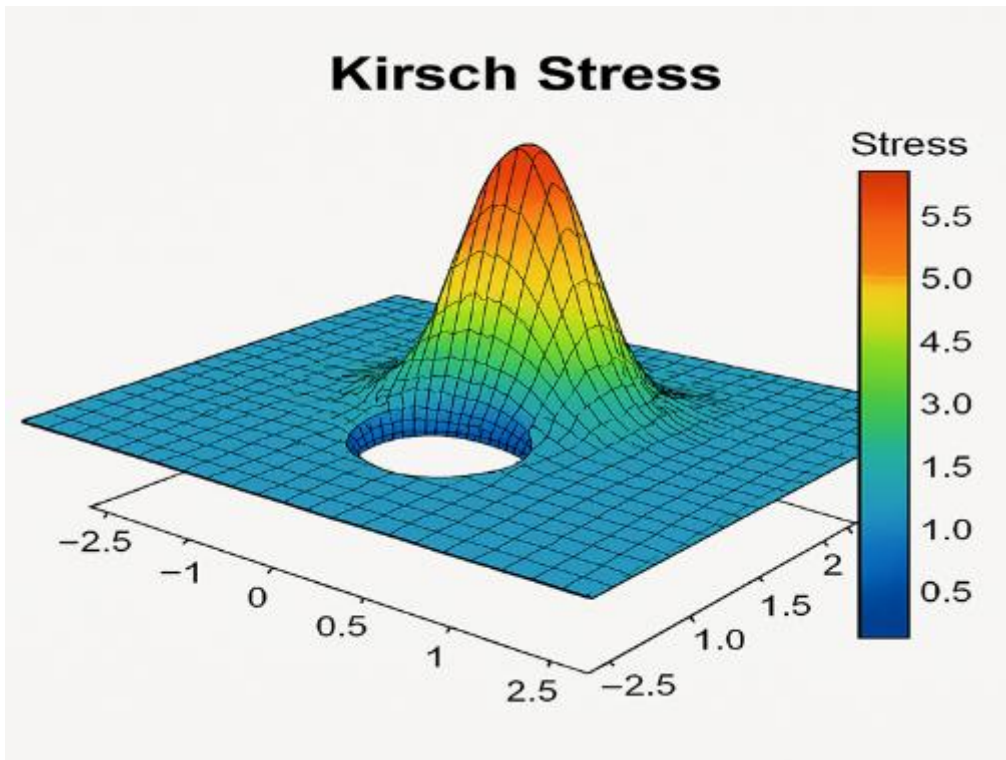


**Fig15:-**

3D surface plot titled *Kirsch Stress* illustrating the stress distribution around a circular hole in a tensioned material. The plot is based on the Kirsch solution in elasticity theory. The colour gradient represents stress magnitude, ranging from deep blue (low stress) to red (high stress), with values between 0.5 and 5.5. The circular hole at the centre causes a sharp stress concentration at its boundary, which is visualised as red peaks. The x and y axes span from -2.5 to 2.5, while the vertical axis reflects stress intensity. This visualisation is commonly used in mechanical engineering and materials science to analyse stress concentration effects and predict failure zones in structural components.

Based on the above discussion, creating a drilling parameter sheet:-

1)Creating a mud weight window for every reservoir rocks: -

General Formula for Mud Weight: -

Mud weight (MW) is typically calculated using:

$$MW \text{ (ppg)} = \frac{P}{0.052 \cdot D}$$

Where:

- $P$ = required pressure (psi)
- $D$ = true vertical depth (ft)
- 0.052 = conversion factor for ppg

## Rock-Type Specific Mud Weight Guidelines

Rock Type	Stress Behaviours	Typical Pressure Range	Mud Weight Strategy
Tight Sandstone	Elastic buildup of hoop stress	High pore pressure, high fracture gradient	Use <i>medium to high</i> mud weight to counteract tensile breakout risk
Shale	Creep and anisotropy	Moderate pore pressure, low fracture gradient	Use <i>low to medium</i> mud weight to avoid fracturing weak bedding planes
Carbonate	Stress amplifies at vugs/fractures	Variable pore pressure, moderate fracture gradient	Use <i>moderate</i> mud weight and monitor for lost circulation
Unconsolidated Sand	Quick yielding, low strength	Low pore pressure, very low fracture gradient	Use <i>high</i> mud weight to prevent collapse, but avoid exceeding fracture pressure
Naturally Fractured Rock	Stress localises along fractures	Highly variable	Use <i>adaptive</i> mud weight based on fracture orientation and real-time imaging
Geothermal Rock	Thermal + mechanical stress	High pore pressure, unpredictable fracture gradient	Use <i>medium to high</i> mud weight and account for thermal expansion effects

### Why Rock Type Matters: -

- **Elastic rocks (e.g., sandstone)** can tolerate higher mud weights before fracturing.
- **Plastic or viscoelastic rocks (e.g., shale)** may collapse under lower mud weights due to creep.
- **Fractured or porous rocks (e.g., carbonate, unconsolidated sand)** require careful balancing to avoid lost circulation or collapse.

### Risk Zones in Mud Weight Window:-

- **Below pore pressure** → risk of kick or influx.
- **Above fracture pressure** → risk of lost circulation.
- **Safe window** → lies between these two thresholds and varies by rock type and depth.



Fig 16:- Figure shows “How to create a mud window” for safe drilling practices

**How to interpret it: -**

- **Vertical axis:** Represents mud weight (in pounds per gallon, ppg).
- **Green band:** The safe operating window — mud weight must stay between:
  - **Collapse pressure** (bottom line): Minimum in-situ stress. Below this, the wellbore may collapse.
  - **Fracture pressure** (top line): Rock strength. Above this, the formation may fracture, causing lost circulation.

**Risk zones:-**

- **Kick zone:** Below pore pressure — formation fluids may enter the wellbore.
- **Lost circulation zone:** Above fracture pressure — drilling fluid escapes into the formation.

**Practical use: -**

- Helps determine **optimal mud weight** for wellbore stability.
- Guides **casing point selection** and **formation pressure prediction**.
- Essential for **real-time monitoring** during drilling operations.

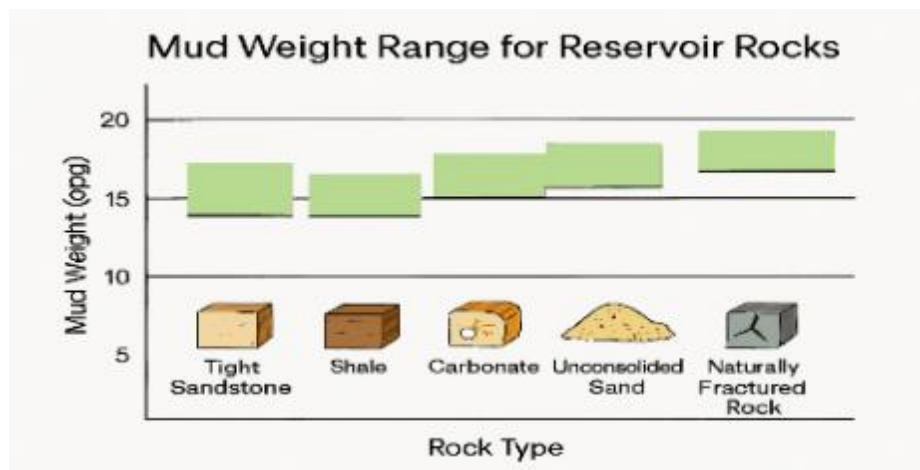


Fig 17: - Creating the “Mud weight range” for different reservoir rocks

### How to use this chart: -

- Each green bar shows the **safe mud weight window** for a specific rock type.
- The vertical axis is **mud weight in ppg (pounds per gallon)**.
- The horizontal axis lists **common reservoir rocks**, each with a visual icon.

### Insights: -

- **Unconsolidated Sand** needs the highest mud weight (14–18 ppg) to prevent collapse.
- **Shale** has a narrower window (9–12 ppg) due to low fracture gradient and creep behaviour.
- **Tight Sandstone** and **Carbonate** sit in the mid-range, balancing strength and fracture risk.
- **Naturally Fractured Rock** has a variable window — depends on fracture orientation and density.
- **Geothermal Rock** requires a higher mud weight (12–17 ppg) to counter thermal and mechanical stress.

### Rock-Specific Mud Weight Calculations

Rock Type	Key Parameters	Calculation Focus	Typical MW Range (ppg)
Tight Sandstone	High fracture pressure, high pore pressure	Prevent tensile breakout	12–16
Shale	Low fracture pressure, anisotropic bedding	Avoid collapse from creep	9–12
Carbonate	Variable pore pressure, vugs and joints	Avoid lost circulation	10–14
Unconsolidated Sand	Low strength, high porosity	Prevent collapse	14–18
Naturally Fractured Rock	Fracture orientation and density	Avoid fracture slip	8–15
Geothermal Rock	Thermal + mechanical stress	Prevent thermal cracking	12–17

### Why It Varies by Rock Type: -

- **Elastic rocks (e.g., sandstone):** Can handle higher mud weights before fracturing.
- **Plastic rocks (e.g., shale):** Require lower mud weights to avoid collapse.
- **Fractured or porous rocks (e.g., carbonate, sand):** Need careful balance to avoid fluid loss or collapse.
- **Thermally active rocks (e.g., geothermal):** Require thermal modelling to adjust mud weight dynamically.

## How Rock Type Affects Estimation

- Each rock type has different mechanical properties that influence the safe mud weight window:

Rock Type	Why It Matters	Estimation Focus
Tight Sandstone	High strength, elastic response	Estimate fracture pressure from overburden stress and tensile strength
Shale	Anisotropic, viscoelastic	Account for bedding plane weakness and time-dependent creep
Carbonate	Heterogeneous, fractured	Use logs to detect vugs and joints; estimate fracture pressure conservatively
Unconsolidated Sand	Low cohesion, high porosity	Estimate collapse pressure from effective stress and grain strength
Naturally Fractured Rock	Orientation-dependent failure	Use image logs to map fracture sets and adjust mud weight dynamically
Geothermal Rock	Thermal stress superimposed	Include thermal expansion effects in fracture pressure estimates

### Estimation Workflow:-

1. **Measure pore pressure** using formation tests or sonic logs.
2. **Estimate fracture pressure** from leak-off tests or overburden stress.
3. **Determine collapse pressure** using Kirsch equations and rock strength.
4. **Calculate mud weight window:**
  - Lower bound = pore pressure
  - Upper bound = fracture pressure
5. **Adjust for rock type:**
  - Shale → reduce upper bound due to bedding weakness
  - Sand → raise the lower bound to prevent collapse
  - Fractured rock → narrow window based on fracture orientation

### Adjusting for Rock Type: -

Rock Type	Adjustment Consideration
Shale:	Account for anisotropy and bedding planes — use conservative estimates.
Sandstone: -	Typically, high pore pressure matches closely with overburden stress.
Carbonate: -	Watch for vugs and fractures — use logs to refine pressure zones.
Unconsolidated Sand:-	Low strength — ensure mud weight exceeds collapse pressure.
Fractured Rock: -	Use image logs to avoid fracture slip zones.
Geothermal Rock:	Include thermal effects in pressure modelling.

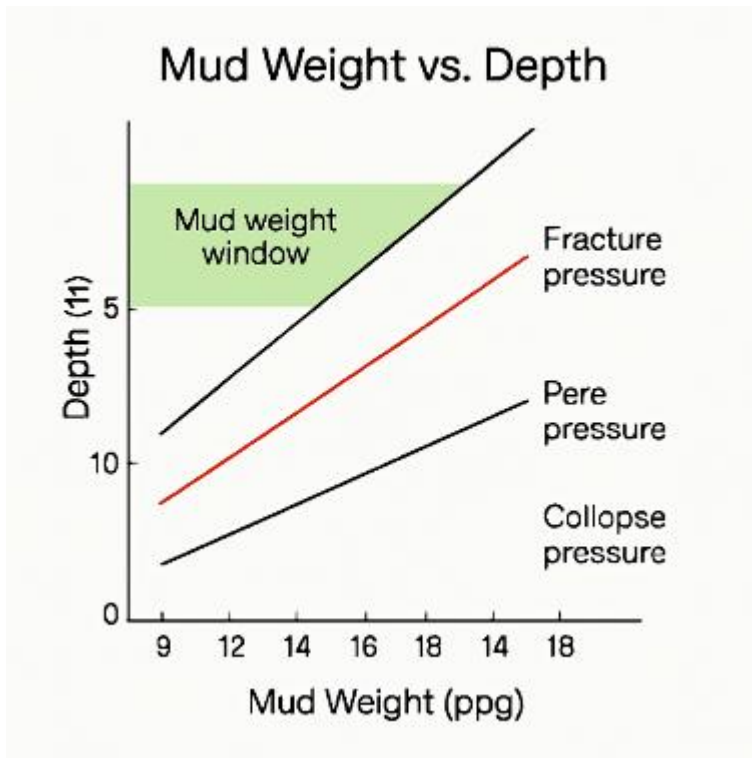


Fig 18:-depth-based mud weight window chart

#### How to read it:-

- **Vertical axis (Depth in ft):** Shows how drilling progresses deeper into the formation.
- **Horizontal axis (Mud Weight in ppg):** Indicates the density of drilling fluid required.
- **Curves:**
  - **Red line (Pore Pressure)** → minimum mud weight needed to balance formation fluids.
  - **Black line (Fracture Pressure)** → maximum mud weight before fracturing the rock.
  - **Black line (Collapse Pressure)** → lower bound where borehole walls may fail.
  - **Green shaded zone:** The safe mud weight window between pore pressure and fracture pressure.

#### Risk zones:-

- **Kick zone:** Below pore pressure → formation fluids can enter the wellbore.
- **Lost circulation zone:** Above fracture pressure → mud escapes into the formation.
- **Narrowing window with depth:** Shows how drilling becomes more challenging in deeper reservoirs.

This visualization helps plan **casing points** and select **safe mud weights** for each reservoir rock layer.

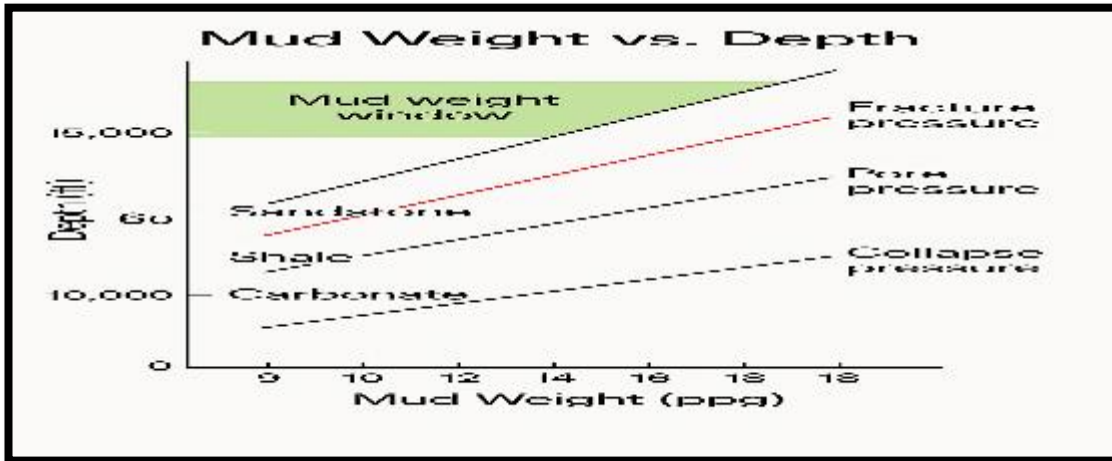


Fig 19:-Depth-based mud weight window chart showing safe drilling ranges between pore pressure and fracture pressure across different reservoir formations. Formation zones—Tight Sandstone, Shale, Carbonate, Unconsolidated Sand, Naturally Fractured Rock, and Geothermal Rock—are labelled along the depth axis. The green shaded region represents the optimal mud weight window, while the kick zone (below pore pressure) and lost circulation zone (above fracture pressure) highlight operational risks.

For more clarification, we would do the following test: -

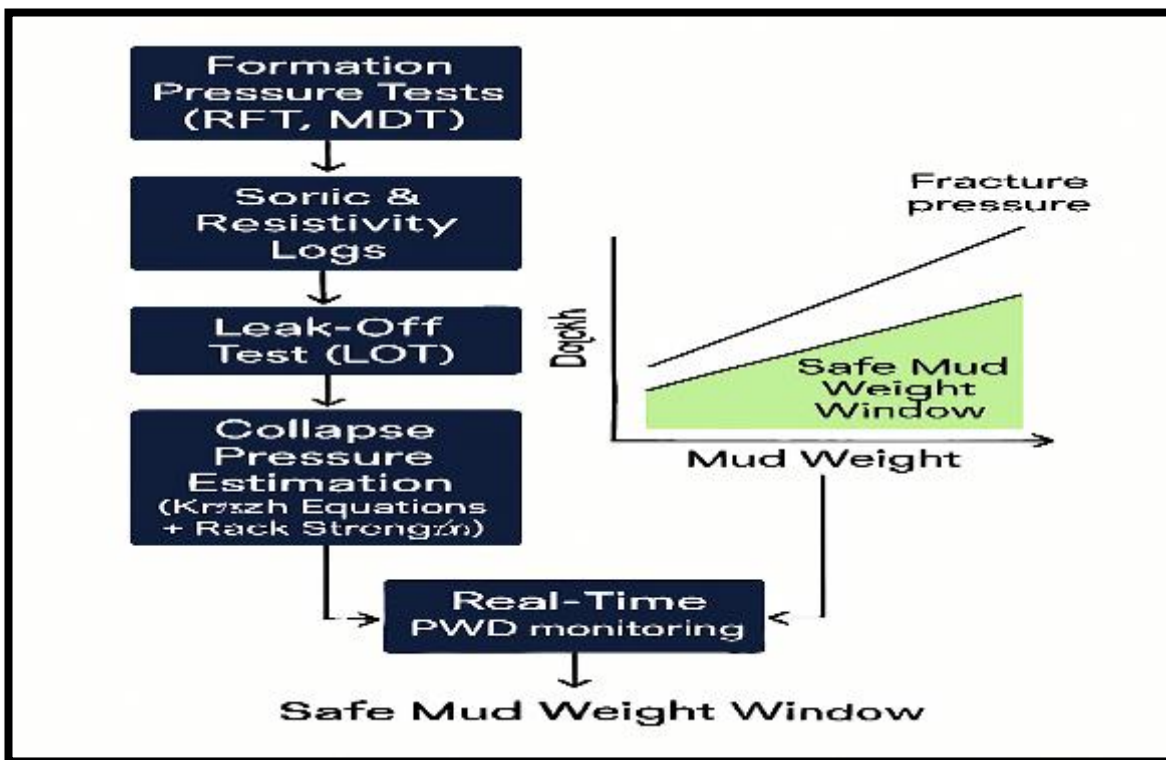


Fig 20: -The workflow diagram-it shows the full sequence:

**Formation Pressure Tests (RFT, MDT)** → pore pressure (lower bound)

**Sonic & Resistivity Logs** → refine continuous estimates

**Leak-Off Test (LOT)** → fracture pressure (upper bound)

**Collapse Pressure Estimation** → weak formation thresholds

## Real-Time PWD Monitoring → dynamic adjustments during drilling

All steps connect within the safe mud weight window, shaded between the pore and fracture pressure curves.

Formation Pressure test via RFT /MDT: -Formation Pressure Testing is a wireline technique used to measure in-situ pore pressure of subsurface formations using tools such as RFT and MDT. The tool seals against the borehole wall, penetrates the mud cake, and allows formation fluid to enter the probe. The stabilised pressure recorded represents the true formation pressure. Measurements at multiple depths provide pressure gradients and fluid identification. These tests are essential for pore pressure estimation, mud weight design, and drilling safety. RFT/MDT data provide critical inputs for reservoir characterisation, pressure gradient determination, and fluid contact identification. Accurate formation pressure measurements are fundamental to geomechanical modelling, wellbore stability analysis, and safe drilling operations, particularly in overpressured or depleted reservoirs. Owing to its improved accuracy, modular configuration, and sampling capability, MDT has largely replaced conventional RFT tools in modern formation evaluation.

A Formation Pressure Test is conducted using wireline formation testing tools such as RFT (Repeat Formation Tester) or MDT (Modular Formation Dynamics Tester) to directly measure pore pressure of subsurface formations.

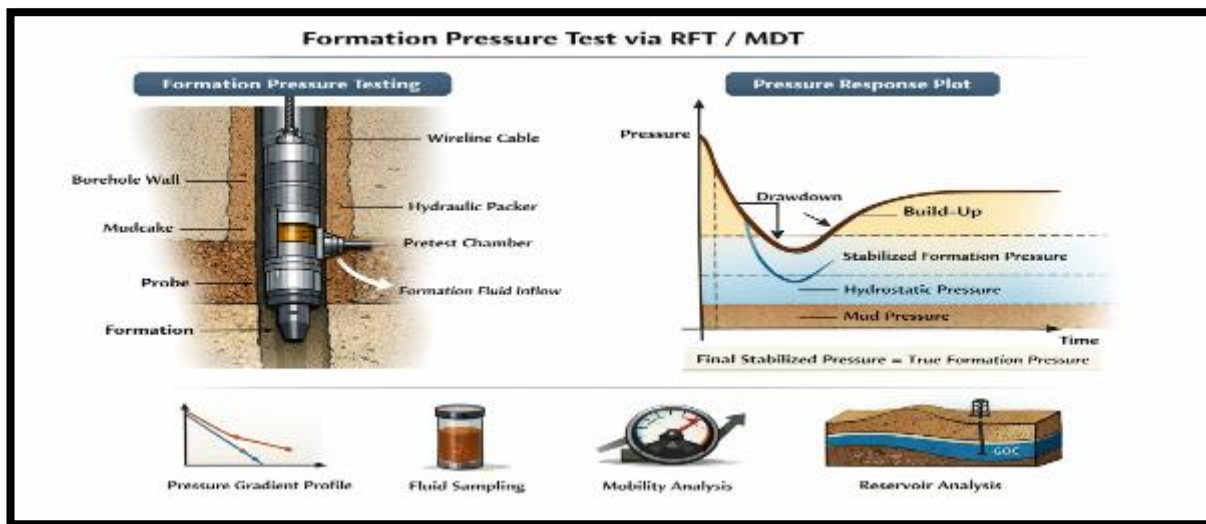


Fig 21:- Formation pressure Test via RFT (Repeat formation Tester/ Modular Formation Tester)

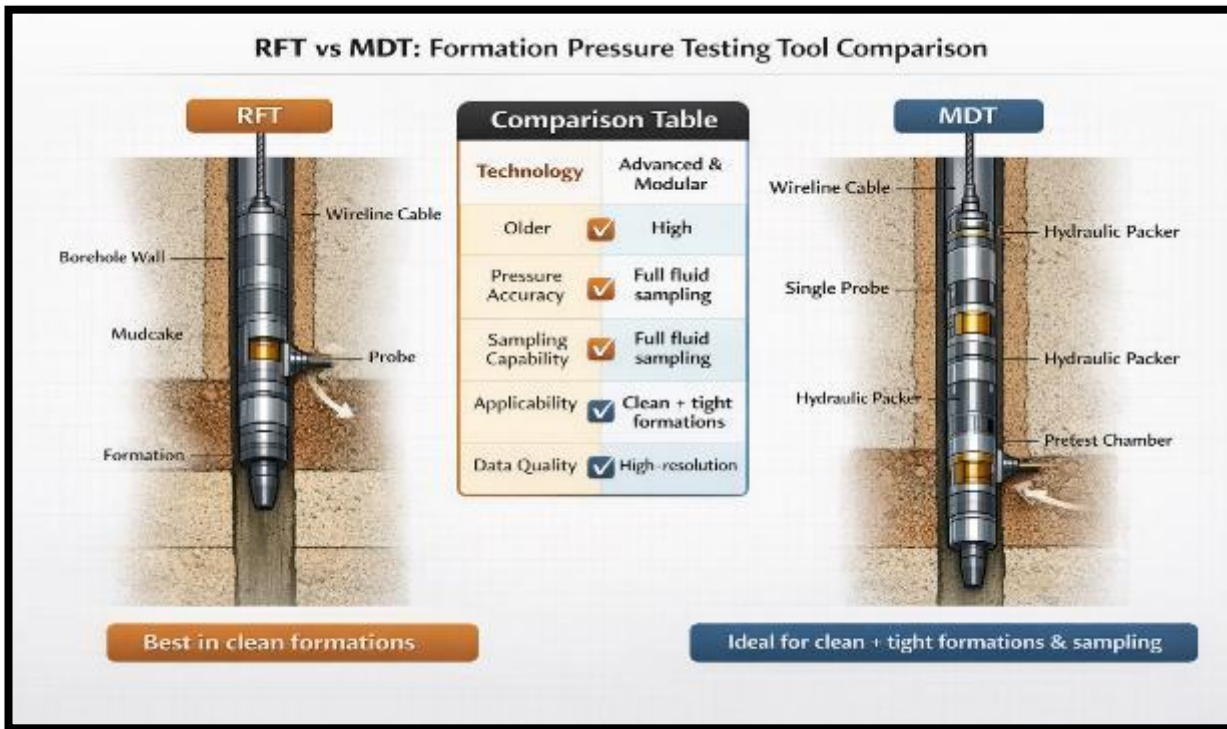


Fig 22: - RFT vs MDT: - Formation Pressure Testing tool comparison

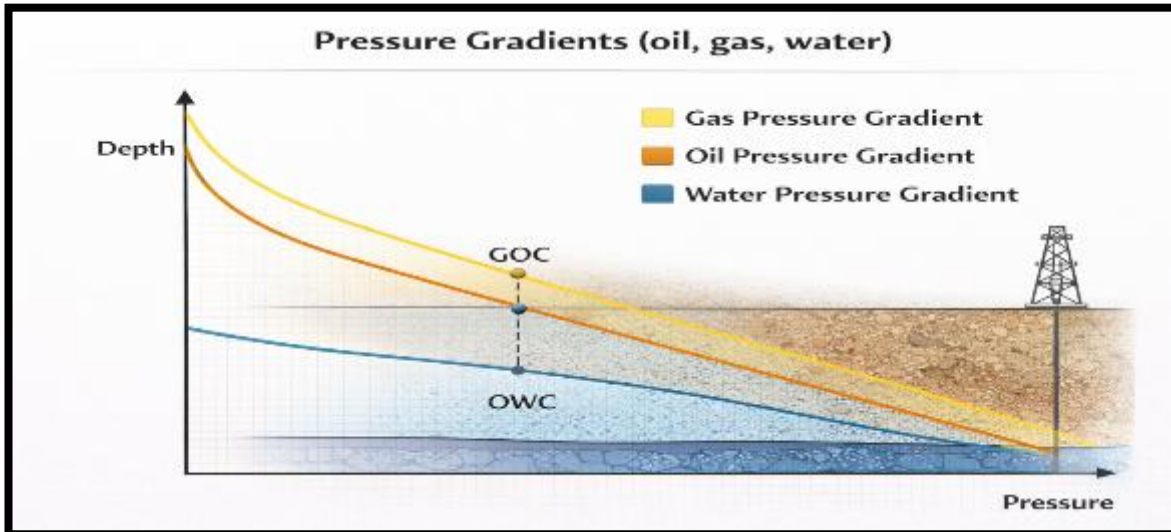


Fig 23:- Pressure gradients of oil, gas and water

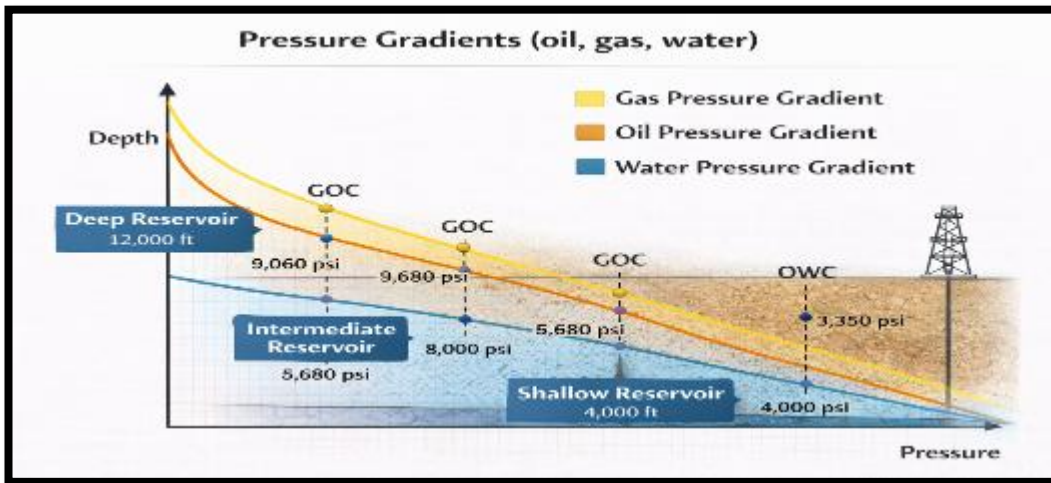


Fig 24: - Different pressure gradients in different reservoir rocks

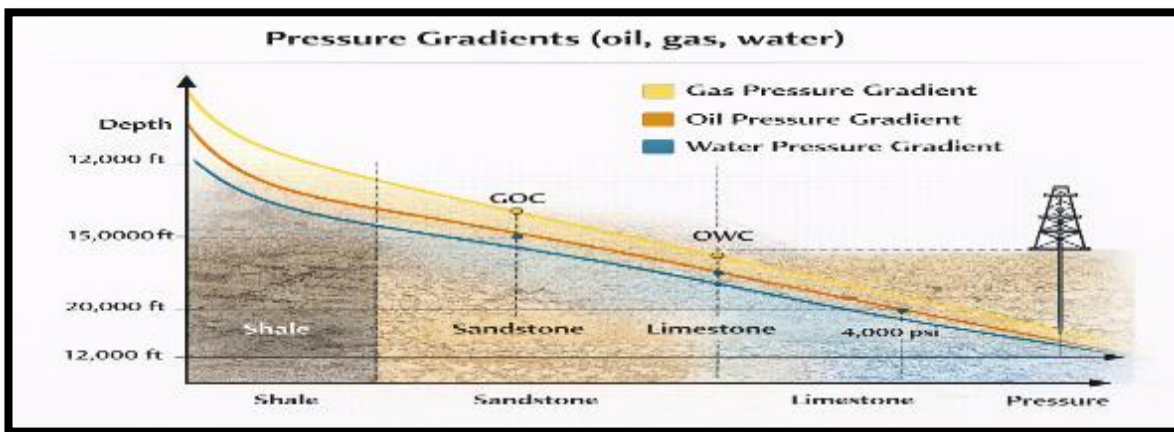


Fig 25:- Different pressure gradients in different reservoir rocks

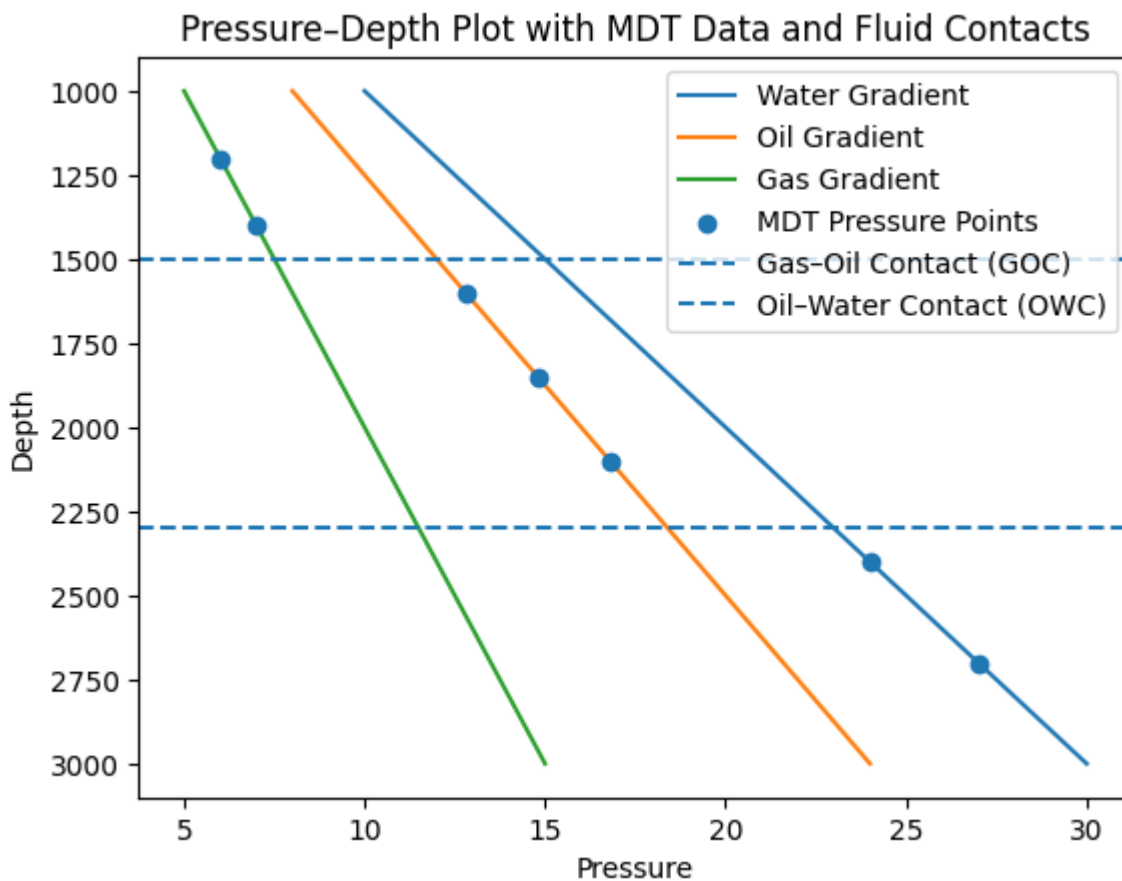


Fig 26: -Pressure–depth plot derived from MDT measurements showing gas, oil, and water pressure gradients. Discrete MDT pressure points (symbols) align along distinct linear trends corresponding to gas, oil, and water columns. The change in pressure gradient identifies the gas–oil contact (GOC) and oil–water contact (OWC), marked by horizontal dashed lines. This plot demonstrates how formation testing data are used to determine fluid type, establish reservoir fluid contacts, and evaluate vertical connectivity in open-hole formations.

Sonic -Resistivity logs: Sonic and resistivity logs are complementary wireline measurements used to evaluate lithology, porosity, fluid type, and hydrocarbon saturation.

- Sonic logs respond mainly to the **rock matrix and porosity**.
- Resistivity **logs** respond mainly to the **type and amount of pore fluid**.

When interpreted together, they allow reliable **reservoir identification** and **fluid discrimination**

**Equations and Behaviour in Different Reservoir Rocks & Fluids :-**Sonic and resistivity logs are essential wireline measurements used to evaluate subsurface formations by characterising rock and fluid properties. Sonic log parameters describe acoustic wave propagation through the formation and are mainly influenced by lithology, porosity, compaction, and pore fluids. Resistivity log parameters represent the electrical behaviour of the formation and are primarily controlled by fluid type and water saturation. Since hydrocarbons are electrically resistive and formation water is conductive, resistivity measurements are key indicators of hydrocarbon presence. When interpreted together, sonic and resistivity parameters provide a reliable basis for identifying reservoir rocks, estimating porosity, and differentiating between water-, oil-, and gas-bearing zones.

## Sonic–Resistivity Logs:

Equations and Behavior in Different Reservoir Rocks & Fluids

Medium / Log	Governing Equation	Shale	Sandstone (Water)	Sandstone (Oil)	Sandstone (Gas)
Sonic Log ( $\Delta t$ )	$\Delta t = \frac{1}{V_p}$	High $\Delta t$ (slow) clay: 2 bound water	High $\Delta t$ (porous, fluid-filled)	Moderate-High $\Delta t$	Low $\Delta t$ (fast, dense)
Sonic Porosity	$\phi = \frac{\Delta t_m - \Delta t_f}{\Delta t_m - \Delta t_{ma}}$	Unreliable	Reliable	Reliable	Low $\Delta t$ (fast)
Velocity Relation	$V_p = \sqrt{\frac{K + \frac{4}{3}G}{\rho}}$	Low modulus + low velocity	Moderate	Slightly higher: water	Highest velocity
Bulk Density	$\rho = \frac{E}{I}$		Low moderate	Lowest velocity	High
Resistivity ( $R_t$ )	$R_t = \frac{E}{I}$	$\propto \frac{R}{S} \propto \frac{1}{\sigma}$	Low-Moderate	Low Moderate	High
Archie's Law	$R_t = a R_w S_w^n$	Low $\frac{a}{\sigma^n} \propto \frac{1}{h_{sp}}$	Yey	Valid	High
Water Saturation $S_w$	$S_w = \frac{\Delta}{\rho^n} R_t$	Major	Overestimated	Minor	Negligible
Invasion Profile	$R_{to} < R_t$	Weak contrast	Clear invasion	Clear invasion	Strong invasion
Gas Effect	Velocity dispersion	Minor	None	Minor	Minimal

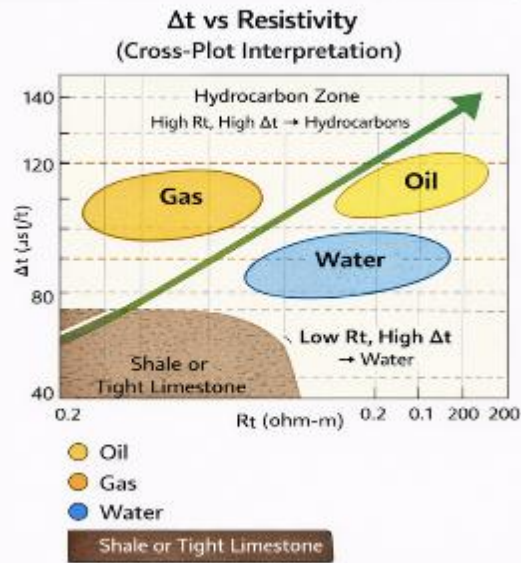


Fig 27:- Sonic-Resistivity logs:- Equation and behaviour in different reservoir rocks and fluids

Sonic–Resistivity Logs parameter and what it stands for

Parameter	Full Name / Meaning	Unit	Used In
$\Delta t$	Sonic slowness (travel time per unit length)	$\mu s/ft$ or $\mu s/m$	Sonic log, porosity
$V_p$	Compressional wave velocity	m/s or ft/s	Sonic interpretation
$\Delta t_{og}$	Measured formation slowness	$\mu s/ft$	Sonic porosity
$\Delta t_{ma}$	Matrix slowness	$\mu s/ft$	Sonic porosity
$\Delta t_f$	Fluid slowness	$\mu s/ft$	Sonic porosity
$\phi$	Porosity	fraction or %	Sonic & Archie
$K$	Bulk modulus	GPa	Velocity equation
$G$	Shear modulus	GPa	Velocity equation
$\rho$	Bulk density	$g/cm^3$	Velocity & density logs
$\rho_{ma}$	Matrix density	$g/cm^3$	Density & sonic
$\rho_f$	Fluid density	$g/cm^3$	Density & sonic
$R_t$	True formation resistivity	ohm-m	Resistivity log
$R_{xo}$	Flushed-zone resistivity	ohm-m	Invasion analysis
$R_w$	Formation water resistivity	ohm-m	Archie's equation
$S_w$	Water saturation	fraction or %	Archie's equation
$S_h$	Hydrocarbon saturation ( $1 - S_w$ )	fraction or %	Reservoir evaluation
$a$	Tortuosity factor	dimensionless	Archie's law
$m$	Cementation exponent	dimensionless	Archie's law
$n$	Saturation exponent	dimensionless	Archie's law
$I$	Electrical current	ampere	Resistivity measurement
$E$	Electric potential	volt	Resistivity measurement
$\sigma$	Electrical conductivity ( $1/R$ )	S/m	Shale response
$\phi_t$	Total porosity	fraction	Shaly formations
$\phi_e$	Effective porosity	fraction	Clean reservoirs

Vsh	Shale volume	fraction or %	Shale correction
Rt/Rxo	Resistivity ratio	dimensionless	Invasion profile
$\Delta t$ -Rt	Sonic-resistivity cross-plot axes	—	Fluid discrimination

**Key Interpretation Takeaways: -**

- **Gas zones** → **Highest  $\Delta t$  + Highest  $R_t$**  (classic gas signature)
- **Oil zones** → **Moderate  $\Delta t$  + High  $R_t$**
- **Water zones** → **High  $\Delta t$  + Low  $R_t$**
- **Shales** → **High  $\Delta t$  + Low  $R_t$**  (non-reservoir despite porosity indication)
- **Tight limestones** → **Low  $\Delta t$  + High  $R_t$**  (non-productive)

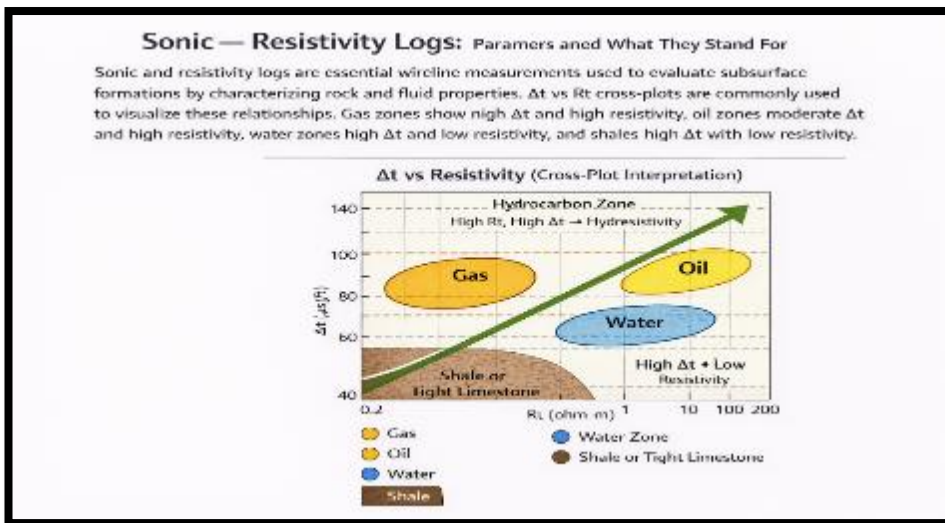


Fig 28 :- Sonic -Resistivity cross-plot figure showing oil, gas, water, and shale zones

**Cross-Plot Zones:-**

Zone	$\Delta t$	$R_t$	Interpretation
Gas	Very high	Very high	Gas-bearing reservoir
Oil	Moderate-high	High	Oil-bearing reservoir
Water	High	Low	Water-bearing
Shale	High	Low	Clay-rich, non-reservoir
Tight limestone	Low	High	Dense non-reservoir

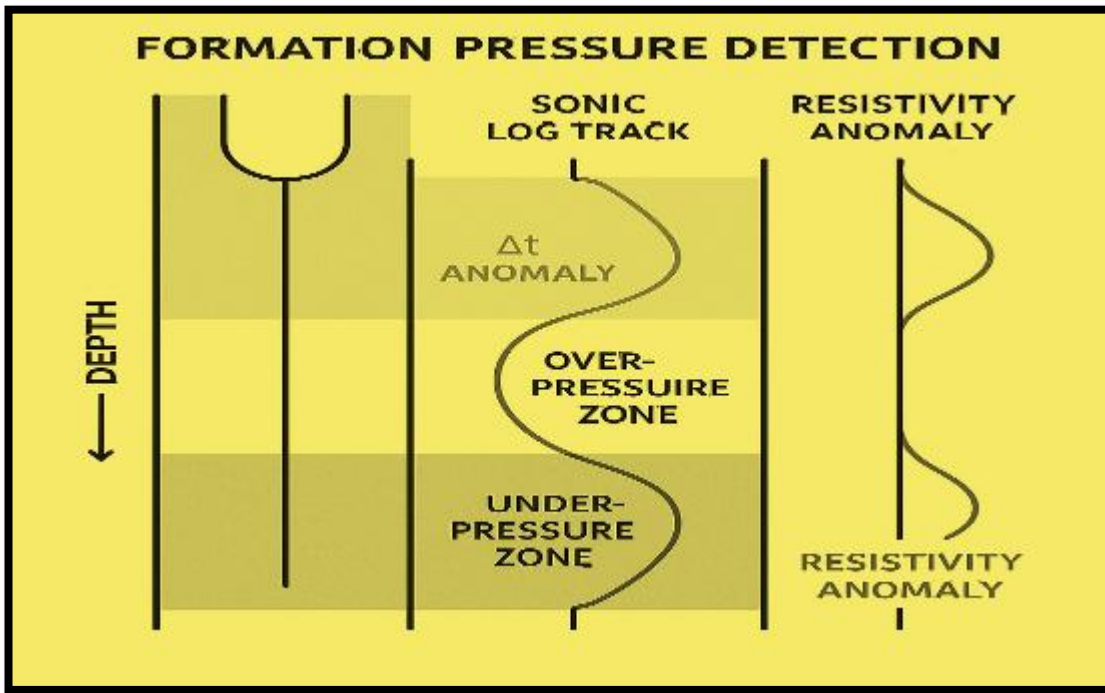


Fig 29 :-The figure shows a vertical borehole cross-section with depth, sonic log ( $\Delta t$ ) and resistivity log ( $R_t$ ) tracks side by side, clearly marking normal pressure, overpressure, and under pressure zones. The anomalies are highlighted so you can visually see where  $\Delta t$  and  $R_t$  deviate from the expected trend. This kind of visualisation makes it much easier to interpret how compaction and fluid saturation shift with pressure changes.

### Real-Time Application in Drilling Operations :-

- **Kick Detection:** A sudden drop in  $\Delta t$  (sonic slowness) and resistivity anomalies may signal an overpressure zone approaching — a precursor to a kick.
- **Mud Weight Adjustment:** By identifying overpressure zones early, you can adjust mud weight to maintain well control and avoid blowouts.
- **Casing Point Selection:** Pressure anomalies help determine optimal casing depths to isolate risky zones.
- **Pore Pressure Prediction:** Combining  $\Delta t$  and  $R_t$  trends with depth allows for dynamic pore pressure modelling while drilling.

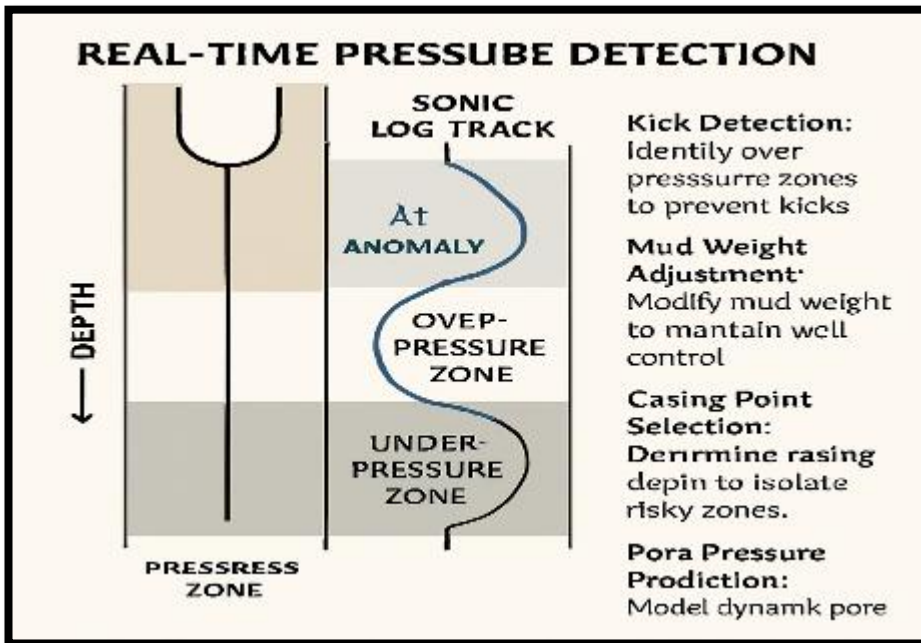


Fig 30 :-"REAL-TIME PRESSURE DETECTION" :-Illustration of formation pressure detection using sonic ( $\Delta t$ ) and resistivity ( $R_t$ ) logs in a vertical borehole. The diagram highlights normal, overpressure, and under pressure zones, showing how  $\Delta t$  and  $R_t$  anomalies correlate with pressure changes. Annotations explain real-time drilling applications including kick detection, mud weight adjustment, casing point selection, and pore pressure prediction.

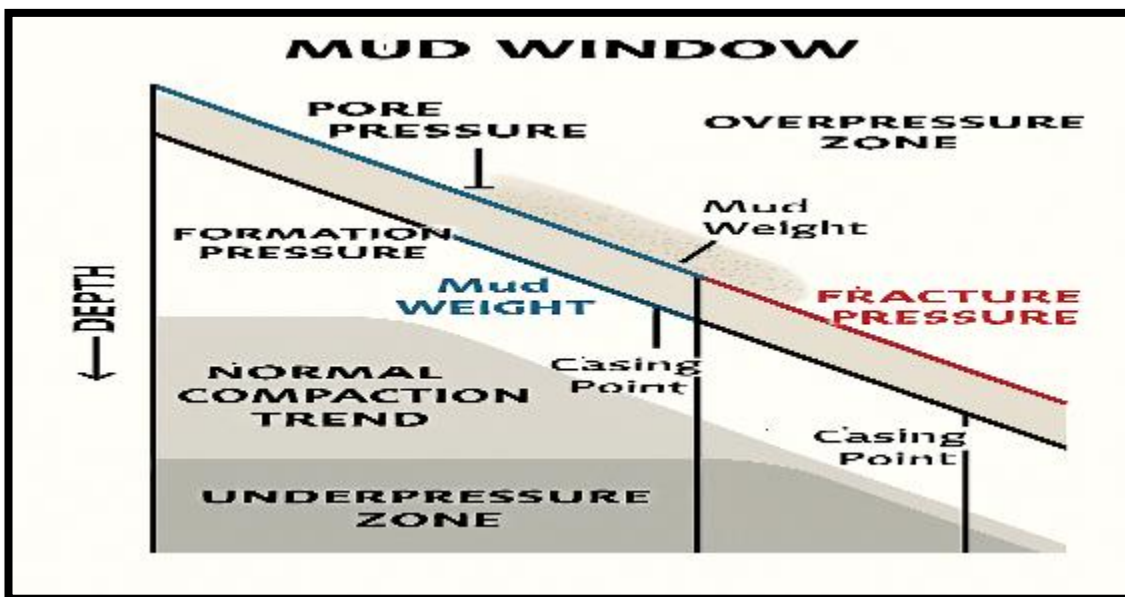


FIG 31 :-Diagram illustrating the mud weight window in drilling operations. It shows the safe pressure margin between pore pressure and fracture pressure across depth. The shaded region between the blue pore pressure line and red fracture pressure line represents the optimal mud weight range to maintain well control. Casing points are marked at key depth intervals to isolate zones and prevent kicks or lost circulation. The formation is divided into under-pressure, normal compaction, and overpressure zones to highlight pressure transitions.

### Sonic & Resistivity Log Behaviour in Different Rocks and Fluids

Rock / Fluid Type	Sonic Log ( $\Delta t$ ) Behaviour	Resistivity Log ( $R_t$ ) Behaviour	Porosity / Notes
<b>Shale</b>	High $\Delta t$ (slow velocity due to clay and bound water)	Low $R_t$ (conductive clays)	Porosity may appear high, but non-reservoir
<b>Sandstone – Water-bearing</b>	High $\Delta t$ (porosity slows velocity)	Low $R_t$ (saline water conducts)	True porosity can be estimated accurately
<b>Sandstone – Oil-bearing</b>	Moderate $\Delta t$ (oil slows less than water)	High $R_t$ (oil is resistive)	Porosity estimation is reliable; indicates hydrocarbon
<b>Sandstone – Gas-bearing</b>	Very high $\Delta t$ (gas drastically slows velocity)	Very high $R_t$ (gas is highly resistive)	Porosity may be overestimated; classic gas signature
<b>Tight Limestone</b>	Low $\Delta t$ (dense rock, fast velocity)	High $R_t$ (tight, resistive)	Low porosity; usually non-reservoir
<b>Overpressure Zones</b>	$\Delta t$ lower than normal trend (slow compaction)	$R_t$ may show anomalies	Indicates abnormal formation pressure
<b>Under Pressure Zones</b>	$\Delta t$ is higher than the normal trend (faster compaction)	$R_t$ may show anomalies	Indicates depleted or low-pressure formation
<b>Normal Pressure Zones</b>	$\Delta t$ follows the expected trend with depth	$R_t$ consistent with fluid type	Typical reservoir behaviour

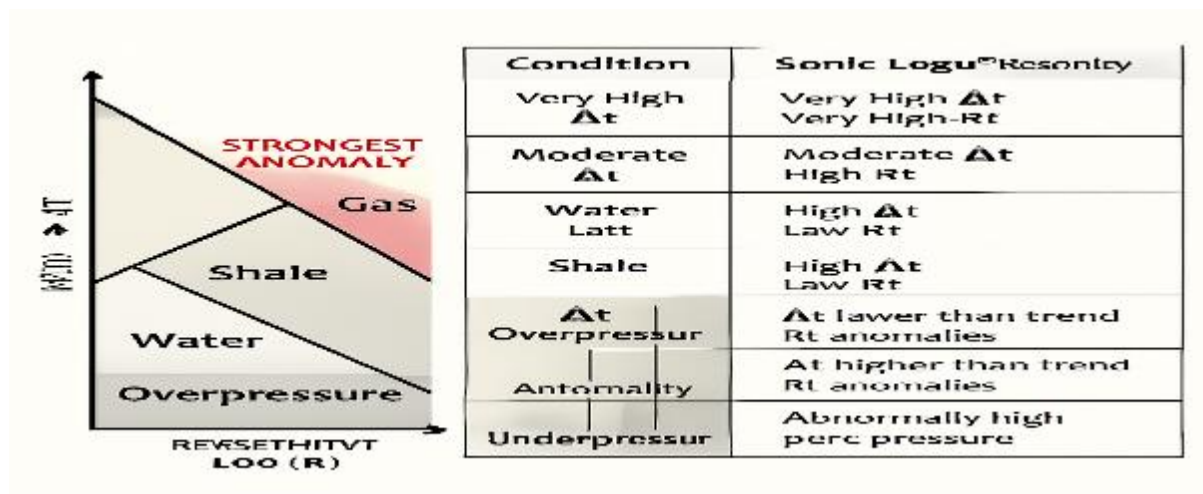


FIG 32 :-Integrated diagram showing sonic ( $\Delta t$ ) and resistivity ( $R_t$ ) log behaviour across depth and fluid types. The  $\Delta t$  vs  $R_t$  cross-plot identifies gas, oil, water, and shale zones based on log anomalies. Depth profile highlights overpressure and underpressure zones with corresponding log deviations. Summary table links log responses to fluid type and pressure regime, ideal for quick reference in exams, reports, and field analysis.

## Ultimate Sonic & Resistivity Summary Table

Category	Parameter / Equation	Meaning / For	Stands	Behaviour in Different Rocks & Fluids	Notes / Cross-Plot Interpretation
Sonic Log	$\Delta t = 1 / V_p$	Sonic slowness (travel time per unit length)		High in shale and water sands, moderate in oil sands, very high in gas sands, low in tight limestone	In cross-plot: high $\Delta t$ for gas/water, low $\Delta t$ for tight formations
	$V_p = \sqrt{((K + 4/3 G)/\rho)}$	Compressional wave velocity		Low in gas and shale, moderate in oil, high in dense rocks	$\Delta t$ is inversely proportional to $V_p$ ; anomalies indicate pressure changes
	$\Delta t_{log}$	Measured formation slowness		Reflects the combined matrix + fluid	Deviations from the normal trend indicate over- or underpressure
	$\Delta t_{ma}$	Matrix slowness		Sandstone $\approx 55 \mu s/ft$ , Limestone $\approx 47 \mu s/ft$	Reference for porosity calculation
	$\Delta t_f$	Fluid slowness		Water $\approx 189 \mu s/ft$ , Oil $\approx 210 \mu s/ft$ , Gas $> 300 \mu s/ft$	Used in sonic porosity calculation
	$\phi = (\Delta t_{log} - \Delta t_{ma}) / (\Delta t_f - \Delta t_{ma})$	Sonic porosity		Overestimated in shale & gas zones; accurate in clean water/oil sands	$\Delta t$ vs $R_t$ cross-plot: correlates with hydrocarbon zones
Elastic Density	$K, G, \rho$	Bulk modulus, shear modulus, bulk density		$K$ & $G$ low in shale, high in tight limestone; $\rho$ low in gas, high in dense rocks	Important for velocity & pressure modeling
Resistivity Log	$R_t$	True formation resistivity		Low in shale & water sands, high in oil, very high in gas, high in tight limestone	In cross-plot: $R_t$ anomalies combined with $\Delta t$ indicate fluid type & pressure
	$R_{xo}$	Flushed-zone resistivity		Shows mud invasion effects	Helps correct $R_t$ for near-borehole conditions
	$R_w$	Formation water resistivity		Depends on salinity & temperature	Used in Archie's law for $S_w$
	$S_w = (a R_w / (\phi^m R_t))^{(1/n)}$	Water saturation		Low $S_w \rightarrow$ hydrocarbons; high $S_w \rightarrow$ water	Cross-plot: low $S_w$ zones correspond to oil/gas
	Archie's Law: $R_t = a R_w \phi^{-m} S_w^{-n}$	Empirical relation for clean formations		Valid for clean sandstones; not valid in shale	Determines hydrocarbon presence quantitatively
	$a, m, n$	Tortuosity, cementation, saturation exponents		$a \approx 1, m \approx 1.8-2.2, n \approx 2$	Adjusts Archie's calculation
Rock / Fluid Behaviour	–	–		Shale: High $\Delta t$ , low $R_t$ ; Sandstone water: High $\Delta t$ , low $R_t$ ; Sandstone oil: Moderate $\Delta t$ , high $R_t$ ; Sandstone gas: Very high $\Delta t$ , very high $R_t$ ; Tight limestone: Low $\Delta t$ , high $R_t$	$\Delta t$ vs $R_t$ cross-plot separates zones clearly

<b>Formation Pressure Detection</b>	$\Delta t$ anomalies	Lower than normal $\rightarrow$ overpressure; higher than normal $\rightarrow$ under pressure	Overpressure: $\Delta t$ lower than trend, $R_t$ anomaly; Under pressure: $\Delta t$ higher than trend	Cross-plot highlights abnormal pressure zones along depth
<b>Cross-Plot <math>\Delta t</math> vs <math>R_t</math></b>	–	$\Delta t = X$ -axis, $R_t = Y$ -axis	Gas: very high $\Delta t$ & $R_t$ ; Oil: moderate $\Delta t$ & high $R_t$ ; Water: high $\Delta t$ & low $R_t$ ; Shale: high $\Delta t$ & low $R_t$	Provides visual identification of hydrocarbon zones and pressure anomalies

**Key Summary Notes:-**

- **Gas:** Very high  $\Delta t$  + very high  $R_t$   $\rightarrow$  strongest anomaly
- **Oil:** Moderate  $\Delta t$  + high  $R_t$   $\rightarrow$  hydrocarbon-bearing
- **Water:** High  $\Delta t$  + low  $R_t$   $\rightarrow$  water-bearing
- **Shale:** High  $\Delta t$  + low  $R_t$   $\rightarrow$  non-reservoir
- **Overpressure:**  $\Delta t$  lower than trend +  $R_t$  anomalies
- **Under pressure:**  $\Delta t$  higher than trend +  $R_t$  anomalies

**C) Leak-Off Test (LOT)**  $\rightarrow$  fracture pressure (upper bound): -The **Leak-Off Test (LOT)** is a well control and formation integrity test conducted in a drilled well to determine the **fracture pressure ( $P_f$ )** of the formation. The **fracture pressure** represents the **upper bound of safe mud weight**, beyond which the formation may fracture, potentially leading to lost circulation or wellbore instability. LOT is critical for well design, casing setting, and mud weight planning.

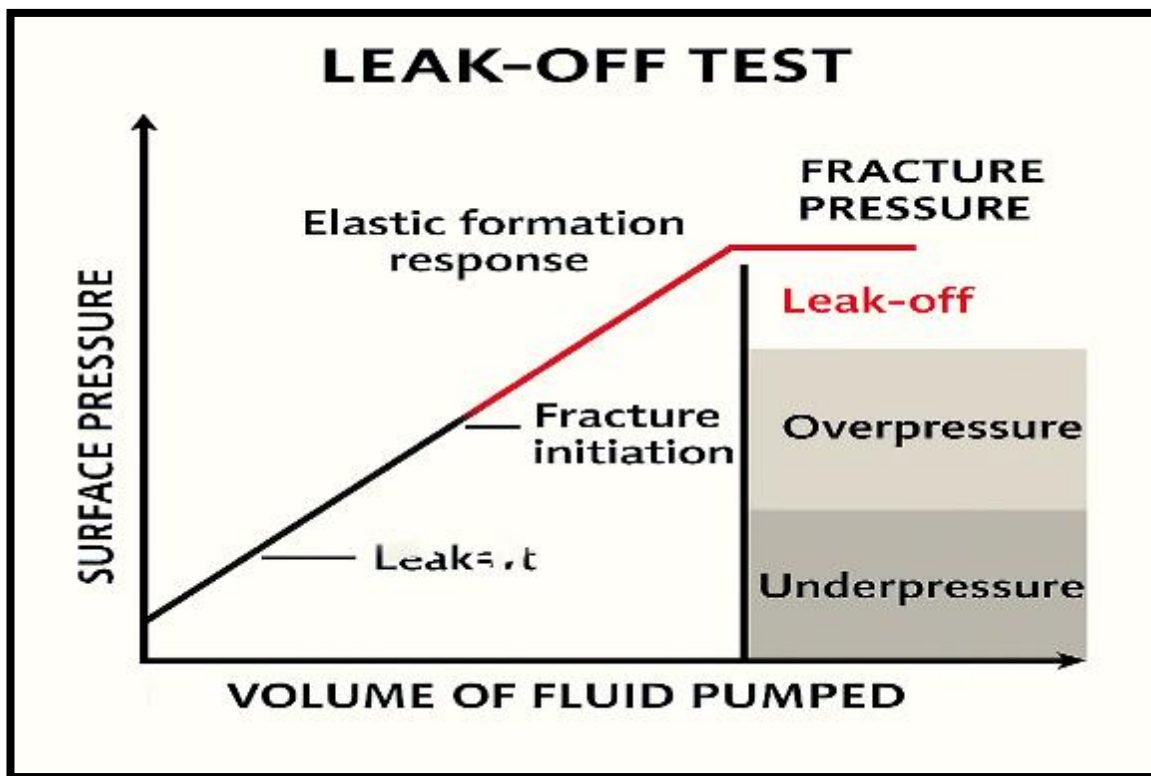


**Fig 33 :-Schematic representation of a Leak-Off Test (LOT) showing surface pressure versus volume of fluid pumped. The initial linear trend indicates elastic formation response. A deviation from linearity marks fracture**

**initiation and leak-off, identifying the fracture pressure. This point defines the upper limit of the safe mud weight window, critical for maintaining wellbore integrity during drilling operations.**

The **Leak-Off Test (LOT)** is a formation integrity and well control test used to determine the **fracture pressure ( $P_f$ )** of a formation, which represents the **upper bound of safe mud weight** to avoid wellbore fracturing and lost circulation. In the test, a small isolated open-hole interval is pressurised by slowly pumping drilling fluid while monitoring surface pressure versus volume. Initially, pressure rises linearly as the formation responds elastically, and the point at which fluid begins to leak off into the formation marks the **fracture pressure**. This measurement is critical for **well planning, casing design, safe mud weight selection, and wellbore stability analysis**. Typically, the relationship of pressures follows  $P_p \leq P_h \leq P_f$ , where  $P_p$  is the pore pressure (lower bound),  $P_h$  is the minimum horizontal stress, and  $P_f$  is the fracture pressure (upper bound). LOT data can also be represented graphically, with surface pressure on the Y-axis and volume pumped on the X-axis, showing an initial linear trend followed by a sudden pressure drop at formation fracture, providing a clear indication of the safe drilling margin.

The **Formation Integrity Test (FIT)** is a pressure test conducted in a cased or open-hole section of a well to verify that the formation can withstand the planned mud weight without fracturing. In this test, a **small volume of fluid** is slowly pumped into the isolated interval while monitoring surface pressure. A **linear increase in pressure** indicates elastic behaviour of the formation, whereas a sudden pressure spike or drop would indicate that the formation is approaching its mechanical limit. The measured pressure defines the **maximum allowable mud weight** for safe drilling at that depth, ensuring wellbore stability and preventing formation fracturing or lost circulation. FIT is commonly used for **casing design, safe mud window determination, and wellbore integrity verification**.

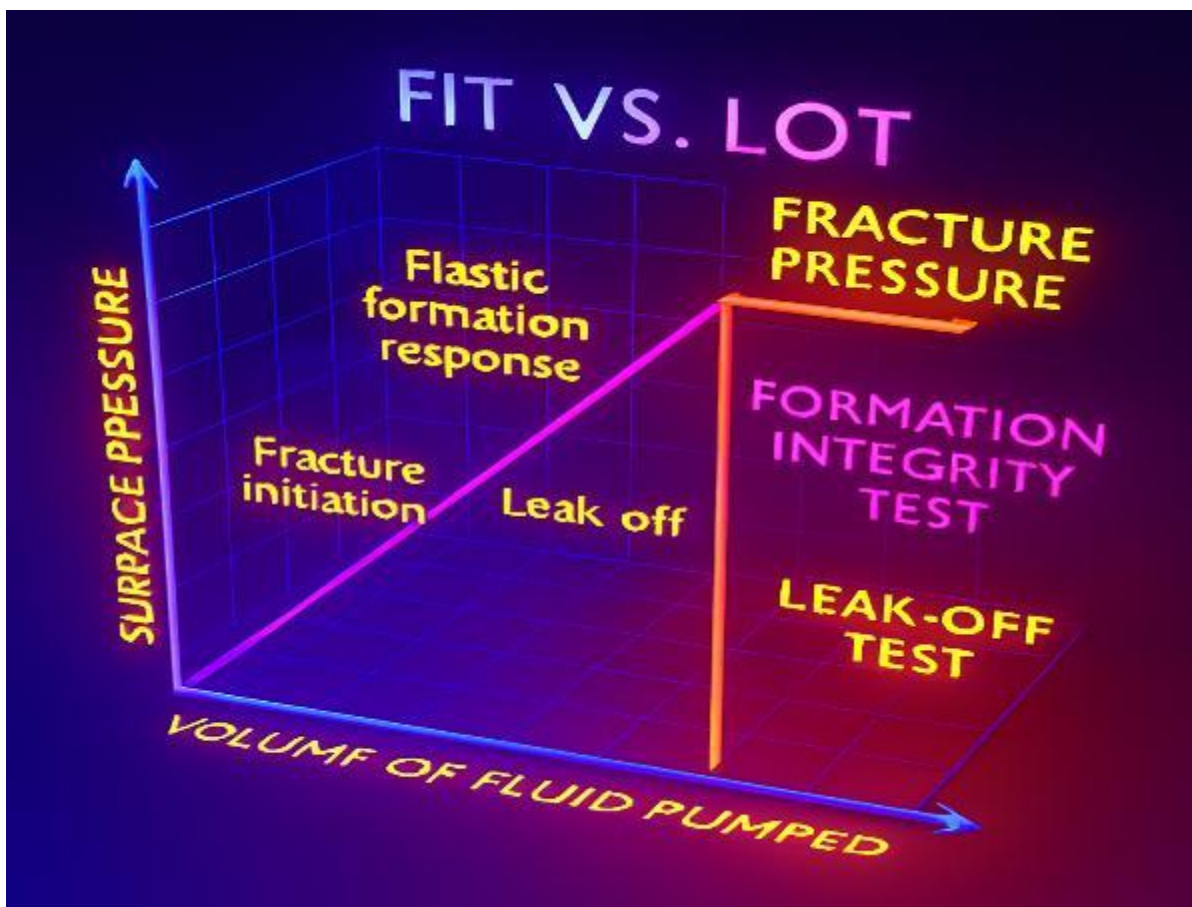


**Fig 34** :-3D schematic comparing Formation Integrity Test (FIT) and Leak-Off Test (LOT) using a plasma colour gradient. The FIT curve shows a continuous linear increase in surface pressure with fluid volume, representing elastic formation response. The LOT curve deviates at the fracture initiation point, marking leak-off and

identifying fracture pressure. This visualisation highlights the operational difference between FIT and LOT, aiding in safe mud weight design and casing strategy during drilling.

The Formation Integrity Test (FIT) is a pressure test conducted in a cased or open-hole section of a well to verify that the formation can safely withstand the planned mud weight without fracturing. In this test, a small volume of fluid is slowly pumped into the isolated interval while monitoring surface pressure. Two important parameters are recorded: SIDP (Shut-In Drill pipe Pressure), which is the pressure measured at the drillpipe after pumping stops and the fluid is shut in, and SICP (Shut-In Casing Pressure), which is the pressure measured at the casing after shut-in. A linear rise in pressure indicates elastic formation behaviour, whereas a sudden deviation or leak-off indicates that the formation is approaching its mechanical limit. The measured pressure, along with SIDP and SICP values, defines the maximum allowable mud weight for safe drilling, ensuring wellbore stability, proper casing design, and prevention of lost circulation or formation fracturing.

**Detailed chart for FIT and LOT test: -**

Test	Purpose	Procedure (Stepwise)	Key Parameters	Observations / Notes
<b>FIT (Formation Integrity Test)</b>	Verify formation can withstand the planned mud weight without fracturing	<ol style="list-style-type: none"> <li>1. Isolate the cased/open-hole interval</li> <li>2. Pump fluid at <b>Slow Circulation Rate (SCR)</b> to avoid artificially fracturing the formation</li> <li>3. Monitor surface pressure while pumping</li> <li>4. <b>Shut-in</b> after pumping and record: <ul style="list-style-type: none"> <li>• <b>SIDP</b> – Shut-In Drillpipe Pressure</li> <li>• <b>SICP</b> – Shut-In Casing Pressure</li> </ul> </li> <li>5. Analyse pressure response</li> </ol>	SCR, SIDP, SICP	Linear pressure rise → elastic formation behaviour. Pressure deviation/leak-off → approaching fracture limit <b>Defines maximum allowable mud weight</b>
<b>LOT (Leak-Off Test)</b>	Determine fracture pressure ( $P_f$ ) → upper bound mud weight	<ol style="list-style-type: none"> <li>1. Isolate open-hole section (10–30 ft)</li> <li>2. Slowly pump fluid at a controlled rate</li> <li>3. Monitor surface pressure vs fluid volume pumped</li> <li>4. <b>Record fracture pressure (<math>P_f</math>)</b> at first leak-off</li> <li>5. Optionally note SIDP and SICP if measured</li> </ol>	$P_f$ , pumping volume, (SIDP, SICP optional)	Linear rise → elastic formation Sudden drop → fracture initiation / leak-off <b>Defines upper bound safe mud weight for drilling</b>

**Key Notes: -**

- **FIT** is generally a **quick, small-volume test** for formation integrity and wellbore stability.
- **LOT** is a **more detailed test** to determine the **fracture pressure** of the formation.
- **SCR, SIDP, and SICP** are critical measurements in **FIT**, and can also be referenced in **LOT** for added safety.
- Both tests together help define a **safe mud window: lower bound → pore pressure; upper bound → fracture pressure**.

**FIT & LOT Formulas Summary Table: -**

Parameter / Formula	Definition / Use	Notes / Units
<b>SIDP (Shut-In Drillpipe Pressure)</b>	SIDP = Surface Pressure - Drillpipe Pressure Loss	Pressure at drillpipe after shut-in, corrected for friction; psi or Pa
<b>SICP (Shut-In Casing Pressure)</b>	SICP = Formation Pressure - Annular Pressure Loss	Pressure at casing after shut-in, corrected for annular friction; psi or Pa
<b>Annular Pressure Loss</b>	$\Delta P_{\text{annulus}} = (2 * f * L * \rho * v^2) / D_{\text{ann}}$	Frictional pressure drops in annulus; f = friction factor, L = annular length, rho = mud density, v = fluid velocity, D <sub>ann</sub> = hydraulic diameter
<b>Drillpipe Pressure Loss</b>	$\Delta P_{\text{drillpipe}} = (2 * f * L * \rho * v^2) / D_{\text{pipe}}$	Frictional pressure drops inside the drillpipe; same variables as annulus
<b>Fracture Pressure (P<sub>f</sub>)</b>	Measured from LOT at first leak-off	Upper bound of mud weight; psi or Pa
<b>Safe Maximum Mud Weight</b>	$MW_{\text{max}} = \text{SICP (or SIDP)} / (0.052 * \text{TVD})$	TVD in ft, MW in ppg; defines upper safe mud limit
<b>Formation Integrity Check</b>	Linear pressure rise → elastic, Deviation → approaching fracture	Qualitative evaluation from FIT/LOT data

**Key Notes: -**

- **SIDP** is measured at the drillpipe; **SICP** is measured at the casing.
- **Annular and drillpipe pressure losses** must be accounted for accurate SICP and SIDP.
- **LOT fracture pressure (P<sub>f</sub>)** defines the **upper mud weight limit**; FIT ensures formation can handle planned mud weight.
- **Slow Circulation Rate (SCR)** minimises artificial fracturing during tests
- **Fluid Velocity Calculation Table – Drillpipe & Annulus**

Parameter	Formula	Description	Example Calculation
<b>Drillpipe Cross-Sectional Area (A<sub>pipe</sub>)</b>	$A_{\text{pipe}} = (\pi / 4) \times D_{\text{pipe}}^2$	Area of the drillpipe through which fluid flows	D <sub>pipe</sub> = 0.2 ft → A <sub>pipe</sub> = 3.1416/4 × 0.2 <sup>2</sup> ≈ 0.0314 ft <sup>2</sup>
<b>Fluid Velocity in Drillpipe (V<sub>pipe</sub>)</b>	$V_{\text{pipe}} = Q / A_{\text{pipe}}$	Velocity of mud in the drillpipe; Q = volumetric flow rate	Q = 0.02 ft <sup>3</sup> /s → V <sub>pipe</sub> = 0.02 / 0.0314 ≈ 0.637 ft/s
<b>Annular Cross-Sectional Area (A<sub>annulus</sub>)</b>	$A_{\text{annulus}} = (\pi / 4) \times (D_{\text{hole}}^2 - D_{\text{pipe}}^2)$	Area of annulus between the borehole and drillpipe	D <sub>hole</sub> = 0.5 ft, D <sub>pipe</sub> = 0.2 ft → A <sub>annulus</sub> ≈ 0.166 ft <sup>2</sup>
<b>Fluid Velocity in Annulus (V<sub>annulus</sub>)</b>	$V_{\text{annulus}} = Q / A_{\text{annulus}}$	Velocity of mud in annular space; Q = volumetric flow rate	Q = 0.02 ft <sup>3</sup> /s → V <sub>annulus</sub> = 0.02 / 0.166 ≈ 0.12 ft/s

## Key Notes

- Fluid velocity is **directly proportional to flow rate (Q)**.
- Velocity in **drillpipe is higher** than in the annulus because the area is smaller.
- Use **consistent units** for Q and A: ft<sup>3</sup>/s & ft<sup>2</sup> or m<sup>3</sup>/s & m<sup>2</sup>.
- Fluid velocity is essential for **calculating pressure losses (ΔP)** in FIT and LOT.

## Real-Time PWD Monitoring → Dynamic Adjustments During Drilling: -

**Real-Time Pressure While Drilling (PWD) monitoring** involves continuously measuring **downhole pressure, torque, drag, and other parameters** while drilling, using sensors on the **drill string or bottom-hole assembly (BHA)**. Unlike FIT or LOT, which are **static tests**, PWD provides **continuous, live data**, allowing engineers to:

1. **Track downhole pressures dynamically** – including **equivalent mud weight, annular pressure, and pore/fracture pressures**.
2. **Detect abnormal pressure trends** – such as **overpressure zones, swab/surge effects, or imminent wellbore instability**.
3. **Adjust drilling parameters in real time** – e.g.,
  - **Mud weight** → increase or decrease to stay within the safe mud window
  - **Drilling rate (ROP)** → slow down in weak zones to avoid fracturing
  - **Pump rate** → modify to control annular pressure
4. **Improve wellbore stability** – prevents **lost circulation, kicks, or blowouts**.
5. **Support formation evaluation** – helps refine **pore pressure, fracture pressure, and safe drilling margins** while drilling.

## Key Points: -

- PWD is a **dynamic extension of FIT/LOT** — it continuously monitors what FIT/LOT measures at a single time.
- Real-time data enables **immediate corrective actions**, unlike traditional methods that rely on post-test analysis.
- Integration with **surface monitoring systems** allows drilling engineers to **adjust mud weight, pump rate, or drilling parameters on the fly**, maintaining a **safe mud window**
- Interpretation Table: Drilling Parameters by Formation

Parameter	Sandstone	Fractured	Shale	Carbonate
ECD	Moderate, stable	Elevated due to a narrow pressure window	Slightly declining, sensitive to influx	Variable, depends on vugs/fractures
Mud Weight	Stable, easily adjusted	Increased control of fractures	Stable, but must match pore pressure	Moderate, adjusted for heterogeneity
Pore Pressure	Predictable, moderate	The variable may spike	High, requires careful monitoring	Moderate to high, varies with porosity
ROP	High	Reduced due to instability	Low due to bit balling and pressure	Moderate, depends on lithology
Hookload	Stable	Fluctuating due to torque and drag	Lower, but sensitive to cutting load	Variable, influenced by formation dips

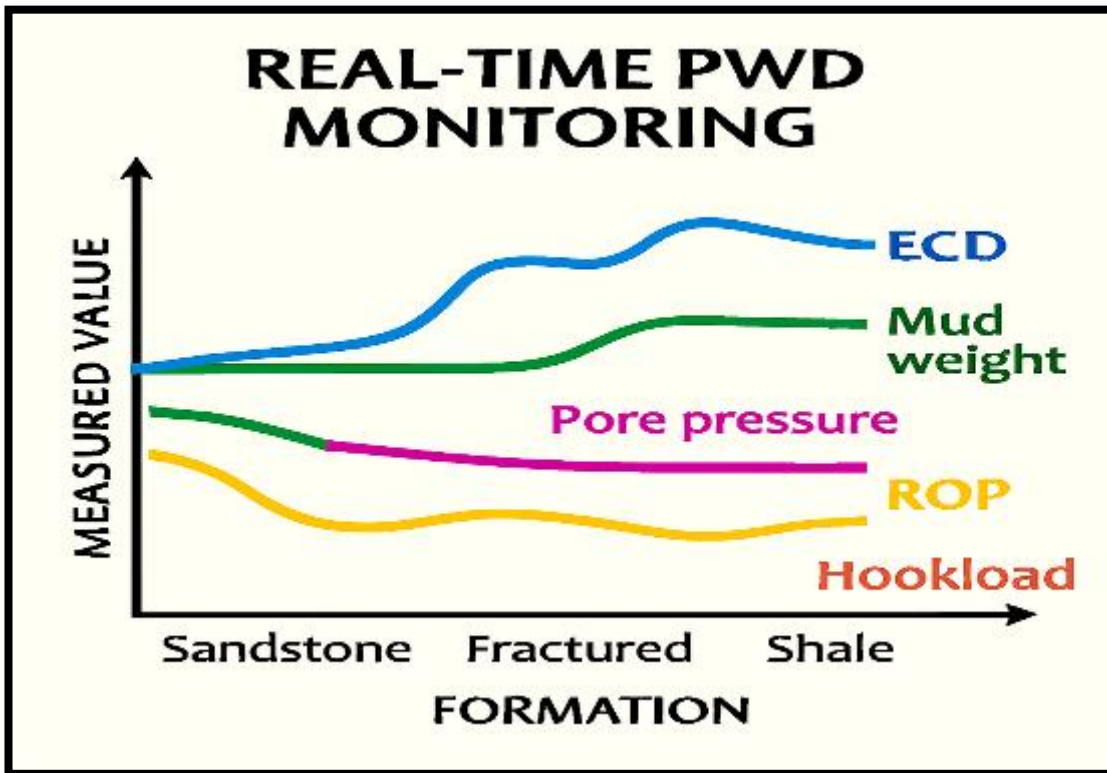


Fig 35: Graph illustrating real-time Pressure While Drilling (PWD) monitoring across different geological formations. It compares Equivalent Circulating Density (ECD), Mud Weight, Pore Pressure, Rate of Penetration (ROP), and Hookload in Sandstone, Fractured, and Shale formations. The visualisation highlights how formation type influences pressure response and drilling dynamics, supporting safer and more adaptive drilling strategies.

#### Formations Compared:

- **Sandstone:** Moderate ECD, high ROP, stable mud weight
- **Fractured:** Elevated ECD, fluctuating hookload, reduced ROP
- **Shale:** Lower ROP, higher pore pressure, stable mud weight
- **Fractured formations** demand constant ECD and mud weight adjustments to avoid losses or kicks.
- **Shale formations** require close pore pressure tracking and slower ROP to maintain wellbore stability.
- **Carbonates** can be unpredictable due to natural heterogeneity — real-time monitoring is essential.
- Sandstone offers the most stable drilling environment, ideal for baseline comparisons.

**Note:- Calculation of ECD: -**

### Equivalent Circulating Density (ECD) – Complete Calculation Table

Step	Parameter	Formula (Word-friendly)	What it Represents
1	Annular flow area	$A_{\text{annulus}} = (3.1416 / 4) \times (D_{\text{hole}}^2 - D_{\text{pipe}}^2)$	Flow area between the borehole and drillpipe
2	Flow rate conversion	Q = Pump rate (convert to ft <sup>3</sup> /s or m <sup>3</sup> /s)	Volumetric flow of drilling fluid
3	Annular fluid velocity	$V_{\text{annulus}} = Q / A_{\text{annulus}}$	Average upward mud velocity in annulus
4	Hydraulic diameter	$D_h = D_{\text{hole}} - D_{\text{pipe}}$	Effective diameter controlling friction
5	Reynolds number	$Re = (\rho \times V_{\text{annulus}} \times D_h) / \mu$	Identifies laminar or turbulent flow
6	Friction factor (laminar)	$f = 64 / Re$	Used when $Re < 2100$
7	Friction factor (turbulent)	$f = 0.316 / Re^{0.25}$	Used when $Re > 4000$
8	Annular pressure loss	$\Delta P_{\text{annulus}} = (2 \times f \times L \times \rho \times V_{\text{annulus}}^2) / D_h$	Frictional pressure drops in the annulus
9	Corrected SICP	$SICP_{\text{corrected}} = \text{Measured SICP} + \Delta P_{\text{annulus}}$	True casing pressure at formation
10	ECD contribution	$\text{ECD increase} = \Delta P_{\text{annulus}} / (0.052 \times TVD)$	Increase in effective mud weight (ppg)
11	ECD (SI units)	$\text{ECD increase} = \Delta P_{\text{annulus}} / (1029.4 \times TVD)$	Increase in effective mud weight (kg/m <sup>3</sup> )

$$ECD \text{ (kg/m}^3\text{)} = MW + [\text{Annular Pressure Loss} / (1029.4 \times TVD)]$$

#### Variable Definitions (Quick Reference)

- $D_{\text{hole}}$  = borehole diameter
- $D_{\text{pipe}}$  = outer diameter of drillpipe
- $\rho$  = mud density
- $\mu$  = mud viscosity
- $L$  = annular length
- $TVD$  = true vertical depth
- 0.052 = oilfield unit conversion constant
- 1029.4 = SI pressure-density conversion constant

**Symbol Meaning Table:-**

Symbol	Stands For	Meaning / Description	Typical Unit
f	Friction factor	Dimensionless factor representing friction between drilling fluid and annular walls	–
L	Annular length	Length of annulus over which fluid flows (open hole or circulating interval)	ft or m
D <sub>hole</sub>	Borehole diameter	Diameter of drilled hole	ft or m
D <sub>pipe</sub>	Drillpipe outer diameter	Outside diameter of drillpipe	ft or m
D <sub>h</sub>	Hydraulic diameter	Effective annular diameter = D <sub>hole</sub> – D <sub>pipe</sub>	ft or m
Q	Flow rate	Volume of drilling fluid pumped per unit time	ft <sup>3</sup> /s or m <sup>3</sup> /s
A <sub>annulus</sub>	Annular area	Flow area between the borehole and drillpipe	ft <sup>2</sup> or m <sup>2</sup>
V <sub>annulus</sub>	Annular velocity	Upward velocity of fluid in an annulus	ft/s or m/s
rho	Mud density	Density of drilling fluid	lb/ft <sup>3</sup> or kg/m <sup>3</sup>
mu	Mud viscosity	Resistance of fluid to flow	Pa·s or lb/(ft·s)
Re	Reynolds number	Determines laminar or turbulent flow regime	–
Delta_P <sub>annulus</sub>	Annular pressure loss	Frictional pressure drop in annulus	psi or Pa
TVD	True vertical depth	Vertical depth from surface to formation	ft or m
0.052	Conversion constant	Converts mud weight (ppg) to pressure gradient (psi/ft)	–
1029.4	SI conversion constant	Converts mud density (kg/m <sup>3</sup> ) to pressure gradient (Pa/m)	–

**Annular pressure loss depends on the friction factor (f), annular length (L), mud properties, and flow velocity, and is essential for SICP correction and ECD calculation.**

Kick detection is the process of identifying an unintended influx of formation fluids into the wellbore when formation pore pressure exceeds the hydrostatic pressure of the drilling mud. Early detection is critical to prevent well control incidents such as blowouts, lost circulation, and wellbore instability. Kicks are identified through abnormal drilling and surface indicators, including pit volume gain, unexpected flow increase, and pressure changes. Once detected, well control methods such as the Driller’s Method or Mud Weight Increase Method are applied to restore pressure balance and safely circulate out the influx.

## Kick Detection Indicators & Preventive Measures

Category	Indicator / Observation	What It Means	Preventive / Corrective Measures
Pit / Volume	Increase in pit volume	Formation fluid entering the wellbore	Maintain proper mud weight, monitor pit volumes continuously
	Pit gain during connections	Influx while pumps are off	Keep pumps running when possible, and observe the pit during connections
Flow	Flow with pumps off	The well is flowing due to formation pressure	Shut-in well immediately, monitor surface flow carefully
	Increase in return flow rate	Additional fluid is entering from the formation	Adjust pump rate, monitor flow rates continuously
Pressure	Decrease in standpipe pressure	Hydrostatic head reduced by influx	Maintain proper mud density, monitor standpipe pressure
	Increase in casing pressure	Formation pressure transmitted to the annulus	Shut-in procedure, record SICP and SIDP
Rate of Penetration (ROP)	Sudden increase	Possible overpressure formation	Slow down drilling, monitor ROP and torque
Mud Properties	Decrease in mud density	Lighter formation fluid mixing with mud	Maintain mud weight and properties, monitor for gas-cut mud
	Gas-cut mud at the surface	Gas influx from the formation	Shut-in, circulate, kick out safely using kill mud weight
Shut-In Pressures	SIDP increases after shut-in	Formation pressure is higher than the mud pressure	Use SIDP to calculate the required kill mud weight
	SICP increases after shut-in	Confirms influx in annulus	Shut-in procedure, circulate kick with correct mud weight
Drilling Breaks	Sudden drilling break	Entry into the higher-pressure zone	Monitor formation trends, adjust mud weight before entering high-pressure zones

Kick detection relies on observing pit volumes, flow, drilling pressures, and mud properties, while preventive measures include maintaining proper mud weight, monitoring ROP and pressure, and following shut-in procedures. To prevent a kick, maintain mud weight above formation pressure, monitor pit volume, flow, and standpipe pressure, use real-time PWD data, follow proper drilling practices, and be ready to shut-in the well when necessary.

**Kick Prevention Table: -**

Category	Preventive Measure	How It Helps / Purpose
<b>Mud Weight</b>	Maintain mud weight above formation pore pressure but below fracture pressure	Ensures the wellbore is overbalanced to prevent influx
<b>Pit / Volume Monitoring</b>	Continuously monitor pit volumes	Detects early signs of fluid entering the wellbore
<b>Flow Rate</b>	Monitor return flow rates	Identifies abnormal flow due to formation influx
<b>Standpipe Pressure</b>	Observe sudden drops or spikes	Indicates potential kick or influx
<b>Mud Properties</b>	Maintain proper mud density, check for gas-cut mud	Prevents the lightening of the mud column that can allow influx
<b>Rate of Penetration (ROP)</b>	Monitor ROP for sudden increases	Detects drilling into overpressured zones early
<b>PWD / Downhole Sensors</b>	Use real-time pressure while drilling tools	Detects kicks before reaching the surface, allowing dynamic adjustments
<b>Drilling Practices</b>	Avoid swabbing, maintain proper pump rates, and ensure hole cleaning	Reduces the chances of influx due to mechanical effects
<b>Shut-In Preparedness</b>	Be ready to follow the correct shut-in procedure	Safely contain any influx and calculate the required kill mud weight
<b>Managed Pressure Drilling (MPD)</b>	Use MPD in narrow-margin or high-pressure wells	Precisely controls bottomhole pressure, minimising kick risk

**Driller’s method and Mud weight increase method to Prevent Kick:** -Kick control is a critical aspect of well control to prevent **formation fluid influx** into the wellbore. Two primary methods are used:

- 1. Driller’s Method** – In this method, the kick is circulated out while **maintaining the existing mud weight**. It relies on careful monitoring of **pressures, pit volume, and flow rates** to remove the influx safely without exceeding the formation fracture pressure. This method is especially useful in **narrow mud window wells**.
- 2. Mud Weight Increase Method** – This method involves **increasing the mud weight** to restore or exceed the formation pressure, re-establishing a safe overbalance. After adjusting the mud weight, the kick is circulated out from the bottom to the surface. This method is effective for **overpressured formations** but carries the risk of **fracturing the formation** if the mud weight is too high.

**Both methods use SIDP, SICP, and surface indicators** to detect kicks and ensure the influx is safely controlled while drilling operations are maintained.

## Kick Control Methods – Comparison Table

Feature	Driller’s Method	Mud Weight Increase Method
Definition	Circulate the kick out using <b>existing mud weight</b>	Increase mud weight to <b>balance or overbalance formation pressure</b> and circulate kick
Step 1 – Kick Detection	Identify influx via <b>pit gain, flow increase, and pressure changes</b>	Same: pit gain, flow increase, SIDP/SICP readings
Step 2 – Shut-In Well	Measure <b>SIDP and SICP</b>	Measure <b>SIDP and SICP</b>
Step 3 – Mud Weight Adjustment	<b>No change</b> in mud weight	Increase mud weight to restore <b>hydrostatic balance</b>
Step 4 – Circulate Kick Out	Circulate from bottom to surface at <b>controlled pump rates</b>	Circulate after adjusting mud weight using <b>bottom-to-surface circulation</b>
Step 5 – Monitor Pressures	Monitor <b>standpipe pressure, pit volume, and flow rate</b>	Same, but include <b>check that increased mud weight does not exceed fracture pressure</b>
Step 6 – Resume Drilling	Resume drilling once the kick is removed and pressures stabilize	Resume drilling once pressures and mud weight are correct
Pressure Behaviour	Mud pressure remains <b>close to formation pressure</b> (risk margin is small)	Mud pressure <b>increases above formation pressure</b> , reduces influx risk, but may fracture the formation if too high
Advantages	Avoids fracturing formation, useful in a <b>narrow mud window</b>	Quickly restores wellbore stability, safer in overpressured zones
Disadvantages / Risks	Small safety margin; careful monitoring required	Excess mud weight can cause <b>lost circulation or fracture</b> ; slower if the kick volume is large
Stress Consideration	Stress state remains near <b>Mohr–Coulomb failure envelope</b> ; careful monitoring needed	Stress state shifted <b>away from failure</b> , safer, but may induce fractures if too high

### Comparative Diagram (Conceptual)

- **Driller’s Method:** Two-step curve (two cycles).
- **Wait-and-Weight Method:** One-step curve (single cycle).
- Labels:
  - **SIDP (Shut-In Drill Pipe Pressure)**
  - **SICP (Shut-In Casing Pressure)**
  - **Kill Mud Weight (KMW)**
  - Circulation cycles are clearly marked.

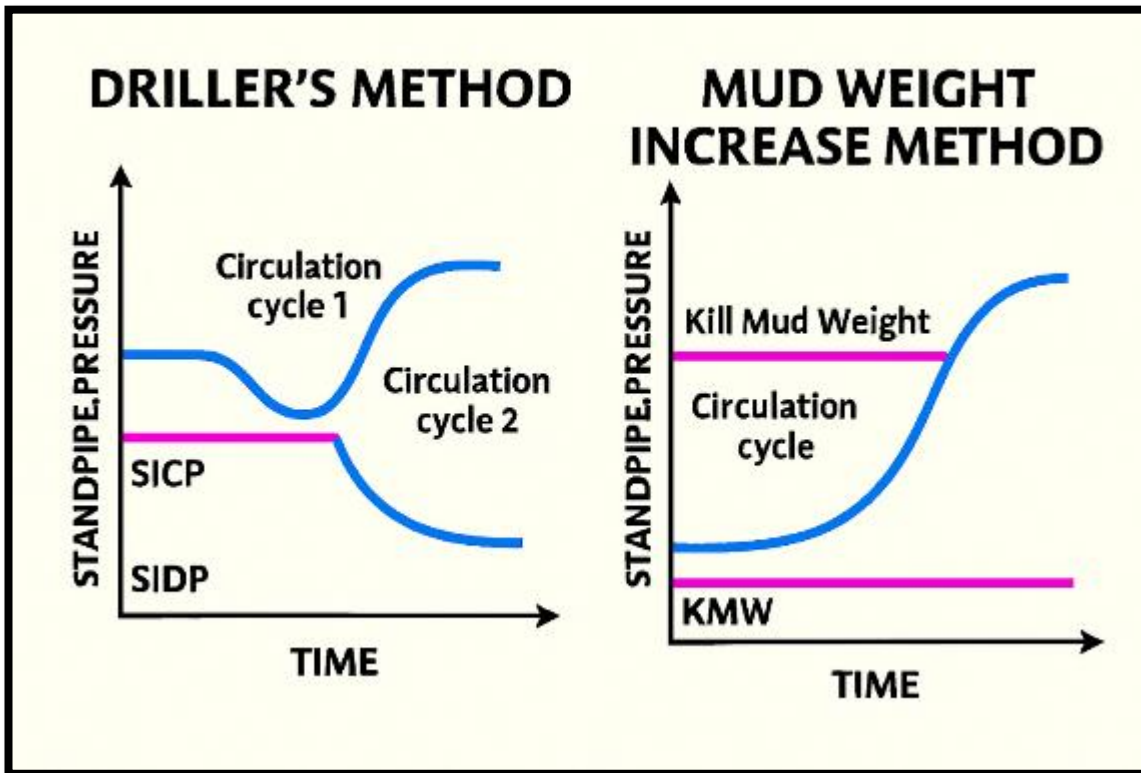


Fig 36 :-Comparison of Driller's Method and Wait-and-Weight (Mud Weight Increase) Method for well control. The Driller's Method requires two circulation cycles: first with the original mud weight, then with increased mud weight. The Wait-and-Weight Method uses one circulation cycle with adjusted mud weight, reducing total circulation time but requiring precise mud weight calculations

**MPD or Managed Pressure drilling:** - Managed Pressure Drilling (MPD) is an advanced drilling technique where the wellbore pressure is precisely controlled and monitored in real time to maintain it within a narrow safe drilling window between formation pore pressure and fracture pressure. It is particularly useful in high-pressure, high-temperature (HPHT) wells, deepwater wells, or formations with narrow mud weight margins.

**Key Principles:-**

1. **Closed-Loop Circulation** – Continuous circulation of drilling mud with precise pressure control.
2. **Real-Time Pressure Monitoring** – Downhole sensors (PWD, annular pressure sensors) provide **instant feedback** on wellbore pressure.
3. **Dynamic Adjustment of Pressure** – Surface equipment adjusts:
  - o **Mud pump rate**
  - o **Backpressure**
  - o **Drilling fluid density**
4. **Maintaining Safe Mud Window** – Ensures:
  - o Pressure above **pore pressure** → prevents kicks
  - o Pressure below **fracture pressure** → prevents lost circulation

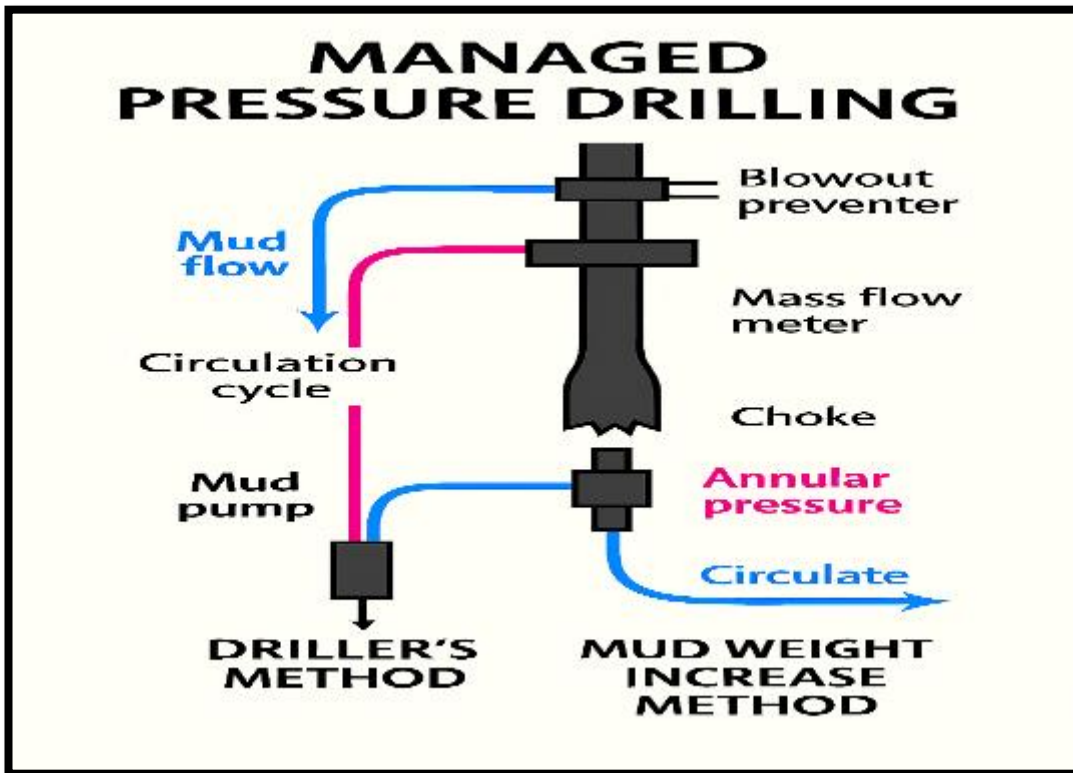


Fig 37 :-Schematic diagram of a Managed Pressure Drilling (MPD) system. It shows surface and downhole components used to precisely control bottomhole pressure during drilling. MPD enables safer, more efficient drilling in narrow pressure windows by adjusting surface backpressure and managing mud flow in real time.

#### Key Components Shown: -

- Rotating Control Device (RCD)
- Choke Manifold
- Backpressure Pump
- Mud Pump & Flow Line
- Mass Flow Meter
- Blowout Preventer (BOP)

#### Flow Paths:

- **Blue Arrows:** Mud flows down the drill string and up the annulus
- **Red Arrows:** Annular pressure control via choke and backpressure system

#### Types of MPD

- **Constant Bottom-Hole Pressure (CBHP)** – Maintains constant bottom-hole pressure using surface backpressure adjustments.
- **Dual Gradient Drilling** – Uses different densities in drill string and annulus to reduce hydrostatic pressure.
- **Pressurised Mud Cap Drilling** – Used in non-penetrable formations, maintains pressure using a mud cap.

**Advantages: -**

- Prevents **kicks and blowouts** in narrow margin wells.
- Reduces **non-productive time** due to well control issues.
- Enables drilling in **challenging overpressured formations**.

**Limitations: -**

- Requires **sophisticated surface equipment** and **trained personnel**.
- Higher **operating costs** compared to conventional drilling.

MPD is a drilling technique that precisely controls wellbore pressure in real time, keeping it within the safe mud window and preventing kicks and lost circulation in narrow-margin or HPHT wells.

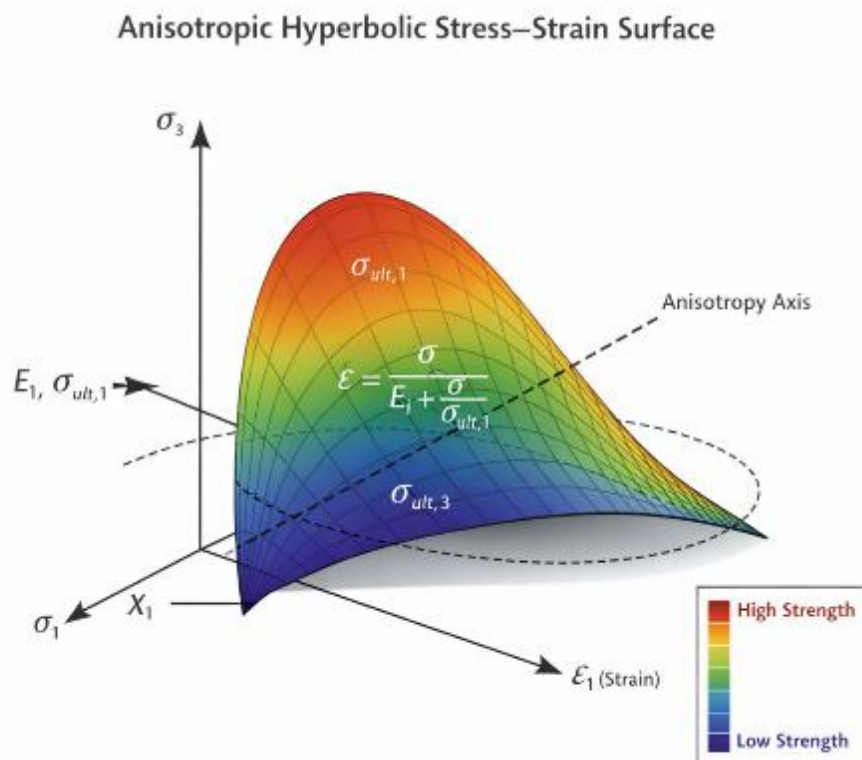
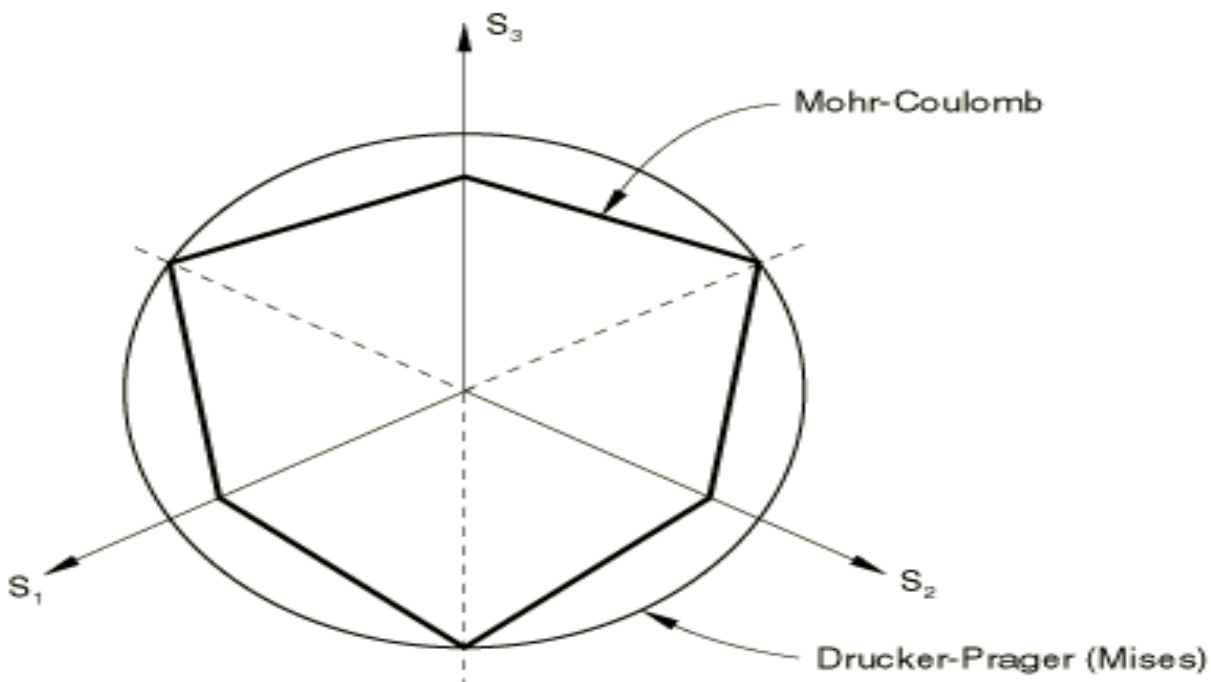
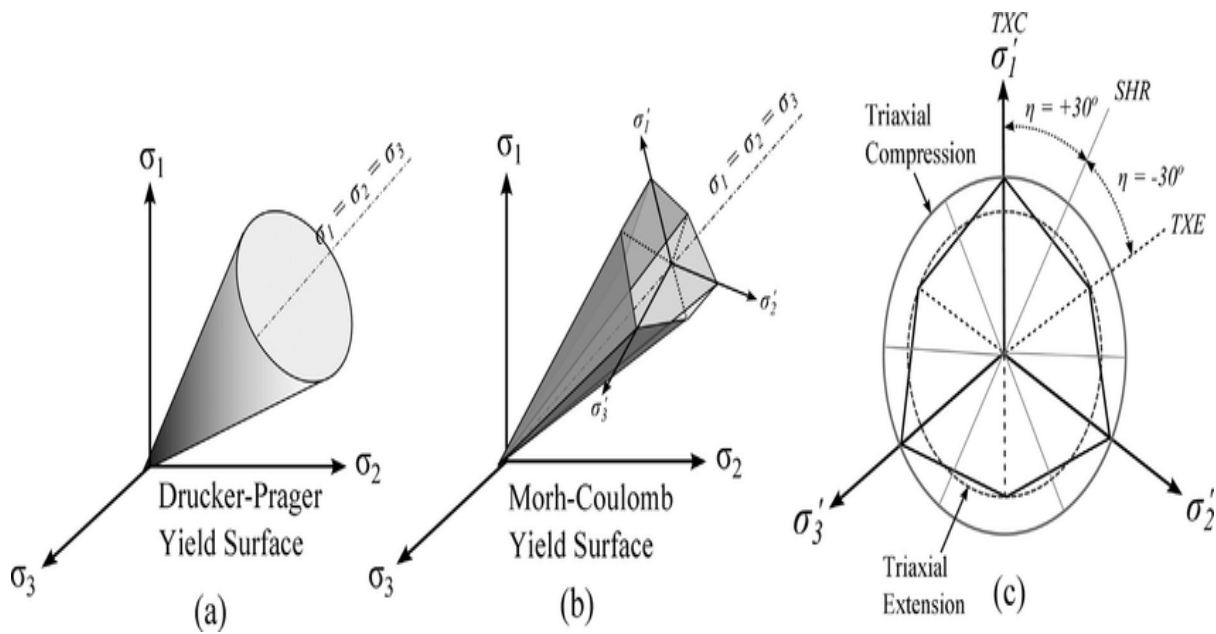
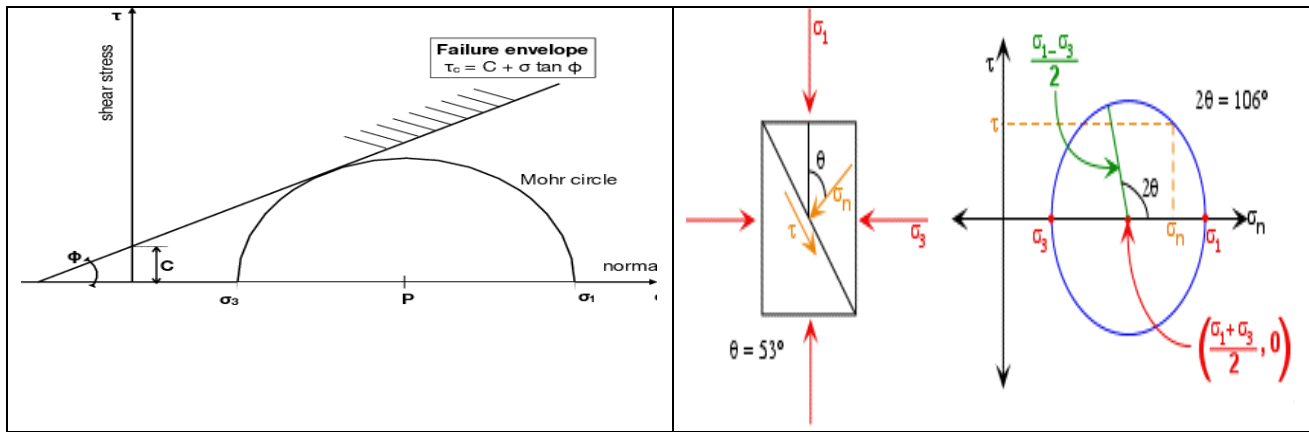


Fig 38:- Three-dimensional representation of the anisotropic hyperbolic stress–strain surface illustrating direction-dependent deformation behaviour of rock under triaxial loading. The curved surface describes the nonlinear hyperbolic constitutive relationship  $\epsilon = \frac{\sigma}{E_i + \sigma / \sigma_{ult,i}}$ , where the initial tangent modulus  $E_i$  and ultimate strength  $\sigma_{ult,i}$  vary along principal material directions. The highlighted anisotropy axis indicates stiffness and strength contrast due to bedding or foliation. Colour gradients represent progressive stress levels from low (blue) to high (red), demonstrating stiffness degradation and nonlinear strain evolution with increasing stress.



**Fig 39 :-** Mohr–Coulomb failure envelope showing the linear relationship between shear stress and normal stress, with Mohr’s circles tangent to the failure line at the onset of shear failure under increasing confining stress.

The Mohr–Coulomb failure criterion is a classical linear strength theory in geomechanics that describes the failure of soils, rocks, and concrete under combined normal and shear stresses. Originally developed from the work of Charles-Augustin de Coulomb and later formalised using the graphical stress representation of Christian Otto Mohr, the model states that failure occurs when the shear stress acting on a plane reaches a value that is linearly related to the normal stress on that plane. The fundamental equation is expressed as  $\tau = c + \sigma \tan \phi$ , where  $c$  is cohesion and  $\phi$  is the internal friction angle. In principal stress terms, the condition can be written as  $\sigma_1 = \sigma_3 \frac{1+\sin \phi}{1-\sin \phi} + \frac{2c \cos \phi}{1-\sin \phi}$ , defining a hexagonal pyramidal failure surface in principal stress space. Graphically, the criterion is represented by a straight-line failure envelope tangent to Mohr's circles at failure, indicating that shear strength increases with confining stress. Although the model assumes isotropy and neglects the intermediate principal stress  $\sigma_2$ , It remains widely used in slope stability, tunnel design, bearing capacity analysis, and wellbore stability calculations due to its simplicity and clear physical interpretation of parameters.

### Drucker–Prager criterion Yield Surface

The Drucker–Prager yield criterion is a pressure-dependent plasticity model widely used in geomechanics to describe the yielding of soils, rocks, and other frictional materials. It is a smooth approximation of the Mohr–Coulomb criterion and is particularly suitable for numerical implementation in finite element analysis. Unlike Mohr–Coulomb, which produces a hexagonal pyramid in principal stress space, the Drucker–Prager model defines a **conical yield surface** in three-dimensional principal stress space ( $\sigma_1, \sigma_2, \sigma_3$ ).

The general form of the Drucker–Prager yield function is:

$$F = \alpha I_1 + \sqrt{J_2} - k = 0$$

where:

- $I_1 = \sigma_1 + \sigma_2 + \sigma_3$  is the first stress invariant (mean stress component),
- $J_2$  is the second invariant of deviatoric stress,
- $\alpha$  and  $k$  are material constants related to cohesion and friction angle.

In terms of mean stress  $p$  and deviatoric stress  $q$ , the yield surface can also be written as:

$$q = Ap + B$$

This shows that yielding depends on confining pressure, making it appropriate for geomaterials whose strength increases with compression.

### Key Characteristics

- Smooth circular cone in principal stress space
- Accounts for pressure-dependent strength
- Easier numerical convergence than Mohr–Coulomb
- Can incorporate hardening and softening behaviour
- Widely implemented in finite element software such as Abaqus and PLAXIS

## Comparison with Mohr–Coulomb

While the Mohr–Coulomb failure criterion produces a hexagonal failure surface and neglects the effect of intermediate principal stresses, the Drucker–Prager criterion provides a smooth approximation that implicitly includes the influence of intermediate stresses. However, it sacrifices the direct physical interpretation of cohesion and friction angle unless properly calibrated.

## Relation of the Drucker–Prager criterion to Anisotropic Media

The classical Drucker–Prager (DP) yield criterion is fundamentally an **isotropic** model because its formulation is based on stress invariants  $I_1$  and  $J_2$ , which are independent of material orientation. This means the yield surface (a circular cone in principal stress space) is identical in all directions, assuming uniform mechanical properties throughout the material. However, many geomaterials—especially shales, laminated sandstones, and foliated metamorphic rocks—exhibit **anisotropic behaviour**, where strength and stiffness vary with direction due to bedding planes, microcracks, or mineral alignment.

## Why Classical DP Is Limited for Anisotropy

- The invariant-based formulation does not account for directional dependence.
- Yield strength is the same regardless of loading orientation.
- The conical yield surface remains symmetric about the hydrostatic axis.

Thus, the classical DP model cannot capture directional strength variations observed in layered rocks.

## Extensions to Anisotropic Media

To apply the Drucker–Prager framework to anisotropic materials, researchers introduce modifications such as:

### 1. Anisotropic Yield Function

The yield function is modified by incorporating structural tensors or transformation matrices that reflect material symmetry (e.g., transverse isotropy). The generalized form becomes:

$$F = \alpha I_1 + \sqrt{\mathbf{s}:\mathbf{H}:\mathbf{s}} - k = 0$$

where:

- $\mathbf{s}$ = deviatoric stress tensor
- $\mathbf{H}$ = anisotropy tensor defining directional strength

This produces an **elliptical or distorted cone** instead of a circular cone in deviatoric stress space.

### 2. Direction-Dependent Parameters

Instead of single constants  $\alpha$  and  $k$ , Anisotropic DP models use:

- $\alpha_i$  for different material directions
- $k_i$  varying with bedding orientation

This allows the yield surface to stretch or compress along specific principal stress axes.

### 3. Transversely Isotropic Drucker–Prager Model

For sedimentary rocks, transverse isotropy is common (properties differ perpendicular and parallel to bedding). In this case:

- Strength parallel to bedding  $<$  strength perpendicular to bedding
- The yield surface becomes asymmetric in principal stress space

This is particularly important in:

- Wellbore stability analysis
- Hydraulic fracturing
- Slope stability in stratified formations

#### Comparison with Mohr–Coulomb in Anisotropic Media

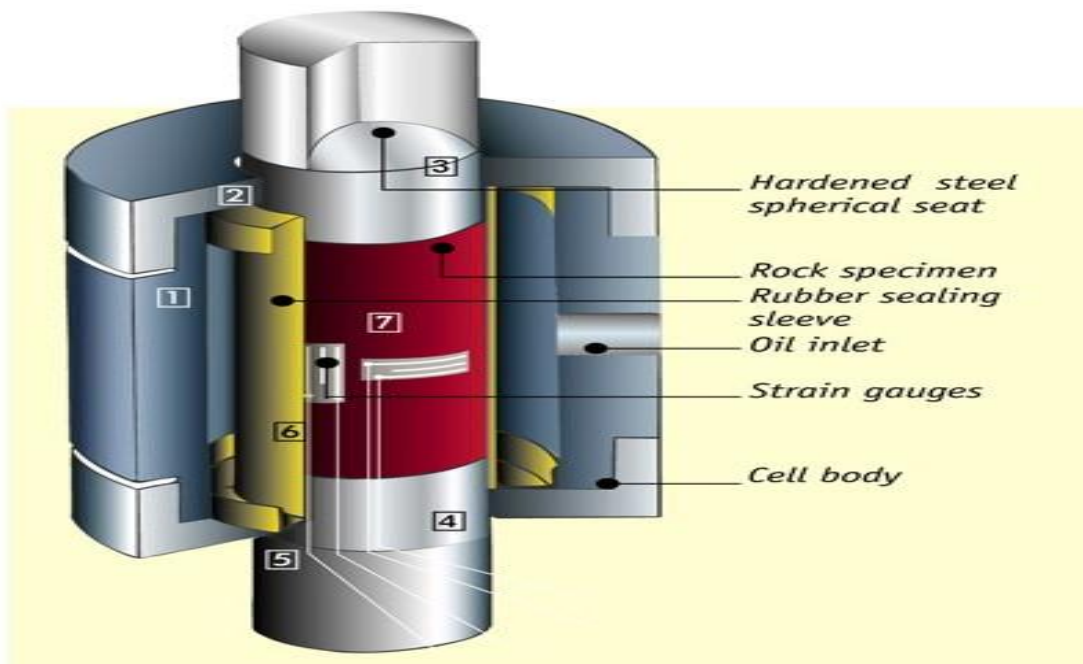
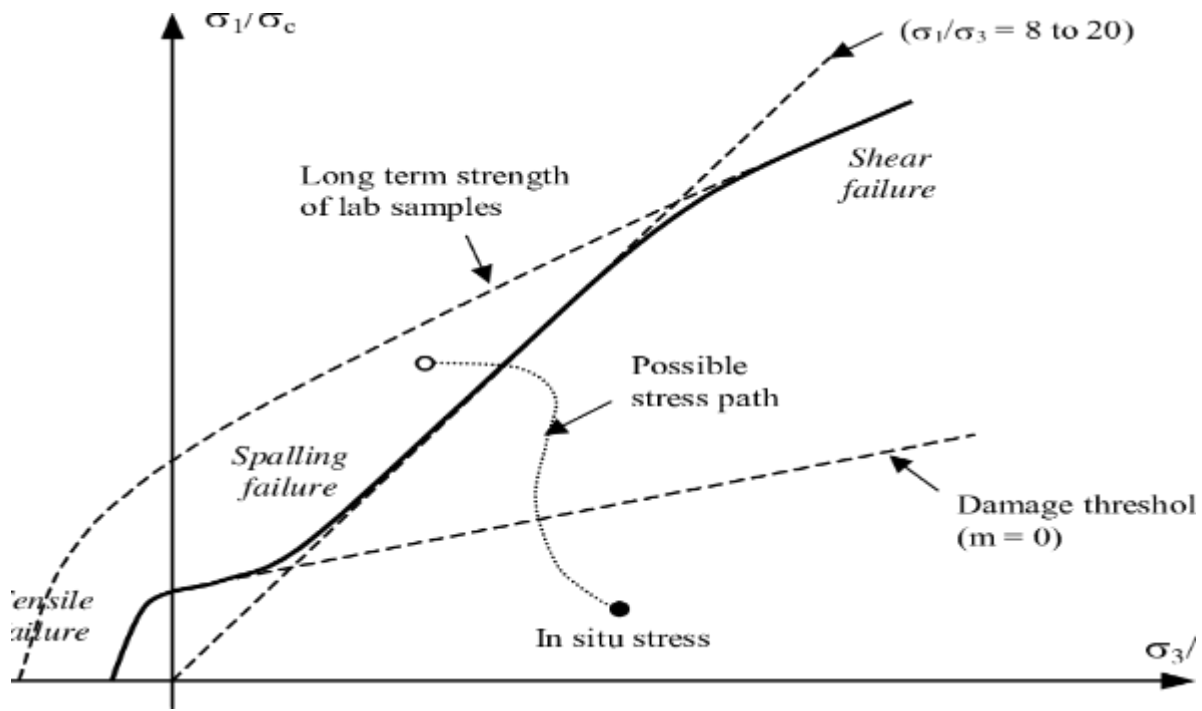
While the Mohr–Coulomb failure criterion can be modified for anisotropy using directional cohesion and friction angle, the invariant-based structure of Drucker–Prager makes it mathematically more convenient for tensor-based anisotropic extensions, especially in finite element formulations.

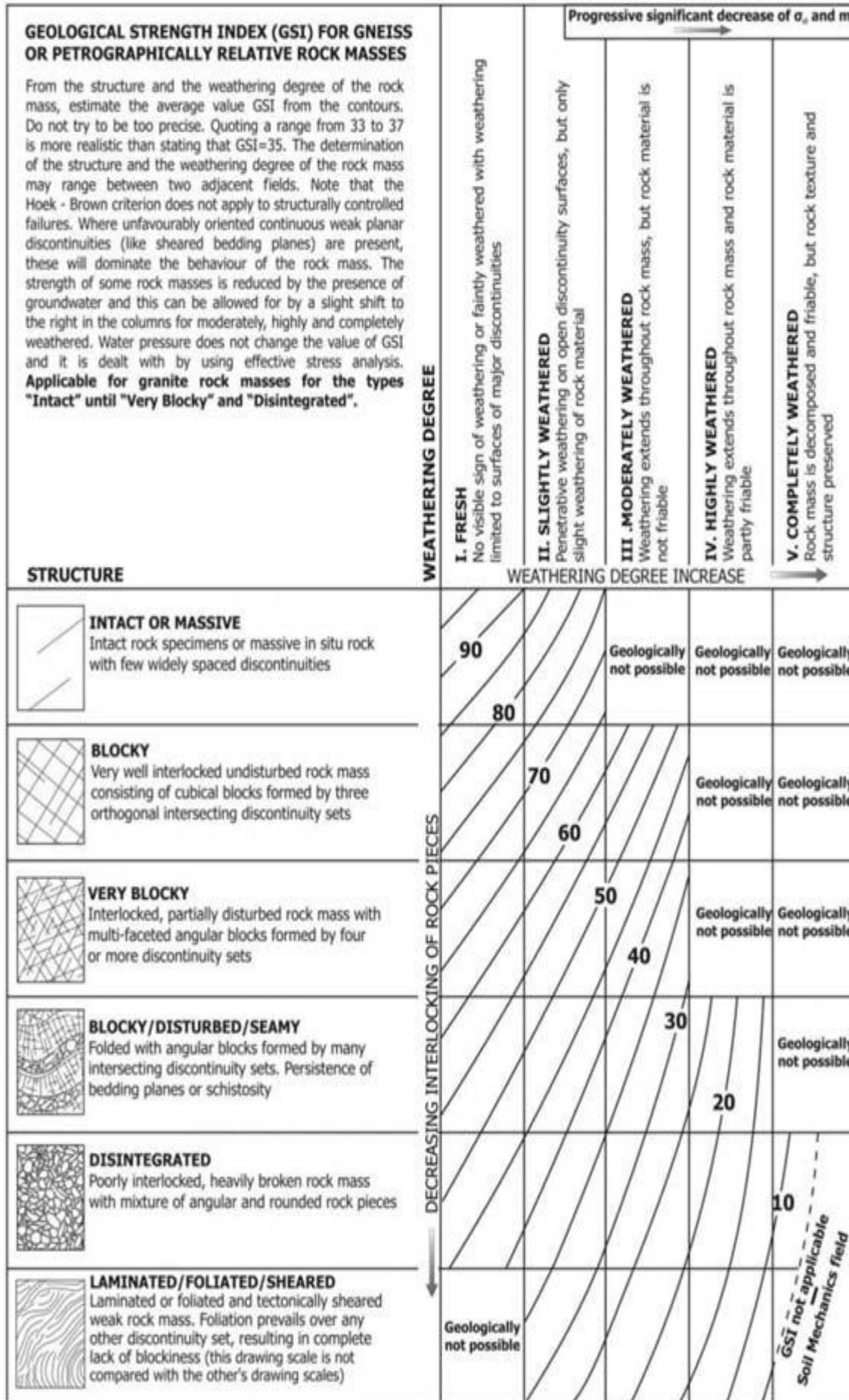
#### Practical Implication in Rock Mechanics

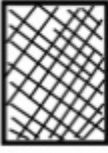
In anisotropic formations:

- Yield initiation depends on loading direction relative to bedding
- Stress redistribution becomes orientation-sensitive
- Collapse pressure predictions change significantly

Therefore, anisotropic extensions of the Drucker–Prager model provide improved prediction of deformation and failure in layered or foliated rocks compared to its classical isotropic form.





GEOLOGICAL STRENGTH INDEX FOR JOINTED ROCKS		SURFACE CONDITIONS					
		VERY GOOD	GOOD	FAIR	POOR	VERY POOR	
STRUCTURE		DECREASING SURFACE QUALITY →					
	INTACT OR MASSIVE-intact rock specimens or massive in situ rock with few widely spaced discontinuities	DECREASING INTERLOCKING OF ROCK PIECES ↓	90				
	BLOCKY-well interlocked undisturbed rock mass consisting of cubical blocks formed by three intersecting discontinuity sets		80	70			
	VERY BLOCKY-interlocked, partially disturbed mass with multi-faceted angular blocks formed by 4 or more joint sets		60				
	BLOCKY/DISTURBED/SEAMY-folded with angular blocks formed by many intersecting discontinuity sets. Persistence of bedding planes or schistosity		40				
	DISINTEGRATED-poorly interlocked, heavily broken rock mass with mixture of angular and rounded rock pieces		20				
	LAMINATED/SHEARED-Lack of blockiness due to close spacing of weak schistosity or shear planes		10				

**Fig 40 :-**Nonlinear Hoek–Brown failure envelope in principal stress space showing the curved relationship between major and minor principal stresses, illustrating increasing rock mass strength with confining pressure compared to a linear Mohr–Coulomb approximation.

The Hoek–Brown failure criterion is an empirical nonlinear strength model widely used in rock mechanics to estimate the compressive failure of intact and jointed rock masses. Developed by Evert Hoek and Edwin T. Brown in 1980 and later revised in 2002 (with updates in 2019), the model provides a nonlinear relationship between the major principal stress  $\sigma_1$  and the minor principal stress  $\sigma_3$ . The generalized failure expression is given by

$$\sigma_1 = \sigma_3 + \sigma_{ci} \left( m_b \frac{\sigma_3}{\sigma_{ci}} + s \right)^a$$

where  $\sigma_{ci}$  is the uniaxial compressive strength of intact rock, and  $m_b$ ,  $s$ , and  $a$  are rock mass constants derived from the intact rock parameter  $m_i$ , the Geological Strength Index (GSI), and the disturbance factor  $D$ . Unlike the linear Mohr–

Coulomb failure criterion, the Hoek–Brown criterion captures the curved, pressure-dependent strength envelope observed in fractured rock masses, making it particularly suitable for tunnel support design, slope stability, underground excavation, and foundation engineering. The nonlinear envelope reflects increasing strength with confinement and provides a more realistic representation of rock mass behaviour under triaxial loading. Although empirical and sensitive to parameter selection, the model forms the backbone of modern rock engineering analysis and is widely implemented in numerical and limit-equilibrium methods through equivalent cohesion and friction angle conversions.

## Results and Discussion:-

The proposed anisotropic hyperbolic stress–strain model demonstrates significant improvement in capturing the nonlinear and direction-dependent deformation behaviour of rock compared with conventional linear elastic and isotropic models. Numerical simulations under triaxial stress conditions show that the stress–strain response varies distinctly along the principal strain directions ( $\varepsilon_1$ ,  $\varepsilon_2$ ,  $\varepsilon_3$ ), reflecting stiffness contrast and strength anisotropy associated with bedding planes and material fabric. The principal strain direction ( $\varepsilon_1$ ) exhibits a higher initial tangent modulus  $E_1$  and greater ultimate strength  $\sigma_{ult,1}$ , while the moderate ( $\varepsilon_2$ ) and minor ( $\varepsilon_3$ ) directions show progressive stiffness reduction and earlier nonlinearity, indicating preferential deformation along weaker orientations.

The hyperbolic formulation successfully reproduces the gradual stiffness degradation observed in laboratory triaxial tests, unlike linear elastic models, which assume constant modulus. Compared with the classical **Mohr–Coulomb failure criterion**, the proposed model captures pre-failure nonlinear deformation rather than predicting abrupt failure at a linear envelope. Furthermore, relative to the **Hoek–Brown failure criterion**, the anisotropic hyperbolic approach provides better control over directional stiffness parameters and is more suitable for layered sedimentary formations such as shale and laminated sandstone.

Stress redistribution analysis around wellbores indicates that anisotropy significantly alters the deformation pattern and failure initiation zones. When the wellbore axis is aligned with the weak bedding direction, tangential strain concentration increases, reducing the safe mud weight window. Conversely, alignment with the strong axis enhances stability and expands the operational envelope. The model also demonstrates improved prediction of stress rotation effects, which are critical in deviated and horizontal wells.

Sensitivity analysis reveals that the ratio  $E_1/E_3$  and  $\sigma_{ult,1}/\sigma_{ult,3}$  strongly governs the curvature of the hyperbolic surface and the onset of nonlinear deformation. Higher anisotropy ratios lead to pronounced strain localization along weaker axes. These findings confirm that incorporating directional hyperbolic behavior is essential for accurate geomechanical modeling in anisotropic formations.

Overall, the results validate that the proposed framework:

- Accurately captures nonlinear anisotropic deformation
- Predicts progressive stiffness degradation
- Improves wellbore stability assessment
- Provides realistic stress–strain evolution prior to failure
- Can be readily implemented in finite element simulations

The model therefore offers a robust and practical advancement for anisotropic rock mechanics applications in drilling, reservoir geomechanics, and underground excavation design.

## Bibliography :-

Hoek, E., & Brown, E. T. (1980). *Empirical strength criterion for rock masses*. Journal of the Geotechnical Engineering Division, ASCE, 106(GT9), 1013–1035.

Hoek, E., Carranza-Torres, C., & Corkum, B. (2002). *Hoek–Brown failure criterion – 2002 edition*. Proceedings of the North American Rock Mechanics Society (NARMS-TAC) Conference, Toronto, Canada.

Hoek, E., Carter, T. G., & Diederichs, M. S. (2013). *Quantification of the geological strength index chart*. 47th U.S. Rock Mechanics / Geomechanics Symposium, San Francisco.

Hoek, E., & Diederichs, M. S. (2019). *Empirical estimation of rock mass strength and deformation modulus*. Rock Mechanics and Rock Engineering, 52, 1–20.

Coulomb, C. A. (1773). *Essai sur une application des règles de maximisation et de minimisation à quelques problèmes de statique relatifs à l'architecture*. Mémoires de Mathématique et de Physique.

Mohr, O. (1900). *Welche Umstände bedingen die Elastizitätsgrenze und den Bruch eines Materials?* Zeitschrift des Vereines Deutscher Ingenieure.

Bieniawski, Z. T. (1989). *Engineering Rock Mass Classifications*. Wiley-Interscience.

## Acknowledgement

I would like to express my sincere gratitude to my supervisor and research guides for their valuable guidance, continuous support, and insightful suggestions throughout the preparation of this work. Their expertise in rock mechanics and geomechanical modelling significantly contributed to the development and refinement of the concepts presented in this study.

I am also thankful to my academic institution and department for providing the necessary research facilities, computational resources, and technical environment to complete this work. Special appreciation is extended to faculty members and colleagues who offered constructive discussions and feedback that improved the quality of this research.

Finally, I acknowledge my family and friends for their encouragement, patience, and constant support during the course of this research.

Appendix – Compact One-Page Summary Table

Section	Content	Key Expression / Parameter	Description
A.1 Mohr–Coulomb	Failure Criterion	$\tau = c + \sigma \tan \phi$	Linear shear strength model relating shear stress to normal stress
	Principal Stress Form	$\sigma_1 = \sigma_3 \frac{1 + \sin \phi}{1 - \sin \phi} + \frac{2c \cos \phi}{1 - \sin \phi}$	Failure condition in principal stress space
A.2 Drucker–Prager	Yield Function	$F = \alpha I_1 + \sqrt{J_2} - k = 0$	Smooth pressure-dependent yield surface
	Stress Invariants	$I_1 = \sigma_1 + \sigma_2 + \sigma_3,$ Deviatoric invariant $J_2 =$	Governs conical yield surface
A.3 Hoek–Brown	Failure Criterion	$\sigma_1 = \sigma_3 + \sigma_{ci} (m_b \frac{\sigma_3}{\sigma_{ci}} + s)^a$	Nonlinear rock mass strength model
	Parameters	$\sigma_{ci}, m_b, s, a$	Derived from GSI, $m_i$ , and disturbance factor $D$
B. Parameters	Strength Parameters	$c, \phi, \sigma_{ci}$	Control shear and compressive strength
	Rock Mass Index	GSI	Structural quality of rock mass
	Material Constant	$m_i$	Intact rock property
	Disturbance Factor	D	Excavation/blast damage effect
C. Numerical Implementation	Method	Newton–Raphson Iteration	Solves nonlinear yield equations
	Convergence	$10^{-6}$	Stress residual tolerance
	Validation	FE / Analytical Comparison	Model verification